CORRELATION BETWEEN HEAD WALL STEEPNESS AND ROCK GLACIER SIZE AND GROWTH ON EARTH AND MARS

A Thesis

Presented to the

Faculty of

California State Polytechnic University, Pomona

In Partial Fulfillment

Of the Requirements for the Degree

Master of Science

In

Geological Sciences

By

Caleb A. Strom

2019

SIGNATURE PAGE

THESIS:	CORRELATION BETWEEN HEAD WALL STEEPNESS AND ROCK GLACIER SIZE AND GROWTH ON EARTH AND MARS
AUTHOR:	Caleb A. Strom
DATE SUBMITTED:	Fall 2018
	Geological Sciences Department
Dr. Nicholas Van Buer Thesis Committee Chair Geological Sciences	______________________________
Dr. Jeffrey Marshall Geological Sciences	______________________________
Dr. Bryan Murray Geological Sciences	______________________________

AKNOWLEDGEMENTS

I would like to thank my advisor Dr. Van Buer for his guidance, helpful feedback, and assistance in obtaining photographs. I would also like to thank Karissa Vermillion and some anonymous scientists and graduate students at the Lunar and Planetary Science Conference for their helpful comments and suggestions during preparation for the thesis.

ABSTRACT

There is growing interest in using rock glaciers in paleoclimate studies on Earth. Rock glaciers are also found on Mars, which suggests that they could also be used for Martian paleoclimate studies. Using rock glaciers to study paleoclimate on multiple planets, however, requires understanding how the response of rock glaciers to climate is affected by non-climatic factors such as headwall or cirque wall steepness, which may vary from planet to planet. The purpose of this study is to determine whether there is a correlation between headwall steepness and rock glacier morphology. In this study, DEMs, analysis tools from ArcGIS, and Google Earth were used to determine the average headwall steepness for individual rock glaciers and compare it with rock glacier height, length, slope steepness, and latitude for 101 individual Earth rock glaciers and 18 out of 50 individual Martian rock-ice features (aspect was also noted for Martian features). Values for these metrics were plotted against headwall steepness and a moderate positive correlation was found between headwall steepness and rock glacier length for Martian rock glaciers, but no correlations were found for terrestrial rock glaciers. If this correlation for Mars is genuine, one possible explanation is that steeper slopes lead to more rockfall, resulting in more debris accumulation and, as a result, larger rock glaciers on Mars. This may not apply to the Sierra Nevada because of a difference in lithology. This tentative correlation means that rock-ice features with steeper headwalls on Mars might have more ice content because of thicker debris mantles and thus appear younger than rock glaciers of similar age with gentler slopes. This would be important for constructing any glacial chronology on Mars and assessing water resources on Earth and is worth further investigation.

TABLE OF CONTENTS

Signature Page…………………………………………………………………………ii

Acknowledgements……………………………………………………………………iii

Abstract…………………………………………………………………………….....iv

List of Figures…………………………………………………………………………vi

List of Tables……………………………………………………………………….....x

List of Equations………………………………………………………………………xi

Introduction……………………………………………………………………………1

Background……………………………………………………………………………12

Methods………………………………………………………………………………..39

Results…………………………………………………………………………………65

Discussion……………………………………………………………………………..82

Conclusion……………………………………………………………………………98

Appendix 1……………………………………………………………………………99

Appendix 2…………………………………………………………………………...127

References……………………………………………………………………………133

LIST OF FIGURES

Figure 1. California Peak rock glacier…………………………………………….....5

Figure 2. Protalus lobes on Axel Heiberg Island…………………………………………6

Figure 3. Protalus rampart or moraine in France…………………………………………7

Figure 4. Protalus rampart and protalus lobe at cliffs of Mynydd Ddu, Wales……….....8

Figure 5. Diagram of rock glacier……………………………………………………..10

Figure 6. Global Earth maps…………………....………………………………………12

Figure 7. Andean rock glacier image and location map………………...………………16

Figure 8. Alps rock glacier image and location map……………………………………18

Figure 9. Himalayan rock glacier image and location map ……………………………..20

Figure 10. New Zealand rock glacier image and location map…………………………22

Figure 11. Global Mars map….…………………………………………………………24

Figure 12. LDA/LVF global location map…………...……………………………….....25

Figure 13. Lobate debris apron (LDA) image and location map………………………...26

Figure 14. Lineated valley fill (LVF image and location map)………………………....27

Figure 15. Sharad radargrams showing subsurface ice…...…………………………......29

Figure 16. Sharad radargrams location map……………………….……………………30

Figure 17. Mars and Earth geologic timescales………………………………………32

Figure 18. Gale Crater global location map…………..……………………………….33

Figure 19. Obliquity example….……...…………….…………………………………..35

Figure 20. Mars obliquity example with ice…….………………………………………36

Figure 21. Historical Martian geologic processes timeline..……….…….……………..38

Figure 22. Rock glacier SNRGLF 85…….…….………………………………………..40

Figure 23. Rock glacier SNRGLF 87……………………………………………………41

Figure 24. Rock glacier SNRGLF 84…………………………………………………....43

Figure 25. Sierra Nevada rock glacier elevation profile example………………………45

Figure 26. Martian Tongue-like shape and transverse ridge example…………………47

Figure 27. Martian Oversteepened front example……………………………………....47

Figure 28. Arsia Mons positive length/width example…………………………………48

Figure 29. Valles Marineris positive length/width example……………………………48

Figure 30. Arsia Mons negative length/width example…………………………………49

Figure 31. Arsia Mons negative length/width example 2………………………………50

Figure 32. Moraine-like feature in Deuteronilus Mensae………………………………51

Figure 33. Longitudinal ridges on VMRGLF 33……………………………………….52

Figure 34. Longitudinal ridges on PTRGLF 27…………………………………………52

Figure 35. Earth glacier with longitudinal ridges……………………………………….53

Figure 36. VMRGLF 27 smooth terrain example……………………………………….56

Figure 37. Polygon example……………………………………………………………..57

Figure 38. PMRGLF 6 HB elevation profile…………………………………………….58

Figure 39. PMRGLF 6 HB image and location map…………………………………….59

Figure 40. PTRGLF 7 HC elevation profile……………………………………………..60

Figure 41. PTRGLF 7 image and location map…………………………………………61

Figure 42. VMRGLF 19 HC elevation profile…………………………………………..62

Figure 43. VMRGLF 19 image and location map……………………………………….63

Figure 44. Sierra Nevada Rock Glacier-like form 92……………………………………65

Figure 45. Sierra Nevada rock glacier map……………………………………………...67

Figure 46. Head wall steepness vs horizontal length graph (SN)……………………….68

Figure 47. Valley wall steepness vs height graph (Mars)………………………………69

Figure 48. Valley wall steepness vs length (Mars)……………………………………...69

Figure 49. Global Mars map showing locations of regional maps………………………70

Figure 50. Valles Marineris map………………………………………………………...72

Figure 51. Valles Marineris rock-ice feature image……………………………………..72

Figure 52. Olympus mons map……………………………………………………………..73

Figure 53. Olympus mons rock-ice feature image………………………………………74

Figure 54. Promethei Terra map…………………………………………………………75

Figure 55. Promethei Terra rock-ice feature image……………………………………...75

Figure 56. Argyr Basin map……………………………………………………………...76

Figure 57. Argyr Basin rock-ice feature image…………………………………………77

Figure 58. Deuteronilus Mensae map…………………………………………………...78

Figure 59. Deuteronilus Mensae rock-ice feature image……………………………...78

Figure 60. Protonilus Mensae map……………………………………………………....79

Figure 61. Protonulus Mensae rock-ice feature image…………………………………..79

Figure 62. Arsia Mons map……………………………………………………………...80

Figure 63. Arsia Mons rock-ice feature………………………………………………....81

Figure 64. Graph demonstrating optimal slope steepness………………………………84

Figure 65. Diagram of Earth and Martian rock glacier flow patterns……………………93

LIST OF TABLES

Table 1. Rock glacier classification schemes……………………………………………….9

Table 2. Morphological criteria for inclusion of Martian rock-ice feature in analysis…..54

Table 3. Data on Sierra Nevada rock glaciers………………………………………………66

Table 4. Table comparing Earth and Martian rock glaciers……………………………...86

LIST OF EQUATIONS

Equation 1. Equation for slope steepness in degrees……………………………………44

Equation 2. Equation for rock glacier length in meters…………………………………44

Equation 3. Equation for rock glacier height in meters…………………………………44

INTRODUCTION

Glacial processes have played a significant role in the climate history of Earth. Over the past 2.5 billion years, Earth has experienced numerous glaciation events. More recent Quaternary glaciation events are indicated by the presence of moraines and other glacial features around the world. At various times during the Quaternary, most of the land in northern hemisphere was covered in ice sheets and glaciers. This is known directly from fossil moraines, drumlins, eskers, and other landforms created by the movement of glaciers. Glaciation events are also known indirectly from paleoclimate studies which have revealed average temperatures as well as fossil flora and fauna which indicate the presence of a glacial climate. In kind, just as paleoclimate studies have illuminated past glaciation, evidence of past glaciation is also useful for inferring past climatic conditions on Earth.

Recent planetary exploration has also revealed that Earth is not the only planet with glacial activity. Evidence has also been found for glaciation episodes on Mars (e.g., Mege and Bourgois, 2011). This makes it possible that glacial chronology could be used to understand the climate of other planetary bodies as well. In order to use glacial chronology to reconstruct the past climate on another planetary body, however, it must be known what factors affect glacial processes on that planet. Modern Mars lacks true ice glaciers, unless debris-covered rock glaciers are included, but it does have possible rock glaciers (e.g., Pierce and Crown, 2003) which are also a feature found in abundance on Earth. Rock glaciers are mixtures of rock debris and ice that form in alcoves or cirques similar to glaciers. Rock glaciers flow in a manner similar to ice glaciers. The response of rock glacier behavior and morphology to climate is not as well studied as the response of ice glaciers to climate, but there is interest in using rock glaciers in paleoclimate studies on Earth. If they can be used on Earth, it is likely that they could also be used for paleoclimate reconstruction on Mars. To accurately interpret the paleoclimatic conditions of ancient Mars, and Earth, using rock glaciers, however, it must be known exactly how rock glaciers respond to climate. For this reason, a study is needed to investigate what factors would influence the response of rock glaciers to climate on Earth and Mars, including non-climatic factors. Focusing on the non-climatic factors implicated in rock glacier behavior and morphology is especially useful since non-climatic factors can cause rock glaciers and other glacial phenomena to respond in unexpected ways to climate.

An example of a potentially significant non-climatic factor in rock glacier morphology is the steepness of the headwall. The headwall, in this case, is the wall of the alcove in which rocky debris accumulates to form the rock glacier. The headwall is also the principle source of the rock debris that composes the rock glacier.

Purpose of this study

The main purpose of this thesis is to determine whether the steepness of the cirque wall or headwall of a rock glacier has a significant influence on the behavior of rock glaciers and other rock-ice features in a way that would be significant for accurately reconstructing climate history on planets with major water-ice cryospheres, essentially Earth and Mars. Headwall steepness is chosen as the focus because steepness is not primarily climate controlled. Rather, slope steepness, or slope gradient, is primarily controlled by tectonic factors (Kirkbride and Brazier, 1995) and lithology (Dorren *et al*, 2004; Marquinez *et al*, 2003; Kirkbride and Brazier, 1995). Headwall steepness is a clear example of a primarily non-climatic factor that could be significant for understanding how rock glaciers respond to climate.

Why study rock glaciers on both Earth and Mars?

Mars is the only planet other than Earth that has evidence of water related glacial activity as shown by evidence of moraines and other features that appear glacial (Arfstrom and Hartman, 2005). There is abundant evidence from images captured by Mars orbiters of potentially glacial landforms created through subsurface flowing ice (Colaprete and Jakosky, 1998; Whalley and Azizi, 2003; Pierce and Crown, 2003). The presence of geomorphological features on Mars that show evidence of having been sculpted by flowing ice demonstrates that ice plays a major role in the Martian surface environment. Most of these features are also probably debris-covered ice flow features of some sort because of the current surface conditions of Mars (Arfstrom and Hartman, 2005; Mahaney, 2007).

Earth and Mars are very different in many ways, but both have water-ice glacial processes that shape their surface environments. Studying rock-ice features on both planets will provide a picture of rock-glacier behavior in response to climate that is more complete and more thorough than one which focuses only on rock glaciers in conditions prevalent on Earth. Furthermore, there is significant scientific interest in unraveling the climate history of both planets, so understanding factors affecting the response of rock-ice features to climate on Mars is scientifically important by itself as well as in reference to Earth. Before investigation into the behavior of rock glaciers on Earth or Mars can be done, however, a more thorough introduction to rock glaciers is necessary.

INTRODUCTION TO ROCK GLACIERS

Rock glaciers are typically defined as poorly sorted, lobate, flowing deposits of rocky material containing silt-sized to boulder-sized angular rock fragments held together by a core of ice or permafrost (Giardino and Vitek, 1988; Whalley and Azizi, 2003). The characteristic features identifying rock glaciers from other lobate deposits in the field are a wrinkled surface caused by a series of transverse ridges (Whalley and Azizi, 2003; Giardino and Vitek, 1988) and a steep front or terminus (Whalley and Azizi, 2003) (Figure 1). In general, most researchers would agree that an oversteepened front, transverse ridges, a lobate shape and continuous flow of material are diagnostic of rock glaciers (e.g., Shroder *et al*, 2000; Whalley and Azizi, 2003; Kirkbride and Brazier, 1995; Figure 1).

In addition to rock glaciers, there are also rock glacier-like features that have some similarity to rock glaciers, but it is not clear that they count as rock glaciers since they do not fit the definition given above, though some authors refer to them as rock glaciers. These are protalus lobes and protalus ramparts (e.g., Whalley and Azizi, 2003; Miller and Westfall, 2008). They are also called valley wall rock glaciers, talus rock glaciers (e.g., Brazier *et al*,1998) and protalus rock glaciers (e.g., Owen and England, 1998) by various authors. The term “valley wall rock glacier” comes from the fact that they tend to form and stay close to the base of a valley wall or cliff wall (Figure 2). Workers in the field refer to the more universally accepted rock glacier type as a “valley floor rock glacier” (e.g., Whalley and Azizi, 2003). This is because it spreads out more onto the valley floor than a protalus lobe or rampart. Valley floor rock glaciers also have a distinctive tongue-like shape (Figure 1). In this study, valley floor rock glaciers will also be called classic rock glaciers.

Figure 1: The California Peak Rock Glacier in the Sangre De Cristo Mountains in Southern Colorado. A classic rock glacier with an over-steepened front, visible transverse ridges, and a vaguely tongue-like shape (adapted from Giardino and Vitek, 1988).

Protalus lobes

Protalus lobes are deposits that occur at the base of cliffs (Figure 2). These features are similar to moraines. They are characterized by steep ridges and often occur far from ice glaciers (Figure 2). They are associated with permafrost and often believed to be held together by interstitial ice (Whalley and Azizi, 2003; Owen and England, 1998).

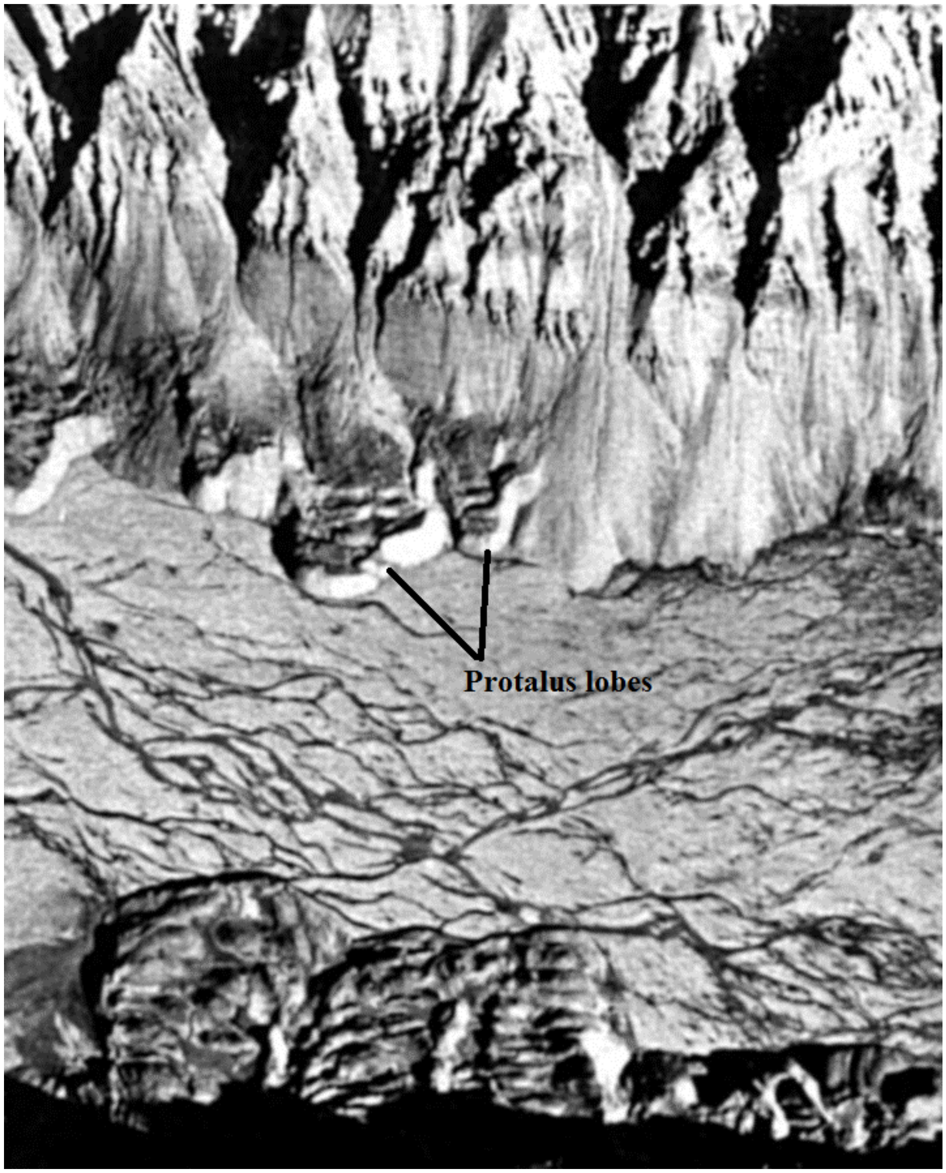

Figure 2: Protalus lobes on Axel Heiberg Island in the Canadian Arctic (adapted from Whalley and Azizi, 2003)

Protalus ramparts

Protalus ramparts are ridges that occur on the edges of a snowfield or small glacier (Figure 3). Protalus ramparts are commonly thought to form from snow accumulating at the foot of a cliff (Figure 4) before becoming covered by debris and, in some cases, compacted into ice (Whalley and Azizi, 2003).

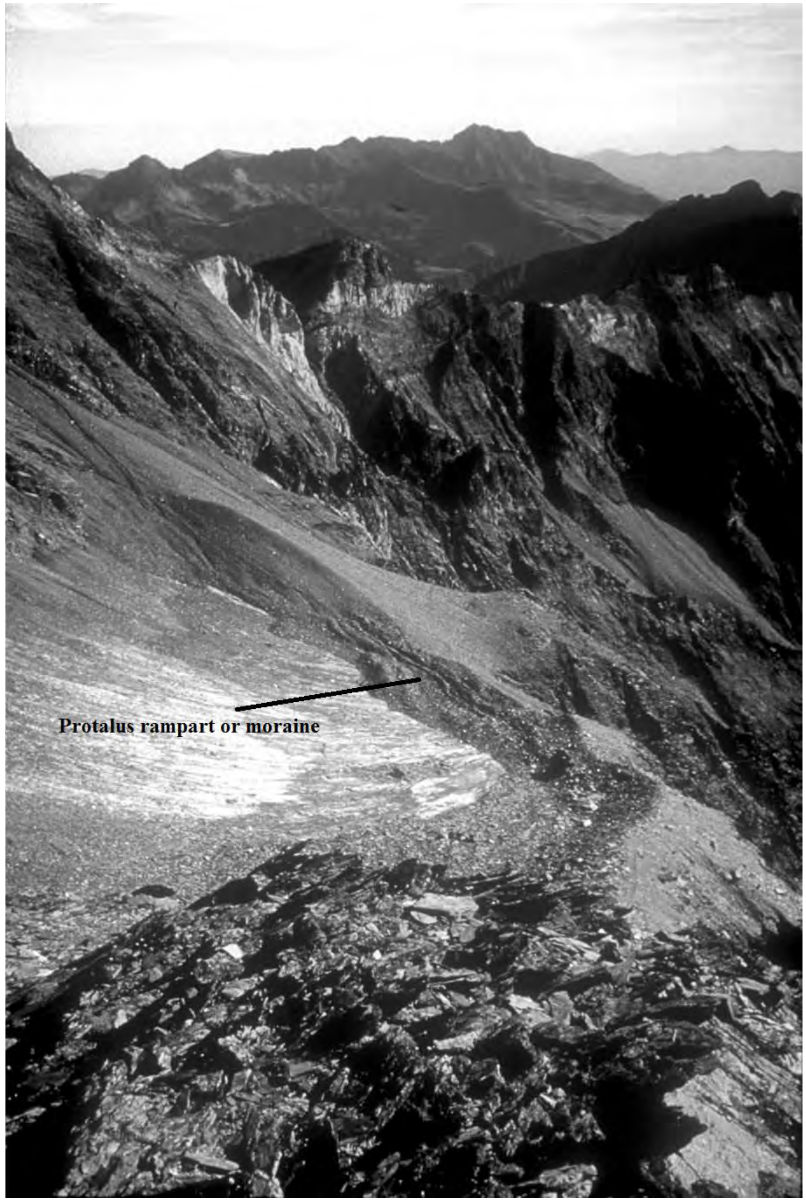

Figure 3: A protalus rampart or moraine in the Pyrenees, France, a glacierette is forming upslope of the feature (Whalley and Azizi, 2003).

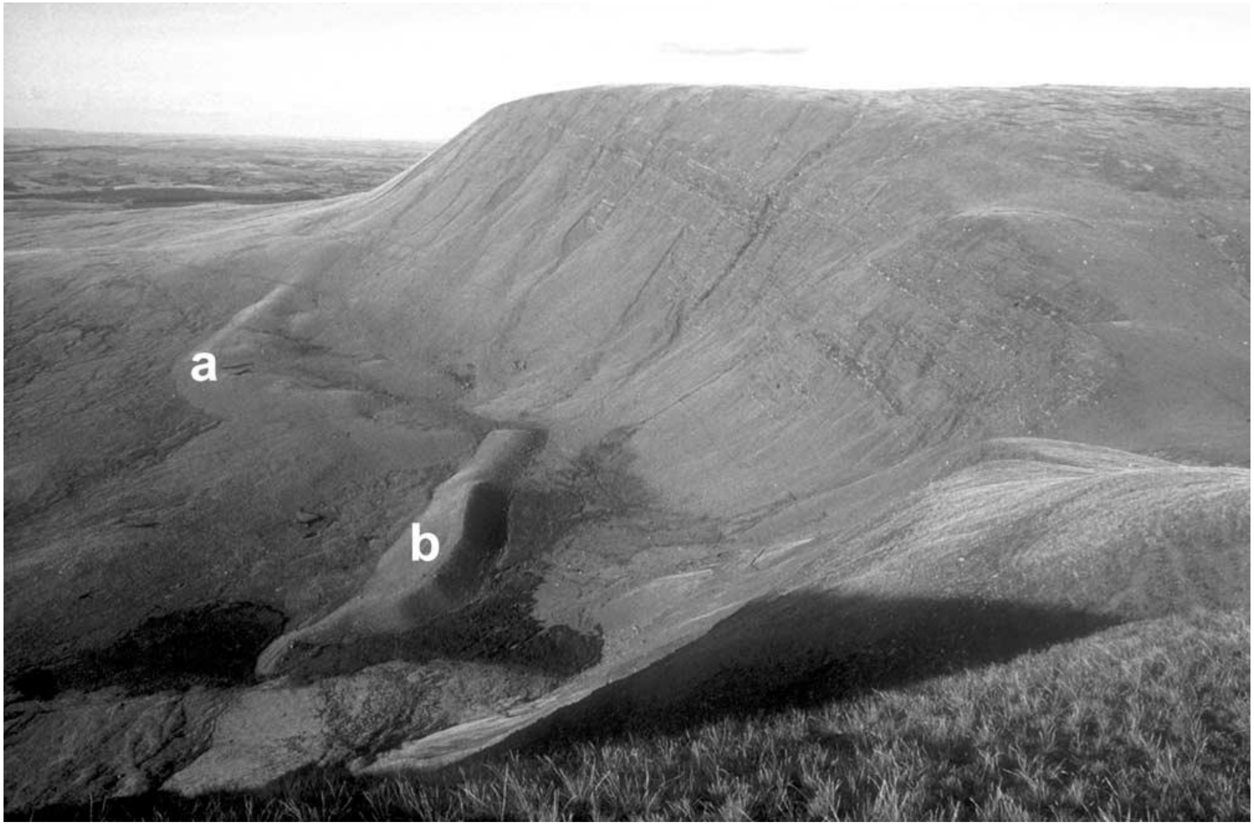

Figure 4: A protalus rampart or moraine (a) and protalus lobe (b) at the cliffs of Mynydd Ddu, Wales, the morphological difference is apparent in the bow-shape of the rampart and the straighter ridge-like shape of the protalus lobe (Whalley and Azizi *et al*, 2003).

These features may not be rock glaciers in a strict sense since they don't appear to exhibit any flow activity, but they are still rock-ice features and many workers in the field call them rock glaciers. Though the focus of this study will be on classic rock glaciers, a typically lobate debris-covered flowing ice body with an oversteepened front and a pattern of transverse wrinkle ridges, other rock-ice features will also be noted since certain rock ice features, such as protalus lobes, do occasionally resemble classic rock glaciers and could be mistaken for them.

Models of rock glacier formation

It should be noted before continuing that there is a controversy regarding the origin of the ice within rock glaciers. There are essentially two views on the origin or formation of rock glaciers: a glacial origin and a permafrost origin (Whalley and Azizi, 2003; Miller and Westfall, 2008; Brazier *et al*, 1998; Giardino and Vitek, 1988; Table 1).

Origin-based classification	Morphology-based classification
“Glacial-derived” rock glaciers	Tongue-shaped for “valley floor” rock glaciers
Permafrost derived rock glaciers	Protalus lobes or “valley wall” rock glaciers

Table 1: The above table demonstrates the two different classification schemes for rock glaciers. Rock glaciers based on ice origin are divided between permafrost and ice glacier derived. Based on morphology, they are divided between valley floor and valley wall rock glaciers or tongue-shaped rock glaciers and protalus lobes respectively.

Glacial model

According to this model, rock glaciers begin as ice glaciers which become covered by a mantle of rock debris eroding from the cirque wall (Figure 5). Over time, the debris becomes thick enough that there is more rock debris than ice making up the bulk of the glacier, making it a rock glacier (Whalley and Azizi, 2003).

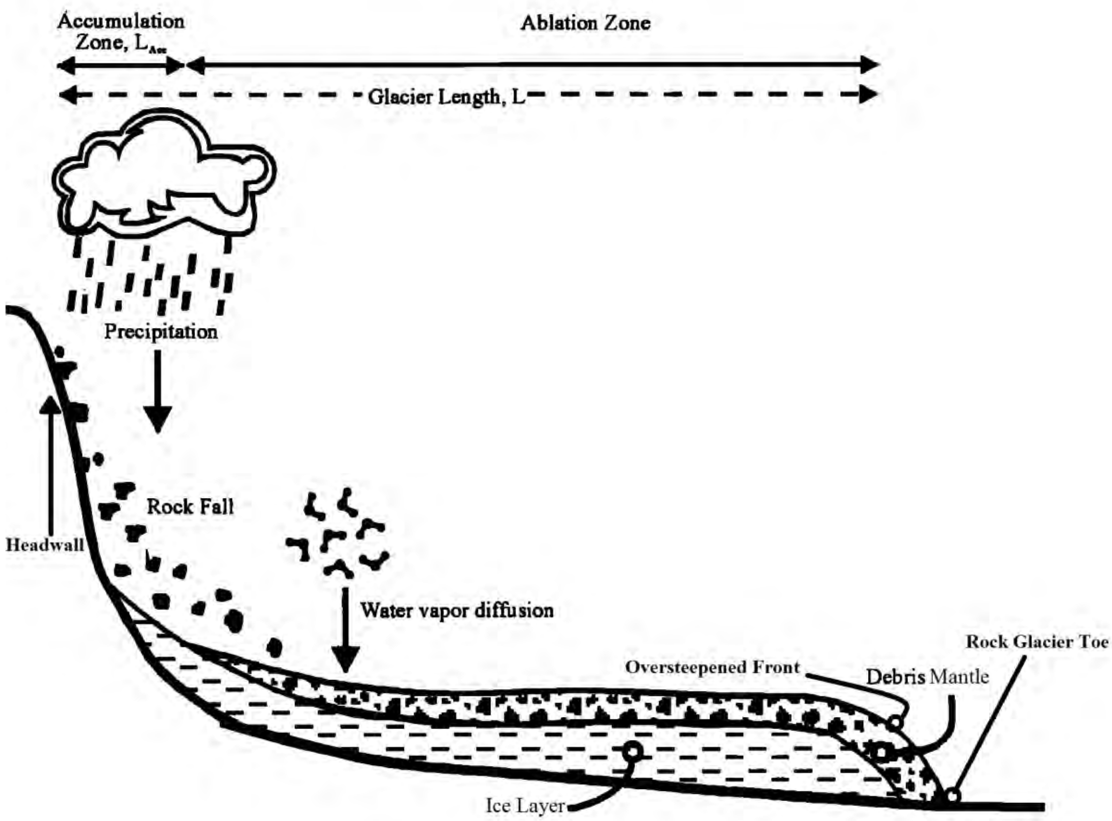

Figure 5. A diagram showing all the basic parts of a classic rock glacier assuming a glacial origin, rockfall erodes from the headwall and accumulates at the base. This creates a debris mantle over an ice layer (adapted from Colaprete and Jakosky, 1998).

Permafrost model

It is also possible that rock glaciers form without pre-existing ice. According to the permafrost model, water becomes injected into a debris flow becoming congelation or interstitial ice. Over time, this creates permafrost. Proponents of this view believe that permafrost glaciers occur at a temperature range below about -1 to -2 degrees Celsius (Brenning, 2005; Brazier *et al*, 1998). The permafrost model appears to be the preferred view in Europe where permafrost is often assumed (Roer *et al*, 2008; Brazier *et al*, 1998).

Models and field results compared

Most of the evidence suggests that rock glaciers can form in both permafrost and glacial conditions (Miller and Westfall, 2008; Giardino and Vitek, 1988; Brazier *et al*, 1998), although there are some researchers who dispute this (Haeberli, 2000).

Most researchers advise using a morphological definition of rock glaciers which is not dependent on the origin of ice (Giardino and Vitek, 1988; Miller and Westfall, 2008; Shroder *et al*, 2000). Furthermore, most researchers would agree that classic rock glaciers count as true rock glaciers regardless of whether they primarily form through glacial ice or permafrost. For that reason, classic rock glaciers will be the main subject of this thesis for discussing the implications for rock glacier behavior in response to climate on glacial chronology. Their morphology will also be the main focus since morphological definitions are more useful than genetic definitions in planetary studies since genetic studies often require visiting the feature which would be difficult at this time in the case of Martian rock-ice features.

BACKGROUND

Rock glaciers on Earth

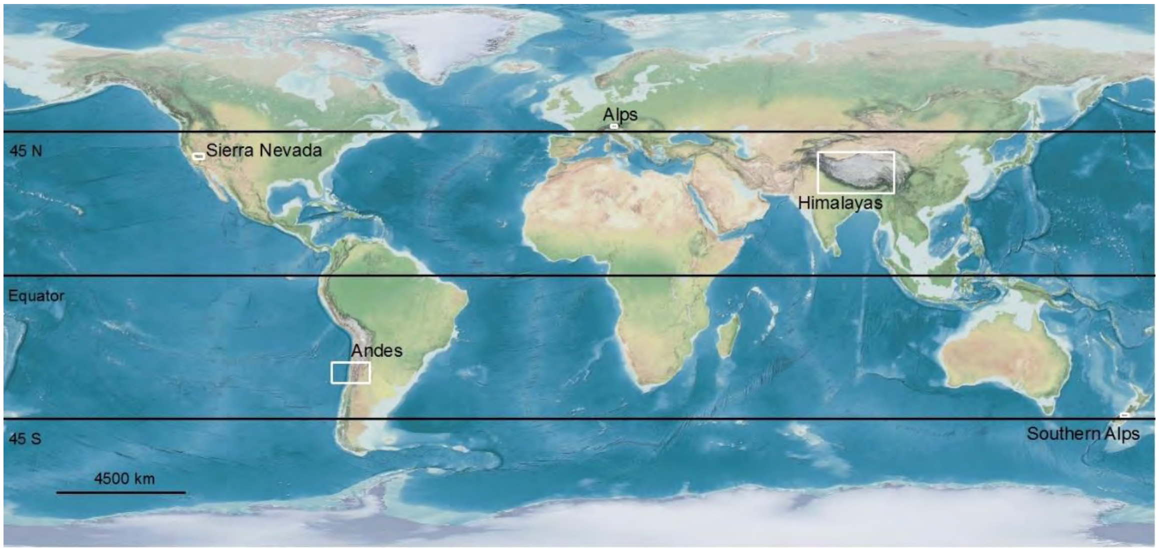

Figure 6: A map showing the major regions which were studied on Earth during this study: the Sierra Nevada, Andes, Alps, Southern Alps of New Zealand, and Himalayas. The specific parts of these mountain ranges that were discussed in project are represented by the white boxes. These white boxes also indicate the locations of regional maps shown later in the thesis.

Sierra Nevada

On Earth, rock glaciers occur in periglacial conditions usually in alpine environments (Giardino and Vitek, 1988; Whalley and Azizi, 2003) at high elevation. For my research, I focused on alpine rock glaciers in the Sierra Nevada. The most common rock-ice features in the Sierra Nevada are classic, valley floor rock glaciers with some protalus lobes and protalus ramparts (Miller and Westfall, 2008). Many Sierra Nevada rock glaciers also appear to be in disequilibrium with the climate and are located in regions where ice glaciers have retreated (Miller and Westfall, 2008). Rock glaciers in the Sierra

Nevada are not well studied. This comparative study, as a result, also provides an opportunity to shed light on the behavior of Sierra Nevada rock glaciers.

Historical context of Sierra Nevada rock glaciers

The Sierra Nevada has experienced several major glaciations in the last 800,000 years (Philips *et al*, 2009). The three latest Pleistocene glaciations are the Tahoe glaciation which occurred around 170-130 Ka (Philips *et al* 2009, Rood *et al*, 2011), the Tioga glaciation which occurred around 28,000-14,500 Ka (Philips *et al*, 2009; Rood *et al*, 2011), and Recess Peak Glaciation which ended about 13 Ka (Philips *et al*, 2009; Bowerman and Clark, 2011). Glaciation events later than the Recess Peak glaciation are controversial, however workers in the field agree that there was at least one instance of neoglaciation in the Holocene, the Matthes glaciation which ended around 200 years ago (e.g., Bowerman and Clark, 2011).

Although no moraines are found dating to periods between the Tahoe and Tioga glaciations, rock flour deposits from Owens Lake and proxy data from Devil's Hole reveal the existence of a period of glacial activity taking place within 80,000-65,000 B.P. (Rood *et al*, 2011). The dearth of moraines to corroborate these finds suggests that the later Tioga glaciation was more extensive and that these moraines were destroyed by obliterative overlap.

Also, according to Bowerman and Clark (2011), there is evidence for two instances of neoglaciation at 5400-4800 BP and at 3200-200 B.P. The later neoglaciation produced the most recent set of moraines belonging to glaciers that retreated at the end of the 19th century. The earlier one, ending around 4800 B.P., is only visible due to spikes in rock flour in nearby lake sediments. Additionally, this data also revealed minor glacial maxima at 2800 B.P., 2200 B.P., 1600 B.P., 700 B.P., and 250-170 B.P. Moraines dating to neoglacial maxima before the Matthes glaciation are not found and were likely lost due to obliterative overlap.

Rock glaciers outside the Sierra Nevada

Other mountains where rock glaciers are common include the Alps (Hippolyte *et al* 2009; Kerschner, 1978; Roer *et al*, 2008), the western Himalaya and Karakoram Mountains (Owen and England, 1998; Jakob, 1992; Shroder *et al*, 2000), the Southern Alps of New Zealand (McGregor, 1967; Brazier *et al*, 1998; Kirkbride and Brazier, 1995), and the Andes (Brenning, 2005; Azocar and Brenning, 2010; Angillieri, 2010). In the Alps, several rock glaciers are associated with the moraines of retreated glaciers (Kerschner, 1978).

Andes

The Chilean Andes are known for having relatively few glaciers, but abundant rock glaciers (Brenning, 2005; Azocar and Brenning, 2010). One likely reason for this is that the Chilean Andes are particularly arid preventing the accumulation of snow leading to ice glaciers. Thus, where there would normally be ice glaciers, there are rock glaciers and debris covered glaciers (Brenning, 2005). Rock glaciers in the Chilean Andes occur sporadically above 3000 m and more commonly above 3500 m leading to the possibility of a permafrost region above 3500 m (Brenning, 2005).

This connection between precipitation levels in the Andes and the occurrence of rock glaciers further affirms how rock glaciers can be used to infer climate conditions. On the other hand, there are possible non-climatic factors such as slope and lithology. Studies by Angillieri (2010) have suggest regions with slopes < 15 degrees and regions with Permo-Triassic non-volcanic, pyroclastic, and intrusive rock debris are most favorable to the formation rock glaciers.

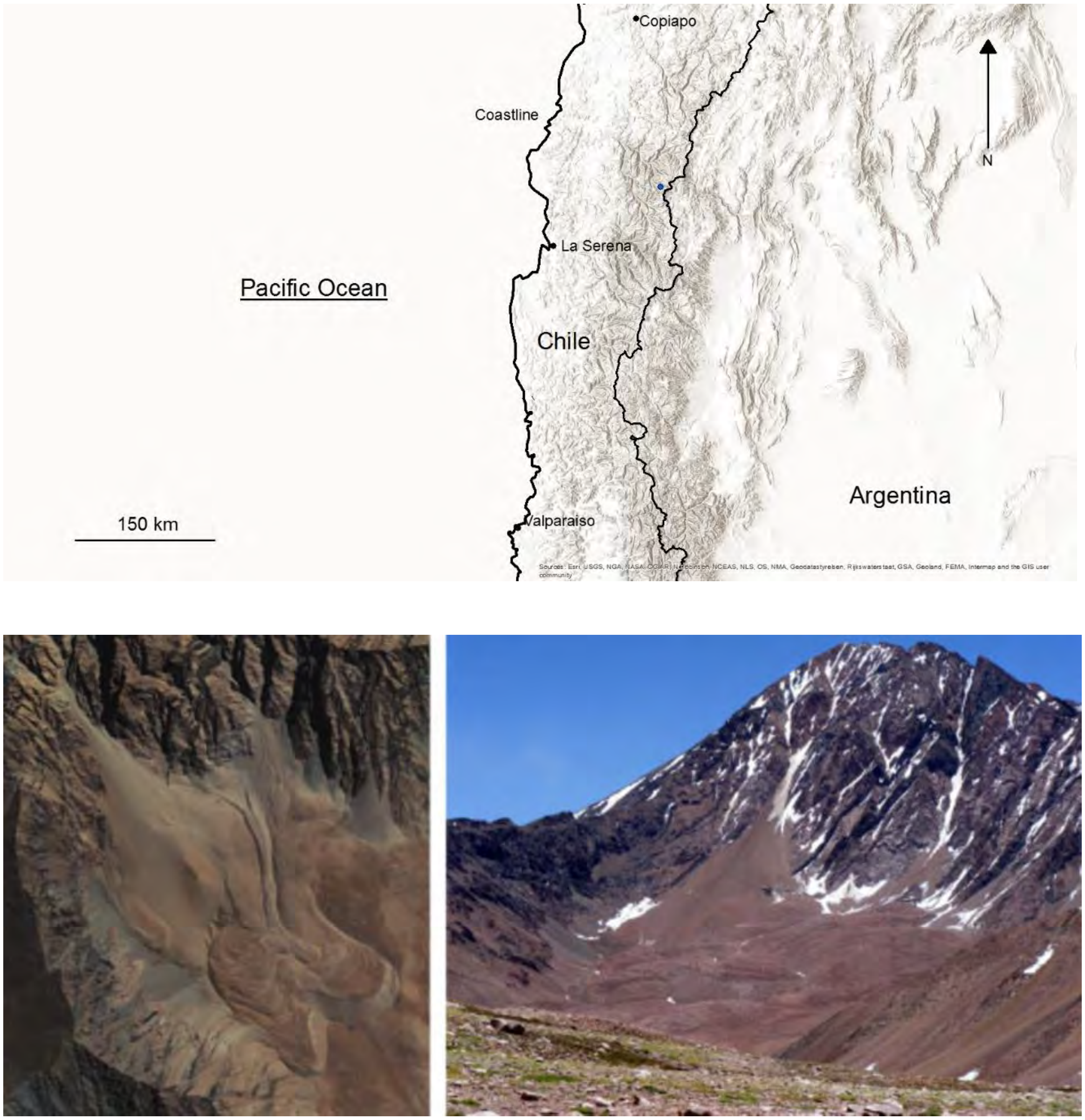

Figure 7: (Bottom) A rock glacier-like feature in in the upper Copiapo River Basin (Above) The map shows the part of central Chile most well known for having an abundance or rock glaciers. The rock glacier represented in the bottom picture is represented by blue dot on the map (adapted from Azocar and Brenning, 2010).

Alps

In Europe, it appears that the permafrost theory of rock glacier origin is favored since rock glaciers in the Alps are often assumed to be associated with permafrost (Hippolyte *et* *al*, 2009; Roer *et al*, 2008; Brazier *et al*, 1998). In certain parts of the Alps, there is a belt of extinct rock glaciers below the current belt of active rock glaciers which likely are associated with glaciation at the end of the Pleistocene (Kerschner, 1978). The terrain covered by rock glaciers in the Swiss Alps is about 5% which is only half the area covered by rock glaciers in the Chilean Andes (Miller and Westfall, 2008). One possible reason for this is that the Alps are a relatively humid mountain range with precipitation levels of 2500 mm per year on average (Brazier *et al*, 1998) while the Childean Andes are more arid with precipitation levels less than 1000 mm per year in some areas (Azocar and Brenning, 2010). As a result, the Alps receive enough precipitation to have more true glaciers.

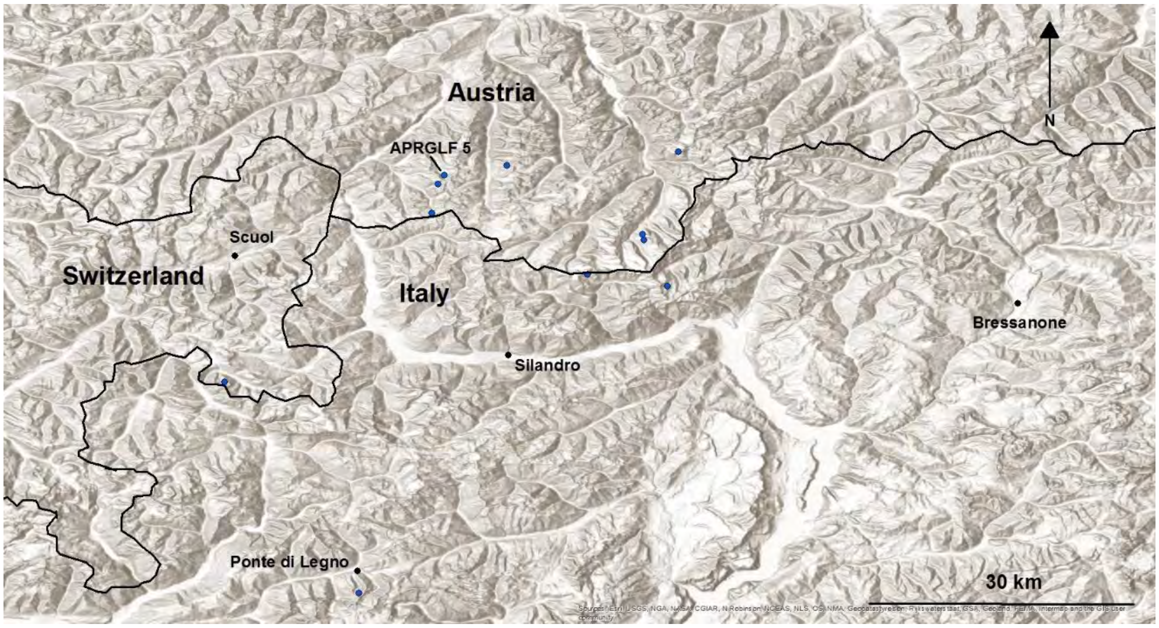

Figure 8: (Below) A rock glacier in the Austrian Alps, (Above) the map shows the locations of the rock glaciers recorded in the Alps. The rock glacier-like features are represented with blue dots. Most of the rock glaciers identified in this study were found in the Austrian Alps nearby the eastern Swiss Alps and the northern Italian Alps.

Himalaya

There have been studies linking Himalayan rock glaciers to permafrost (Jakob, 1992). Another important factor appears to be precipitation levels. Because of the immense size of the Himalaya, precipitation varies considerably across the mountain complex from west to east (Owen and England, 1998). The eastern Himalaya experience significant precipitation because of the summer monsoon of the Indian subcontinent while the western Himalaya are in a rain shadow, significantly reducing precipitation. Rock glaciers are most common at high elevations with low precipitation (Owen and England, 1998) which may explain why they are common in the more arid west (Owen and England, 1998; Shroder *et al*, 2000). This suggests a strong relation between rock glacier formation and climate in the Himalaya.

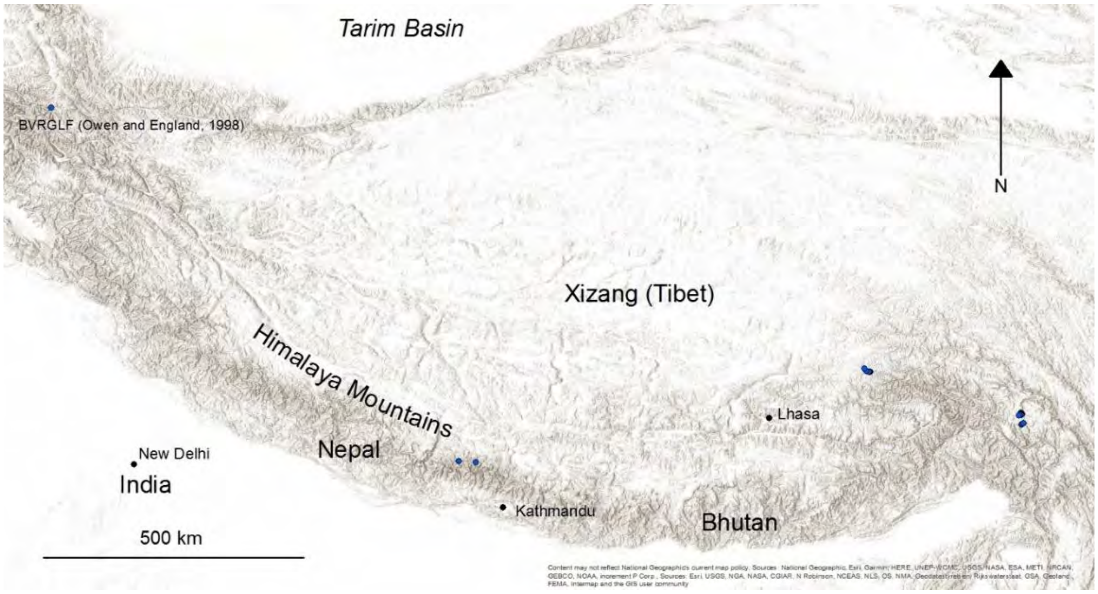

Figure 9: (Below) Rock glacier-like feature in the Bhaga valley in the western Himalaya/Karakoram Mountains (adapted from Owen and England, 1998). In the map (Above), the positions of the rock glaciers are indicated by blue dots.

Southern Alps, New Zealand

New Zealand rock glaciers are found in abundance in the Ben Ohau range of the Southern Alps on the South Island which experienced significant glaciation during the Pleistocene and earlier Holocene (McGregor, 1967, Brazier *et al*, 1998; Kirkbride and Brazier, 1995). Like in the Himalaya, the rock glaciers of the Ben Ohau range are associated with aridity. The rain shadow created by the Main Divide in the Southern Alps results in more glaciers forming closer to the Main divide where there is more precipitation. From west to east, glaciers grade into debris covered glaciers and then into rock glaciers because of the Main Divide (McGregor, 1967; Brazier *et al*, 1998).

In addition to precipitation, the rock glaciers in New Zealand appear to be influenced by factors not related to climate. Rock glaciers tend to form more often in incised canyons with large shadows and where there is abundant rockfall (Brazier *et al*, 1998). According to Brazier *et al*, both of these factors are driven by tectonic uplift of the southern Alps rather than climate and thus will not correlate with climate.

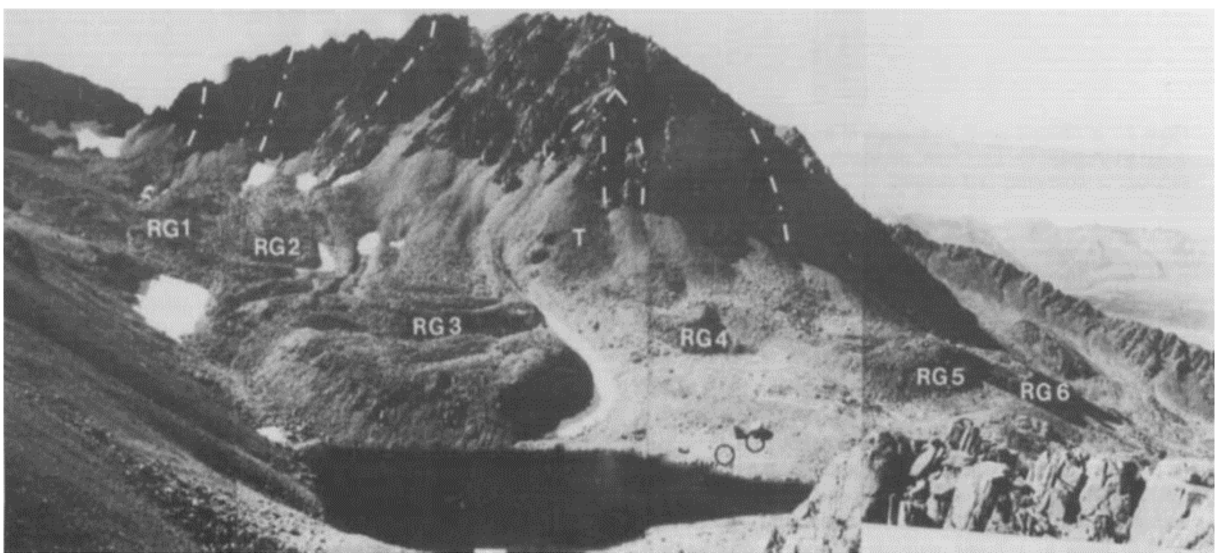

Figure 10: (Below) A series of rock glacier-like features observed by Kirkbride and Brazier (1995) in the Southern Alps near Lake Pukaki. The location the features within the Southern Alps is represented on the regional map by a blue dot (above).

Summary of Earth rock glaciers

On Earth, rock glaciers tend to occur in high elevation alpine physical environments with periglacial climatic conditions. As is seen in the Sierra Nevada, Alps, Himalaya, Southern

Alps, and Andes mountain ranges, rock glaciers tend to occur where temperatures are below freezing but precipitation is insufficient to produce ice glaciers. They also tend to be affected by non-climatic factors such as slope, lithology, and aspect. Rock glaciers have also been used as indicators of permafrost a well as indicators of past glacial conditions. These examples all show the relevance for rock glaciers in studying past climate since it can be used to infer both glacial environments and precipitation rates. Most rock glaciers on Earth are found in high elevation mountain environments like the Sierra Nevada. Other mountain ranges show the same patterns and correlations with respect to rock glaciers as the Sierra Nevada. Because of the similarity between alpine periglacial environments across the globe and the relative accessibility of the Sierra Nevada rock glacier record compared to other sources, the Sierra Nevada rock glacier record can be used as a representative sample for Earth which is how it will be used in this thesis.

Rock glaciers on Mars

For several decades, glacial features have been detected on Mars (Colaprete and Jakosky, 1998; Arfstrom and Hartmann, 2005). The primary regions around which glacial features were identified include Argyre Basin (Pierce and Crown, 2003) and Hellas Basin (Pierce and Crown, 2003; Head and Neukum *et al*, 2005). These regions are in the southern hemisphere at about 45 degrees, mid latitude (Figure 11). Possible glacial or rock-ice flow features have been identified at mid latitudes in the northern hemisphere in what is called the fretted terrain (Head *et al*, 2010) which includes the Deuteronilus and Protonilus regions (Figure 11). Most of the rock-ice features were found at mid-latitudes in the southern and northern hemispheres (Figure 11), though glacial features have also been observed in equatorial areas such as Olympus Mons (Head and Neukum *et al*, 2005) and Valles Marineris (Mege and Bourgois, 2011; Figure 11).

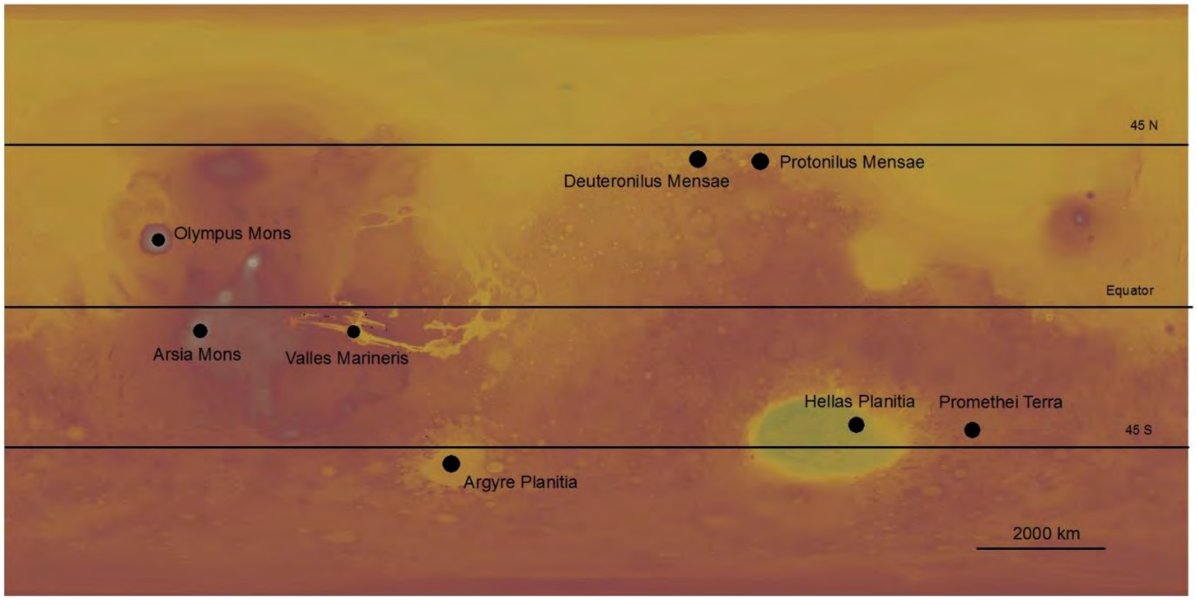

Figure 11: Map showing the location of each region studied. The equator and mid-latitude lines of 45 degrees north and south are also shown for reference. The darker area represents the cratered highlands in the south. The lighter north represents low lying plains that dominate the northern hemisphere.

The glacial features on Mars have been variously called as lobate debris aprons (Head and Neukum, 2005; Pierce and Crown, 2003; Head *et al,* 2010), viscous flow features (Hubbard *et al*, 2011), and lineated valley fill (Pierce and Crown, 2003; Head *et al*, 2010). Debris aprons exhibit well defined flow fronts (Figure 13), have a convex upward surface, and form adjacent to massif slopes (Head *et al*, 2010; Figure 13). Lineated valley fill represents deposits which fill the valley floors between massifs and appear to have flowlines (Head *et al*, 2010; Figure 14). Some have argued that lineated valley fill forms from the merging of these aprons (Pierce and Crown, 2003).

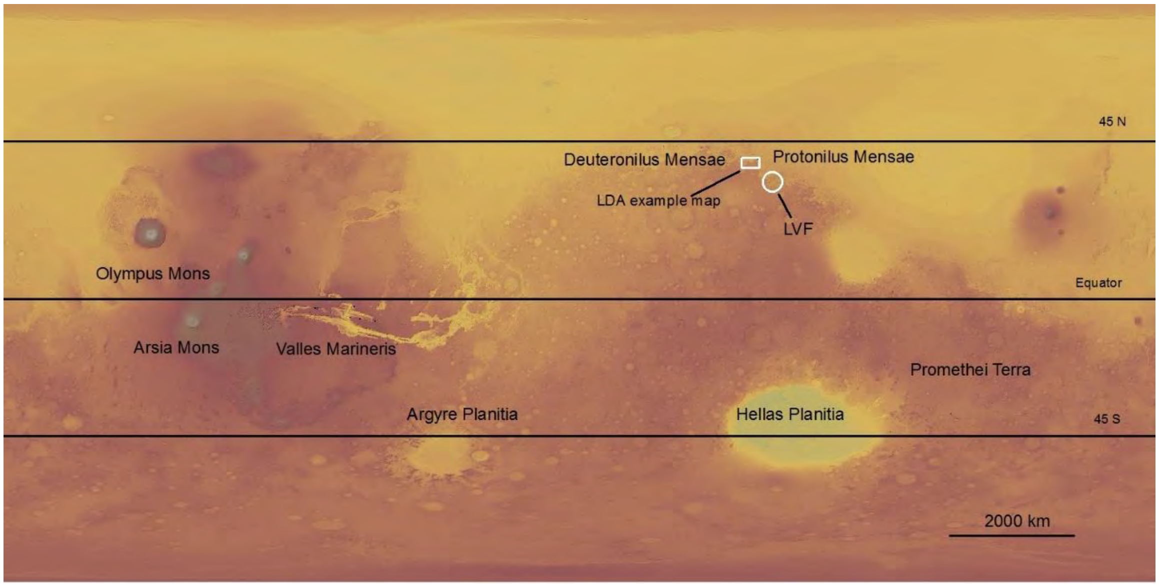

Figure 12: In this global map of Mars, the white box is the location of the map below showing the global location of the massif with the lobate debris aprons (LDA example map) in figure 13 and the lineated valley fill (LVF) in figure 14. The circle is the region in which the example of lineated Valley Fill is most likely located.

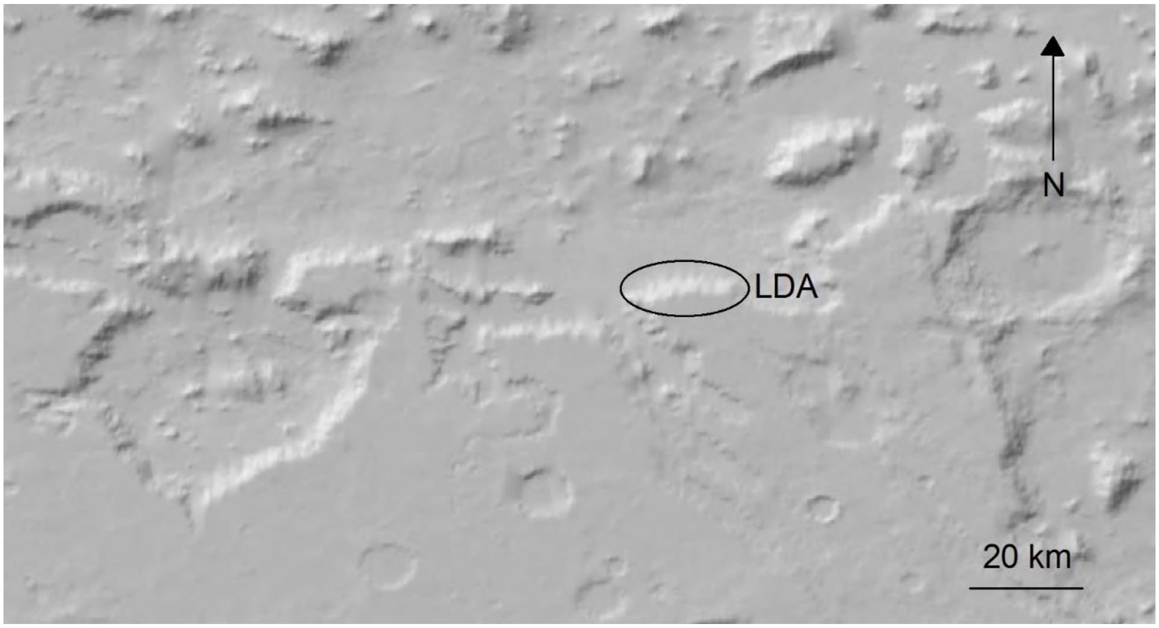

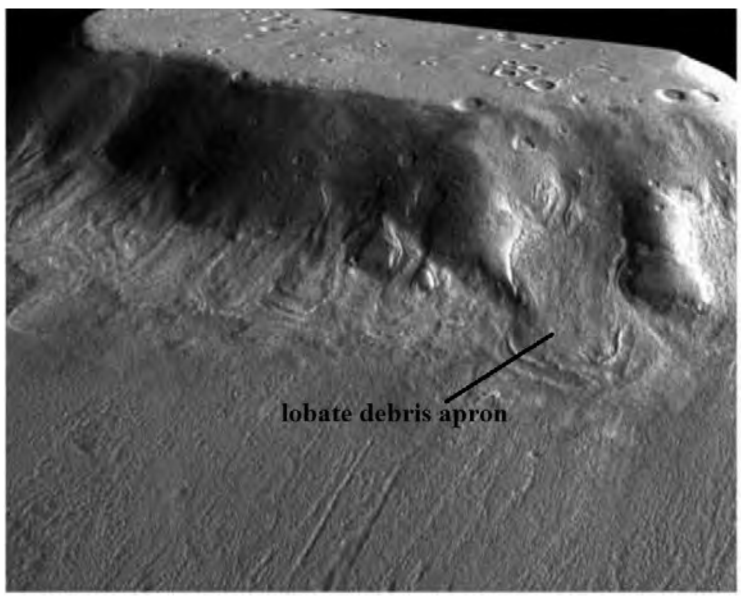

Figure 13: This figure (below) shows lobate debris aprons extending from the cliffs of a massif in the northern hemisphere. The maps above show where it is located within the larger region and where it is on Mars. The lobate debris apron is distinctive because of its lobate shape. It is located southeast of the Protonilus Mensae region (adapted from Head *et al*, 2010).

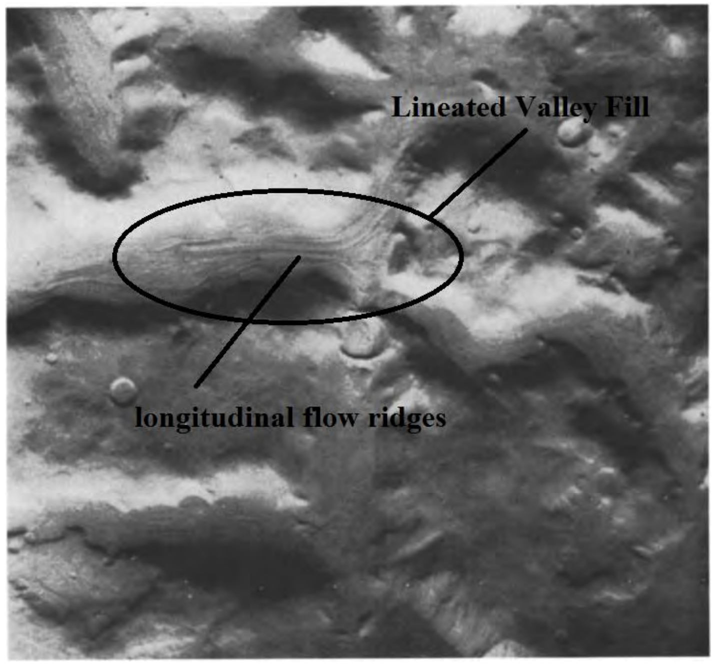

Figure 14: At the center of the image is a valley in which the longitudinal ridges demarcating lineated valley fill (LVF) can be identified (adapted from Colaprete and Jakoski, 1998).

In some areas, these features appear to have undergone significant degradation possibly from sublimation of subsurface ice leaving behind ablation lag and sublimation pits (Head and Neukum, 2005). In other cases, the ice appears to have been covered, or mantled, by a layer of dust leaving smooth areas (Arfstrom and Hartmann, 2005). Although most authors agree that debris aprons, lineated valley fill, smooth mantled terrain, and the moraine-like features are rock-ice forms, their identity is uncertain. Most researchers have suggested that they are rock glaciers (Whalley and Azizi, 2003; Arfstrom and Hartmann, 2005), debris covered glaciers (Pierce and Crown, 2003), or moraines (Arfstrom and Hartmann, 2005). Additionally, some of these features could represent solifluction lobes, which have also been identified on Mars (Johnsson *et al*, 2011).

Detection of subsurface ice on Mars using ground penetrating radar

In some cases, the presence of ice has been confirmed with ground penetrating radar, (SHARAD instrument) on the Mars Reconnaissance Orbiter (Figure 15). Places where subsurface radar has confirmed the existence of ice include and the eastern rim of the Hellas Basin (Holt *et al*, 2008). In the study by Holt *et al*, SHARAD was used on LDAs in the Hellas Basin region to determine the presence of ice within landforms suspected to be rock-ice features. Several LDAs were confirmed in the study to have ice so that the hypothesis that LDAs and other structures are rock-ice features is no longer theoretical in some cases but has been confirmed by evidence (Holt *et al*, 2008; Figure 16). Additionally, neutron and gamma-ray spectrometers on the Mars Odyssey spacecraft have also independently confirmed the existence of subsurface ice on Mars, albeit independent of the structures thought to be rock-ice flow features (Seu *et al*, 2007). Nonetheless, that study further corroborates the reality of subsurface ice on Mars.

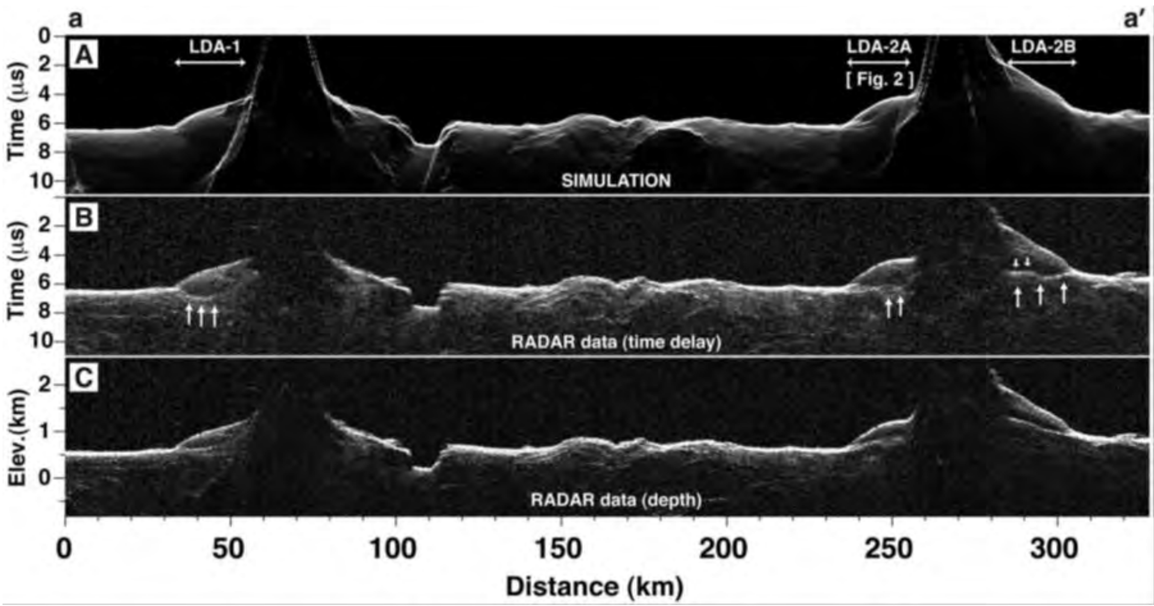

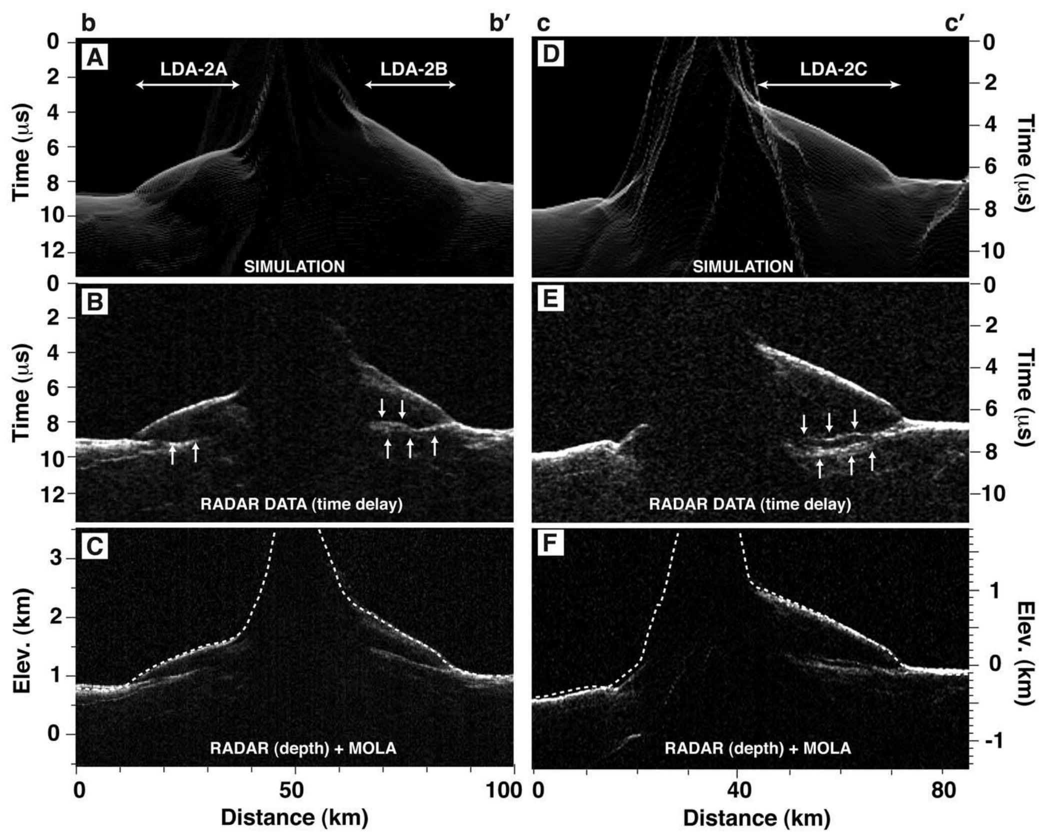

Figure 15: These radargrams represent profiles of lobate debris aprons in the eastern rim of Hellas Basin. The arrows represent areas where the radar reflection does not match what would be expected if the debris aprons were entirely rock debris, suggesting the presence of ice. The above image shows a large-scale view of the area studied and the bottom view shows smaller scale more detailed images of each debris apron (adapted from Holt *et al*, 2008).

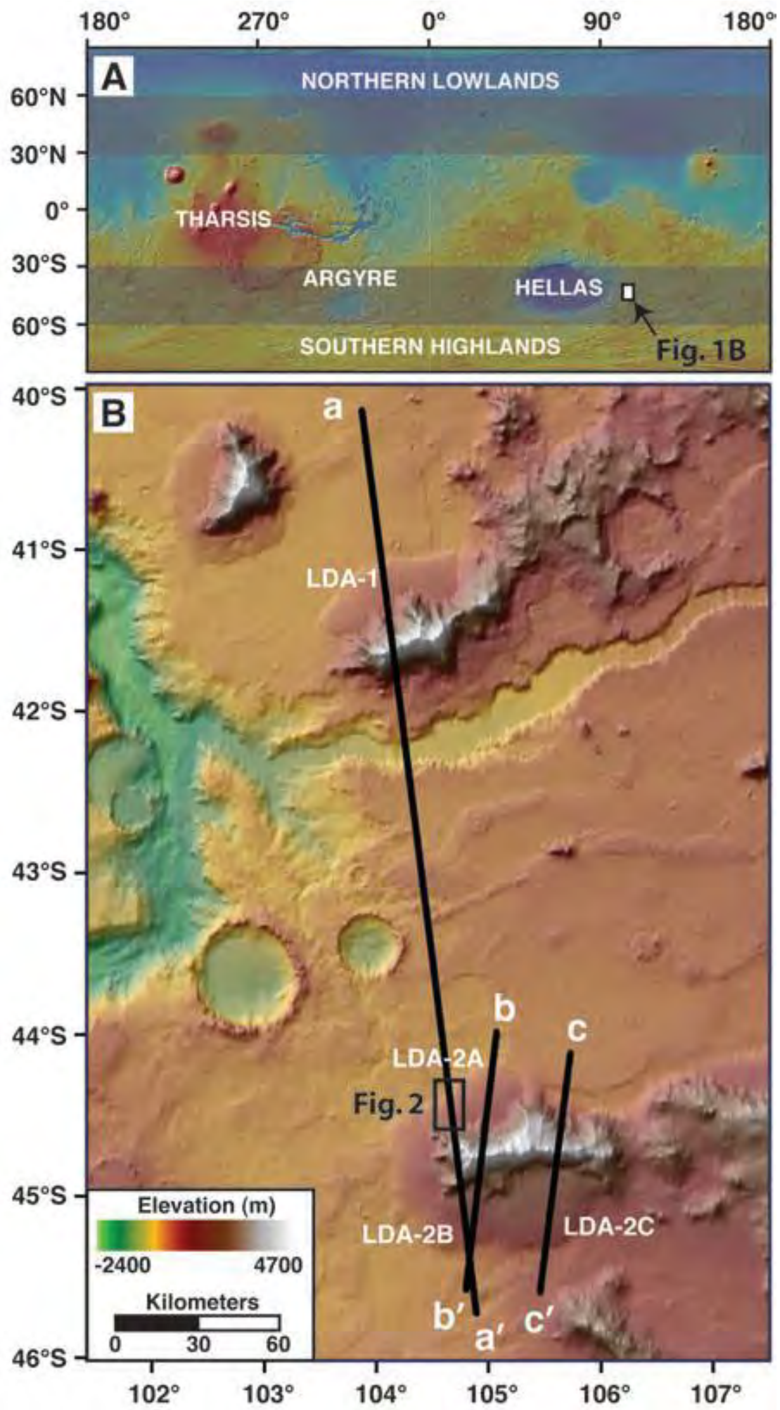

Figure 16: The figure shows the locations of the lobate debris aprons that are studied in cross section. These lobate debris aprons are located on the eastern rim of Hellas basin. LDA 2A-2C were the debris aprons where subsurface ice was detected. The lines show the extent of the cross sections in the figure (adapted from Holt *et al*, 2008).

It is generally agreed that these are related to the movement of ice, but their exact identity and how they fit into the Martian cryosphere is up to debate in many cases. Understanding how rock ice features can be used to interpret past Martian climate requires an understanding of the geological and climatological context of these glacial features which necessitates a review of the geological and climatological history of Mars.

Historical context of Martian rock glaciers

Today, the surface of Mars is covered by a global hyper-arid desert and Mars' atmosphere is too thin to support liquid water for all but very brief and rare periods (Carter *et al*, 2015). There is evidence, however, that in the past Mars was periodically warmer, had a thicker atmosphere and may have supported water ice and limited amounts of liquid water on its surface. (Head and Marchant, 2014; Carter *et al*, 2015; Grotzinger *et al*, 2014; Le Deit *et al*, 2012).

Martian geologic history is divided into four major chronological units, the pre-Noachian, the Noachian epoch, the Hesperian epoch, and the Amazonian epoch (Figure 17). In pre-Noachian times (c. 4.5-4.1 G.a.), Mars was still in the process of formation.

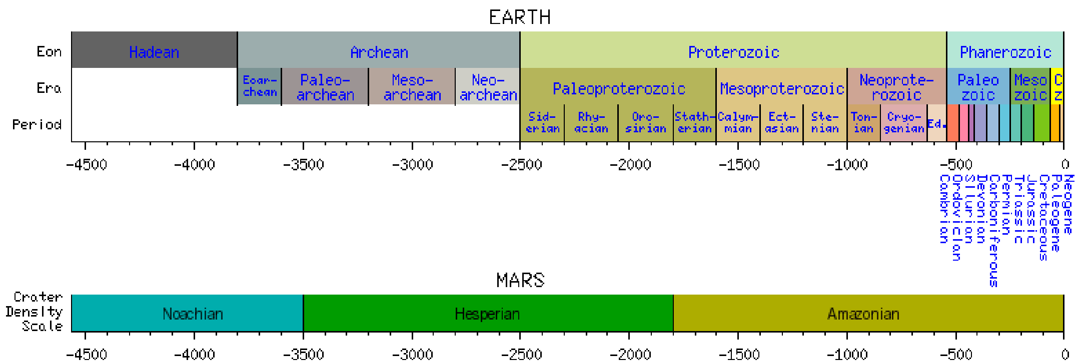

Figure 17: Martian geologic timescale paired with Earth's geologic timescale for reference. The Noachian and Hesperian epochs, corresponding to Earth's Hadean, Archaean, and early Proterozoic eons, were marked by numerous impacts and volcanism. Most rock glacier-like features on Mars probably date to the late Amazonian epoch, corresponding to roughly Earth's Phanerozoic eon (adapted from Gangale, 2010).

Mars experienced a period of intensive impacts from collisions with protoplanetary bodies which is reflected in the heavily cratered highlands in the southern hemisphere. The Noachian Epoch (4.1-3.7 G.a.) is marked by extensive volcanism, particularly in the Tharsis region (Carr and Head, 2010; Wilson and Mustard, 2013), and the formation of lakes and valley networks, suggesting the presence of liquid water. On the other hand, evidence is mounting that Mars was too cold to have oceans and probably had large ice sheets and ice caps which would melt during volcanic eruptions and impacts creating meltwater lakes and river valleys (Head and Marchant, 2014; Carr and Head, 2010; Wadsworth *et al*, 2013). Nonetheless, an abundance of phyllosilicates and other minerals associated with aqueous environments have been identified in Noachian deposits in locations such as Valles Marineris and Gale Crater (Le Deit *et al*, 2012; Roach *et al*, 2010; Grotzinger *et al*, 2014) which suggests that liquid water was at one point widespread on the surface of Mars even if just intermittently and for short periods of time. Geomorphological and sedimentological evidence for lake deposits from observations at Gale Crater (Figure 18) by the Mars Science Laboratory also confirm that liquid water was more widespread during the Noachian (Grotzinger *et al*, 2014).

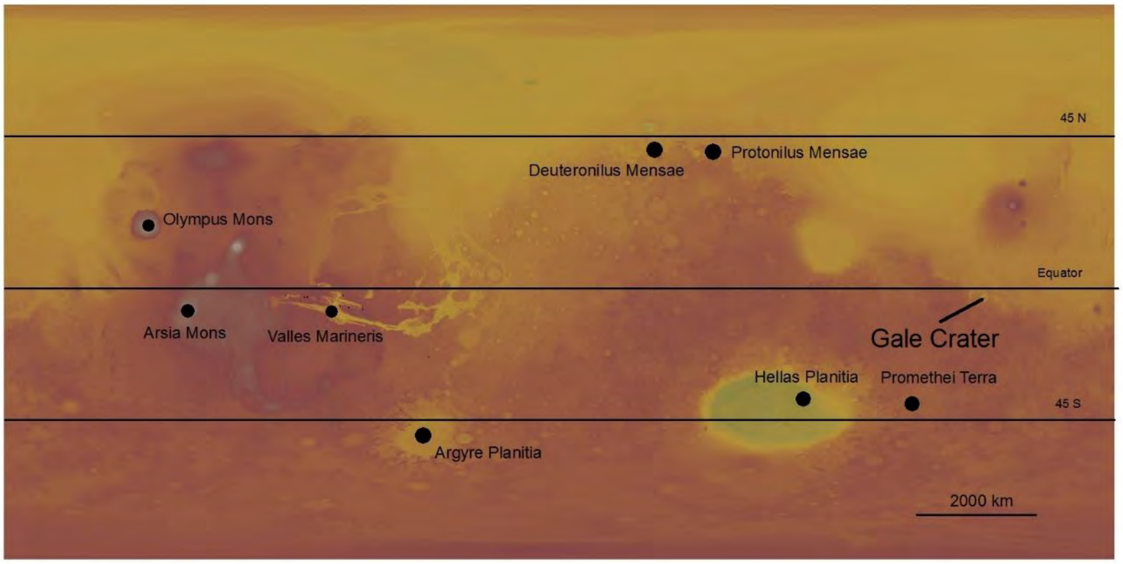

Figure 18: (Above) a global map of Mars showing the location of Gale Crater, the location of a Noachian aged Martian lake deposit.

The Noachian is followed by the Hesperian (3.7-3.0 G.a.) which is characterized hydrologically by the formation of large outflow channels likely related to melting ice (Carr and Head, 2010). Volcanism during the Hesperian was characterized by the formation of extensive ridged plains such as Hesperia Planum (Wilson and Mustard, 2013). It is likely that the younger Amazonian plains in the northern hemisphere are underlain by Hesperian volcanic materials (Carr and Head, 2010). The plains at higher latitudes north and south contain more phyllosilicates and evidence of chemical weathering (Wadsword *et al*, 2013; Carter *et al*, 2015). Weathering could reflect a larger presence of water for limited periods of time. Chemical weathering was present but appears to have significantly decreased (Carr and Head, 2010).

The Amazonian epoch represents the last 3 billion years of the history of Mars. The Amazonian epoch has been marked by sporadic volcanism, lack of significant weathering, and significant ice related processes (Carr and Head, 2010). Although glacial processes were likely active prior to the Amazonian, the most evidence for glacial processes dates to the Amazonian. Most of the moraine-like features, lobate debris aprons, lineated valley fill likely came into existence during the late Amazonian because of their sharpness and lack of erosion and weathering. The polar ice caps of Mars also came into their present form during the late Amazonian (Carr and Head, 2010; Head *et al*, 2010).

The changing obliquity of Mars

There is evidence that the obliquity of Mars has varied significantly over the course of Martian history (Head and Neukum, 2005; Head *et al*, 2010). Obliquity is the angle at which a planet is tilted towards the sun. Obliquity affects the angle of insolation at a planet's surface (Figure 19). The angle of insolation is the angle at which solar radiation hits the surface of a planetary body. A steeper angle of insolation means more direct sunlight, which results in warmer climates and more melting or sublimation of ice. During periods of high obliquity, a planet may be significantly tilted towards the sun resulting in high angle of insolation at the poles (Figure 19). During periods of low obliquity, the angle of insolation is higher at the lower latitudes.

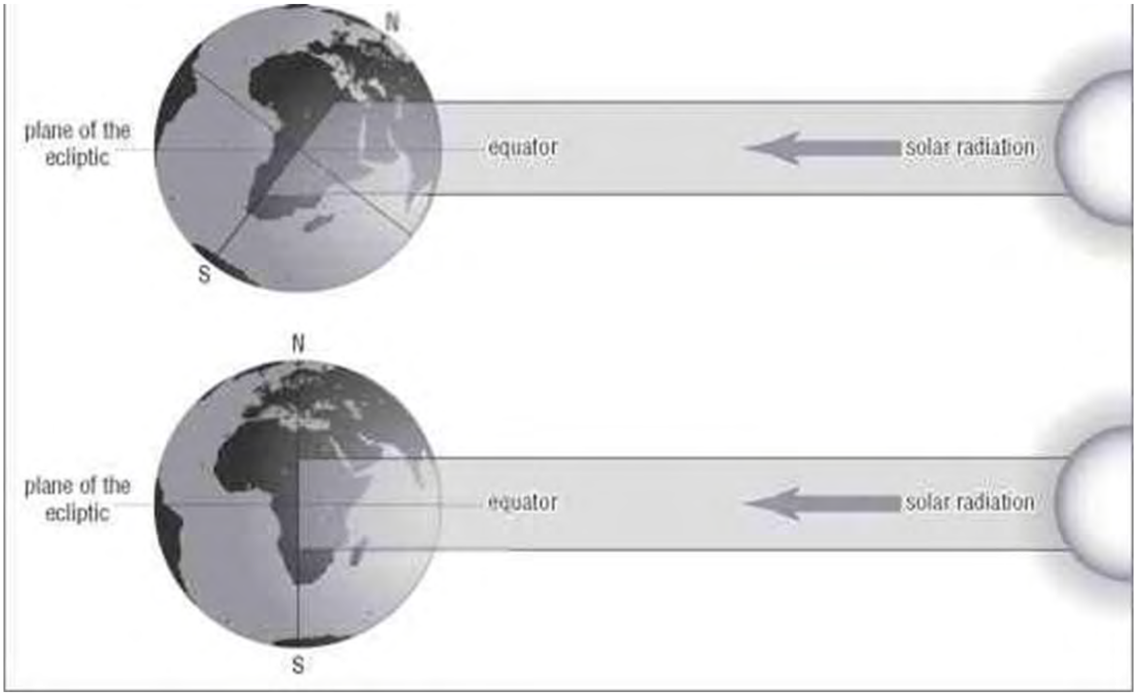

Figure 19: A simple illustration of obliquity, the above situation shows a planet during high obliquity when the angle of insolation is higher and mid latitudes than at the equator because the planet is tilted towards the sun. The situation at the bottom of the figure shows an example where obliquity is close to zero and the angle of insolation is higher at the equator, which will result in a warmer climate at the equator (image credit: www.briangwilliams.us)

All the glacial features are at the mid-latitudes (Pierce and Crown, 2003; Head *et al*, 2010) or in the equatorial regions (Head and Neukum, 2005; Mege and Bourgois, 2011). The current theory for the shift in the belt of rock-ice features is that over the course of Mars' history, the obliquity has changed (Figure 20). At times it has been highly oblique so that the ice at the poles migrates to a belt of ice near the equator (Head and Neukum, 2005; Figure 20). Multiple times over the course of Mars' history, the ice has migrated from the poles to lower latitudes and back as the obliquity has changed (Carr and Head, 2010). Evidence to support this hypothesis is that glacial features tend to form on the pole facing sides of adjacent slopes (Arfstrom and Hartmann, 2005). This would be expected if water ice were to sublimate at the poles and then travel equatorward until being deposited on the nearest pole-facing slope. Over the course of the Amazonian, the obliquity of the planet Mars has been as high as 45 degrees (Head *et al*, 2010), meaning that there would have been times where the poles were receiving more direct sunlight (higher angle of insolation) than lower latitudes and equatorial regions, thus explaining glacial features on Olympus Mons and within Valles Marineris that have been noted by various authors (Head *et al*, 2010; Mege and Bourgois, 2011; Head and Neukum, 2005).

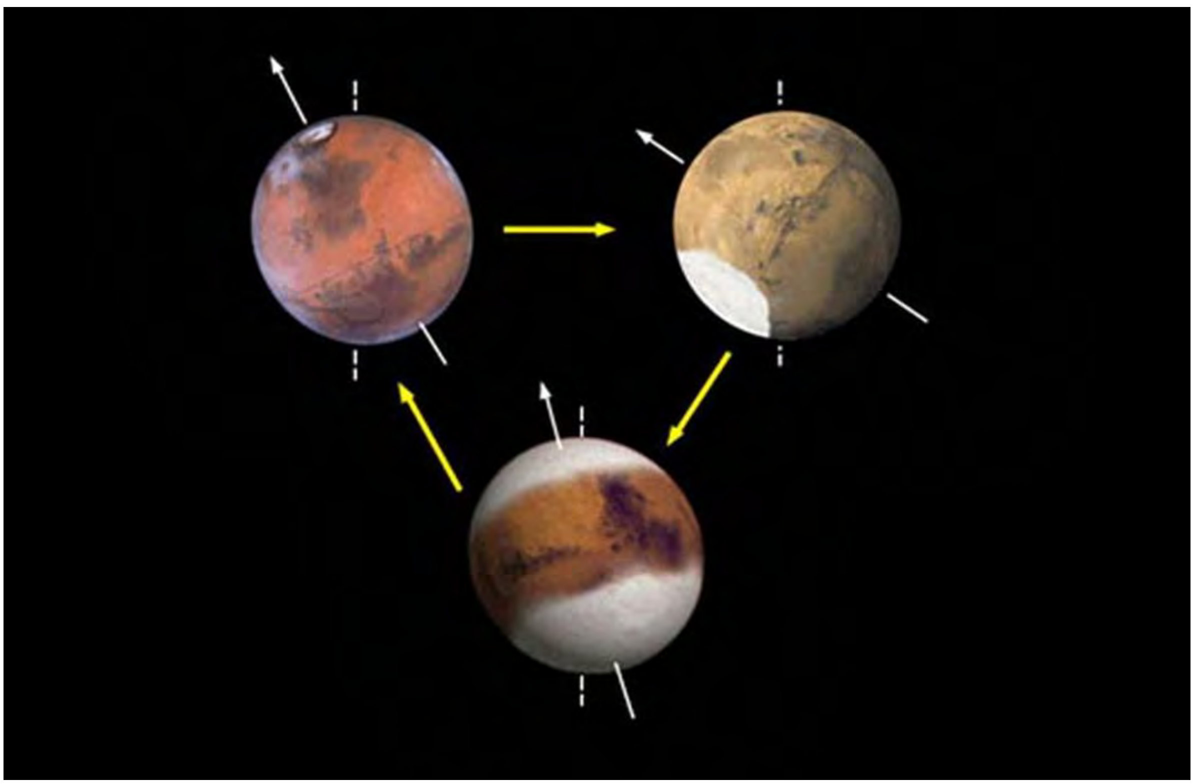

Figure 20: The figure above illustrates how variations in obliquity may affect ice distribution at Mars. During periods of high obliquity, when the rotational axis of Mars is tilted significantly towards the sun, the angle of insolation will be high at the poles resulting in ice becoming destabilized and moving to lower latitudes (Image credit: NASA/JPL).

The picture of early Mars that is emerging is one of a mostly cold and dry climate, not very different from today, punctuated by periods of intensive volcanism and periods following major impacts (Figure 7) during which the surface atmospheric temperature temporarily rose above the freezing point of water, briefly allowing for the existence of open bodies of liquid water on its surface. During these short periods of time, large volumes of water trapped in ice caps may have melted, allowing for the existence of lakes, rivers, or even small seas (Figure 21) in locations such as Gale Crater. As volcanism became less frequent and less intense and the atmosphere became too thin to sustain liquid water, these melting events would have become less frequent and would have eventually stopped (Figure 21). Glacial processes would become the predominant hydrological feature of the planet. For now, researchers have just a broad outline, but a better understanding of the glacial processes that shaped this history may help to further illuminate the history of Mars.

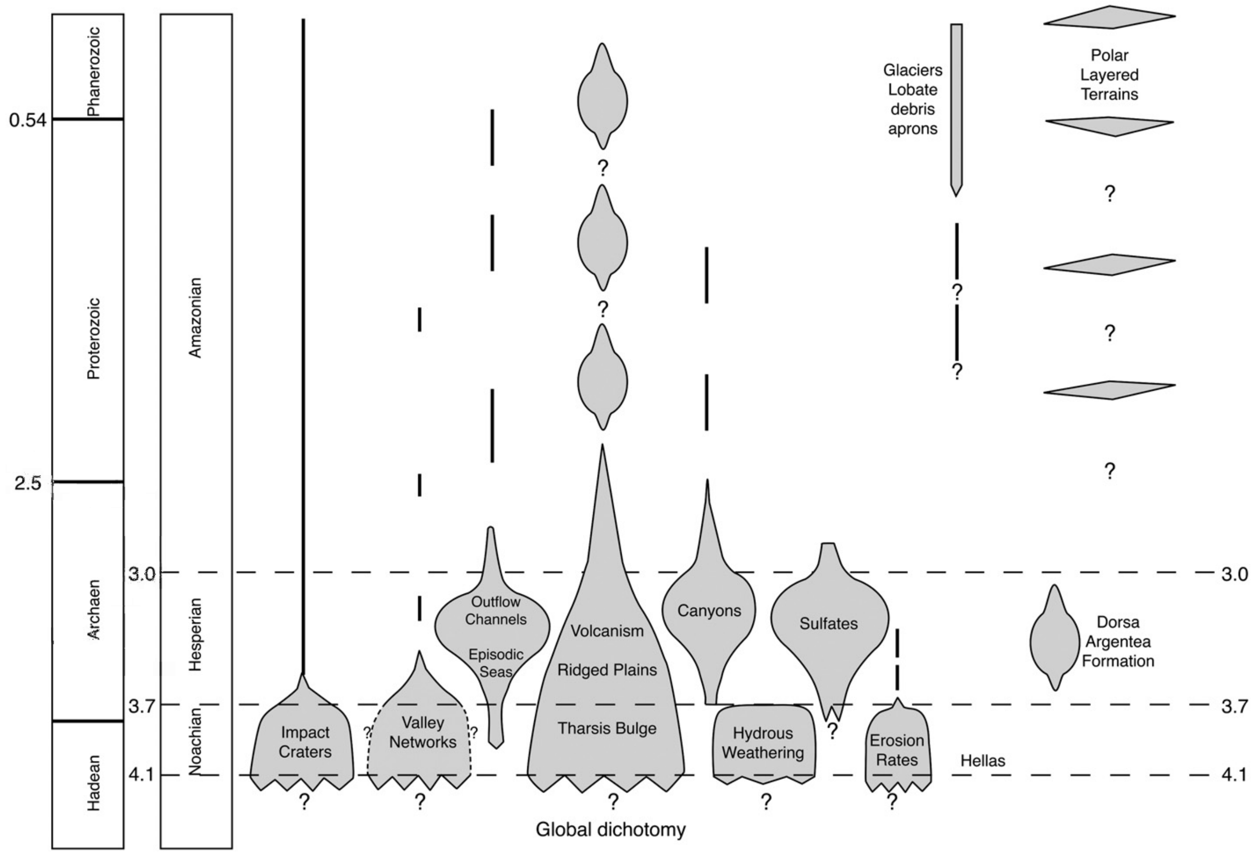

Figure 21: The processes active and predominant in each epoch on Mars are shown. As can be seen, more surface processes driven by water, volcanism, and impacts, appear to taper off towards the Amazonian. An Earth timescale is added for comparison (adapted from Carr and Head, 2010)

METHODS

For my research, I relied primarily on the National Elevation Dataset (NED) and Mars Orbiter Laser Altimeter (MOLA) for altimetry data. With ArcGIS, I used MOLA data to generate slope, hillshade, and aspect maps for Mars and then used polygons to mark off specific features for measurement. I used high resolution Google Earth images to identify potential rock glaciers and then used spatial and statistical analysis tools in ArcGIS to quantitatively analyze the data to determine average valley wall slope, flow feature slope, flow feature length, and aspect within each polygon. I used both graphical and statistical methods to test for correlation, plotting the data and then running a linear regression.

Additionally, I made elevation profiles for each of the rock glacier-like features. For the Sierra Nevada rock glaciers, I used Google Earth to generate the profiles. For Mars, I created the elevation profiles from slope maps using a MOLA-derived DEM (Digital Elevation Model) produced by the USGS astrogeology science center in Flagstaff, Arizona.

In addition to use of remote sensing, I also made one trip in mid-September 2017 to the Sierra Nevada to examine rock glaciers in the field with my advisor, Nicholas Van Buer. On September 16-18, 2017, my advisor and I hiked up to a rock glacier nearby Lake Tinemaha above Big Pine, California. Lake Tinemaha is a lake at an elevation of about 3500 meters (Figure 8). The lake is adjacent to several active rock glaciers. While at Lake Tinemaha, my advisor and I took photographs of the larger rock glacier closest to the lake. The rock glacier is just at the shore of the lake (Figure 22), which suggests that it might be the source of most of the meltwater that makes up the lake. Beneath the elevation of the lake were also several extinct rock glaciers. The difference between the active rock glaciers at higher elevation and the extinct rock glaciers at lower elevation was apparent in the degree of vegetation and visibility of fine-grained material. Active rock glaciers had little or no vegetation on their slopes, and sections of the terminal slopes of the active rock glaciers clearly contained significant amounts of fine-grained material, namely sand and silt (Figure 22, Figure 23). The surficial zones of fine grained material in the slopes of the extinct rock glaciers, on the other hand, were either obscured by extensive vegetation or had been long since removed by erosion from wind and water leaving only boulders and cobbles. The extinct rock glaciers were also a lot more stable than the active rock glaciers. Van Buer and I hiked up the slopes of the extinct rock glaciers to get to Lake Tinemaha but the active rock glaciers were too dangerous to scale because of the threat of triggering a rockslide.

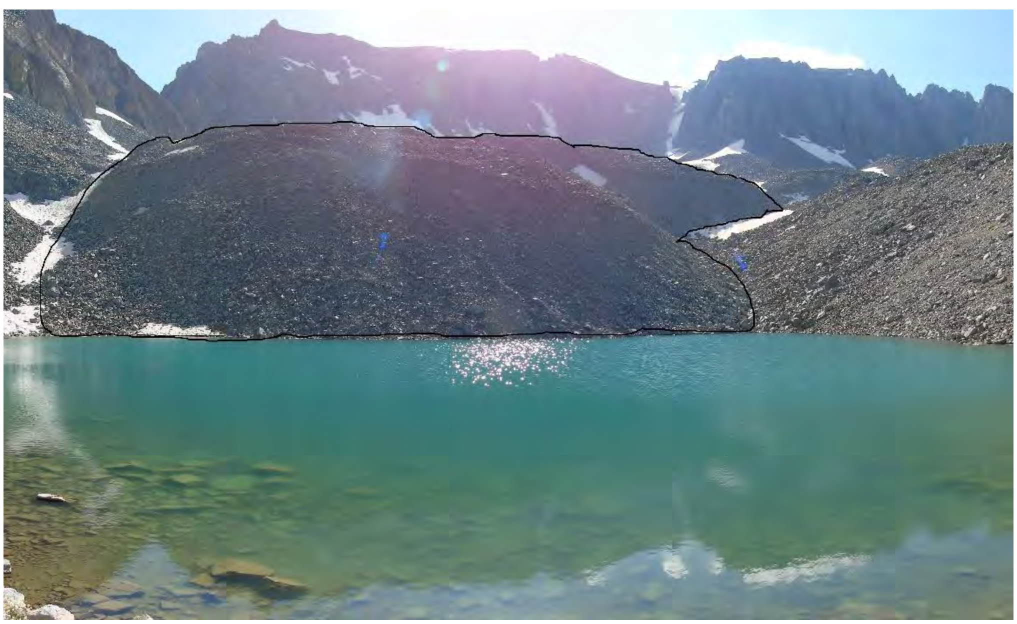

Figure 22: A rock glacier on the shores of Lake Tinemaha at 3500 m elevation. The outlined feature is the rock glacier identified as SNRGLF 85 The lack of vegetation suggests that it is active (Image credit: Nicholas Van Buer)

Figure 23: A rock glacier (SNRGLF 87) at approximately 3000 meters in the Sierra Nevada near Lake Tinemaha. The sparse vegetation cover on its slopes suggests that it is currently active (Image credit: Nicholas Van Buer)

Earth

The location on Earth where I focused my research was the high Sierra Nevada where I recorded and measured 101 rock glaciers. I also identified “valley wall” rock glaciers, protalus lobes, and protalus ramparts. For my purposes, I focused on valley floor rock glaciers which for the rest of the thesis will simply be referred to as “rock glaciers” except if they are being distinguished from protalus lobes. Other rock glacier-like features and glacial features I discuss only qualitatively.

Selection criteria

The criteria used to identify rock glaciers on Earth were based on the classic definition of a rock glacier. Flow features were identified as rock glaciers if they had over-steepened fronts, transverse ridges, and a tongue-like shape. Features which had the characteristics of rock glaciers but that were covered in vegetation were considered to be extinct and were not included in the quantitative analysis.

Quantitative analysis

For each rock glacier, I measured the height, length, steepness angle of the head wall above the rock glacier, the glacier slope steepness angle, and took note of the latitude. For the length and height, I took at least three parallel measurements using the 3D path tool on Google Earth for each rock glacier.

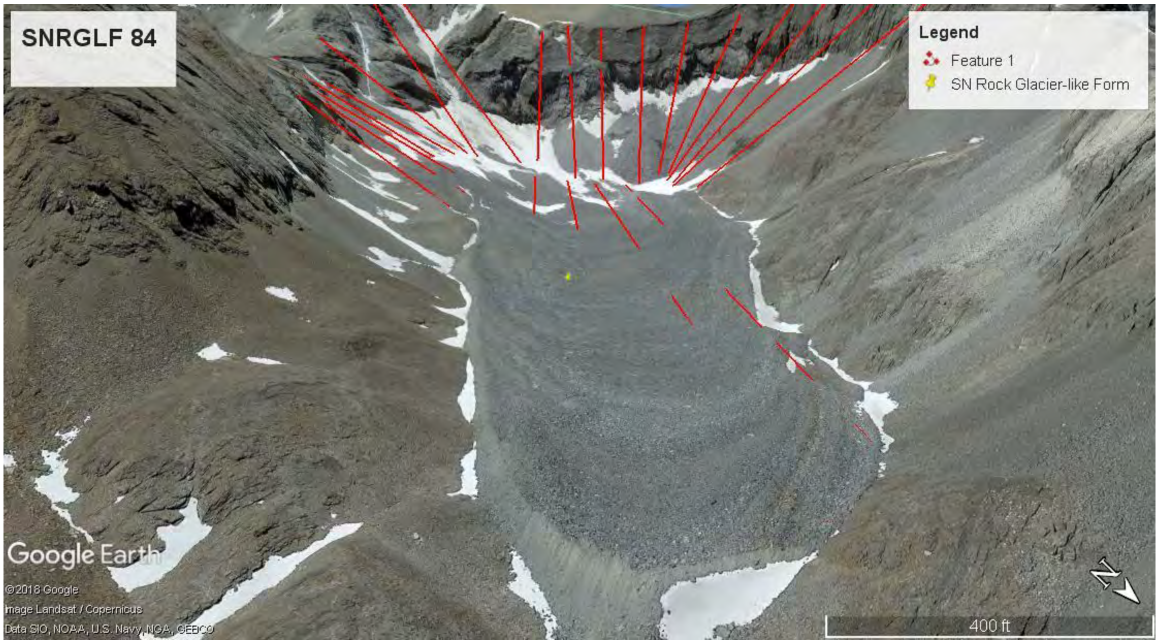

Figure 24: A rock glacier in the Sierra Nevada showing the 3D paths taken along the length of the body and headwall of the rock glacier. The 3D paths are the red lines in the images along which elevation profiles were taken. A minimum of three paths were used for each rock glacier.

I used the elevation profile of the rock glaciers to find the height and length of each path. After I found the height and length of each path, I was able to find the average height and length of each rock glacier. For head wall steepness, I took at least three or four 3D path measurements of the cirque wall of each rock glacier. I used the elevation profile of each 3D path measurement to find the average slope of the valley wall. Since the slope values were given in percentages, I converted the average slope value into a ratio by dividing by 100 and used the arctangent function to find the average head wall steepness angle in degrees for each rock glacier. I also had to convert from miles into kilometers or feet into meters in a few cases because of the settings for Google Earth.

$$\Theta = \boldsymbol{tan^{-1}}(\frac{\boldsymbol{z}}{\boldsymbol{100}})$$

Eq. 1: z is the slope steepness in percentage (%), ϴ is the slope in degrees, the percentage is divided by 100 to get a decimal to which to apply the inverse tangent to get the slope angle in degrees.

$$\boldsymbol{L} = \frac{\sum_{i=1}^{n} \boldsymbol{x}}{\boldsymbol{n}}$$

Eq. 2: The average rock glacier length (L) is equal to the average of the lengths for each 3D path measured in Google Earth. In this case, *n* = total number of paths and *x* is the length of each individual 3D path.

$$\boldsymbol{H} = \frac{\sum_{i}^{n} \boldsymbol{y}}{\boldsymbol{n}}$$

Eq 3: The average rock glacier height (H) is equal to the average of the heights given for each individual 3D path. In this case, *y* is height for each individual 3D path and *n* is the number of paths used to make the average.

To provide an extra parameter, I also used Eq. 1 to find the average slope of each rock glacier. I also recorded the maximum and minimum elevation of each rock glacier by looking at the highest and lowest point of the rock glacier which I defined as the highest and lowest point of the rock glacier covered by a 3D path which I used to measure the feature. The maximum elevation of the rock glacier represents the upper limit of the accumulation zone while the minimum elevation represents the lowest point of the ablation zone unless otherwise noted.

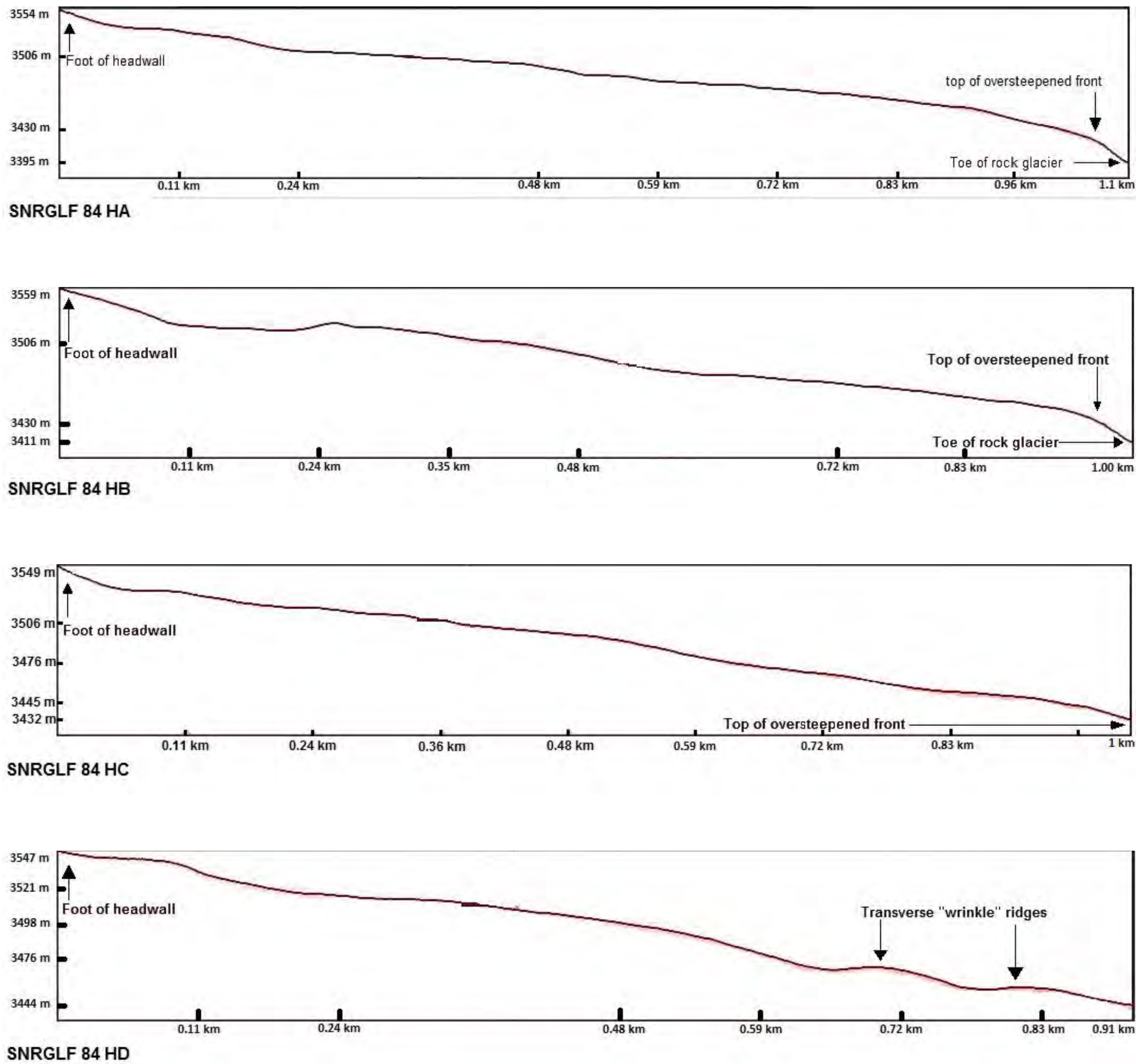

Figure 25: The above images show the four elevation profiles given for above rock glacier SNRGLF 84. Elevation is in feet while the horizontal distance is given in miles. Features such as the foot of the headwall and the top of the oversteepened front are pointed out with arrows. In HD, unusually pronounced transverse ridges are also clearly reflected in the elevation profile. The headwall varies in distinctiveness, being most pronounced in HA and HB.

Mars

A total of 50 potential Martian rock-ice features were identified in this study. I chose to identify 50 rather than 100 rock glaciers because of time constraints and because rock-ice features are less common on Mars than they are on Earth. I mainly focused on valley floor rock glacier-like forms in Valles Marineris, Promethei Terra, Argyre Basin, Deuteronilus Mensae and Protonilus Mensae, I also took note of glacier-like features in the vicinity of Arsia Mons and Olympus Mons. In addition to valley floor rock glacier-like features, I also took note of any possible protalus lobes and ramparts, debris covered glaciers, and ice-rich landslides.

Selection criteria

Rock ice features chosen for analysis were selected on the basis of two main factors: morphological factors and geographic factors.

Morphologically, features were considered potential rock glaciers if they contained at least two of the following features: transverse or "wrinkle" ridges (Giardino and Vitek, 1988; Whalley and Azizi, 2003; Kirkbride and Brazier, 1995; Shroder *et* al, 2000; Figure 26), a tongue-like shape (Figure 26, Figure 27), and an oversteepened front (Whalley and Azizi, 2003; Kirkbride and Brazier, 1995; Shroder *et al*, 2000; Figure 27). The reason that only two of the three were required instead of all three is because of the low resolution of most images.

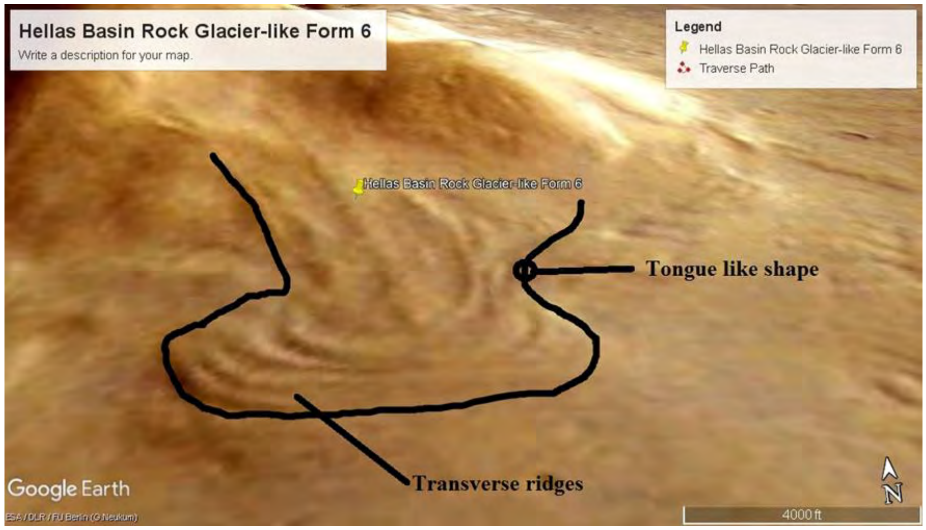

Figure 26: A lobate debris apron adjacent to a massif that shows at least two of the characteristics of a classic rock glacier: a roughly tongue-like shape and transverse ridges

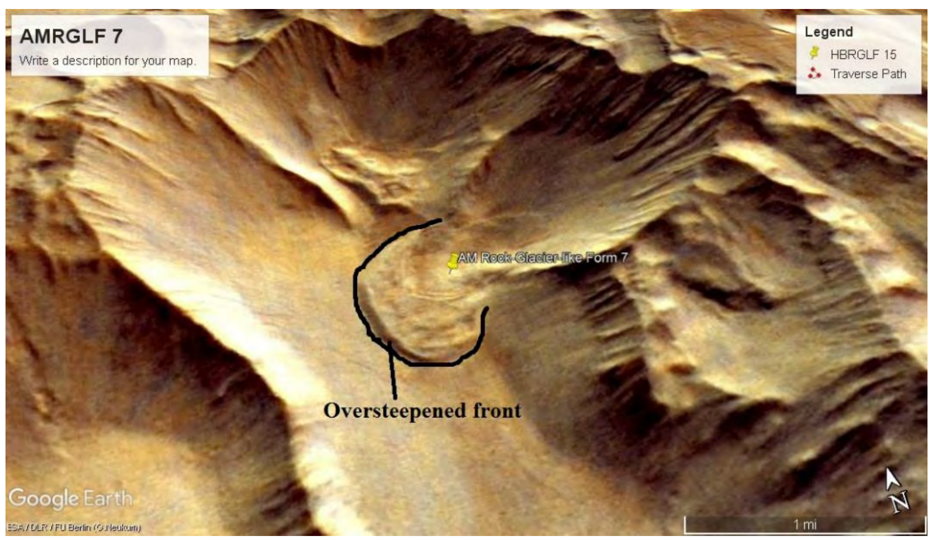

Figure 27: A lobate debris apron on the slopes of Arsia Mons with an oversteepened front (outlined) characteristic of classic rock glaciers.

If a feature appeared to meet at least two of the primary criteria, an additional morphological criterion was also considered to reduce uncertainty: length/width ratio. Features that were longer than they were wide were considered as likely candidates for rock glaciers (Figure 28).

Figure 28: Same rock-ice feature from above, the measurements indicate that the length is greater than the width. As a result, this feature fits the secondary criteria for being considered a potential rock-glacier.

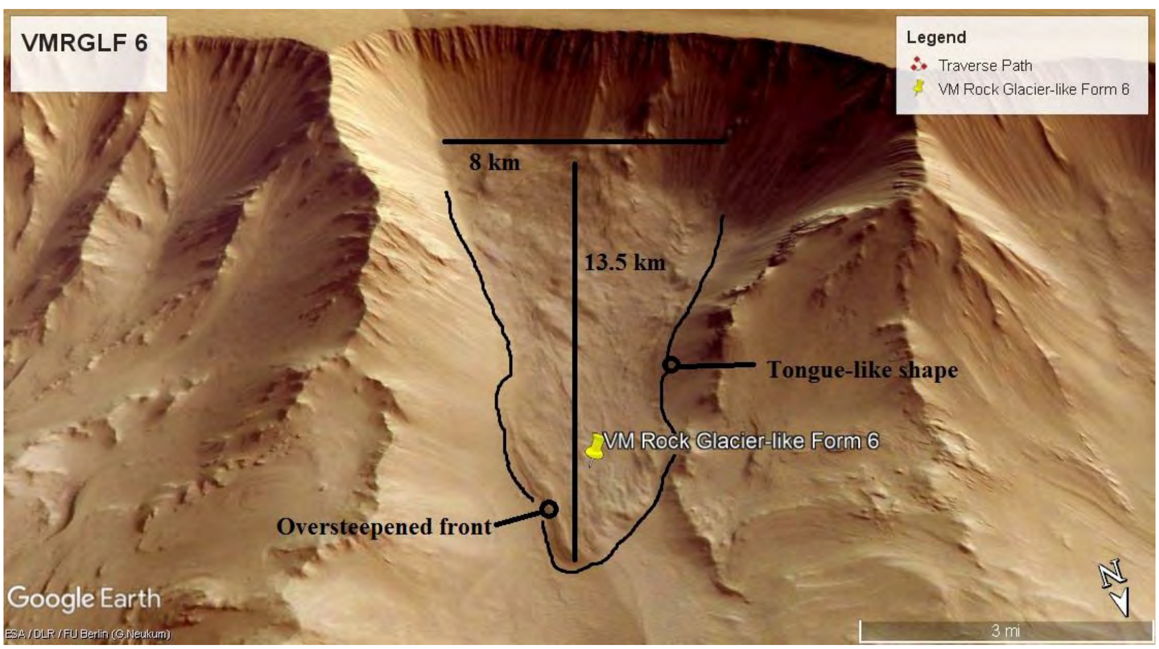

Figure 29: A debris deposit on the southern slopes of Valles Marineris, this deposit also passes the criteria for being considered a potential rock glacier since it has a length greater than its width, it has evidence of an oversteepened front, and a tongue-like shape which are characteristic of rock glaciers on Earth.

Features that had apparent over-steeped fronts and wrinkle ridges but that were wider than they were long (Figure 30) were considered to more likely be protalus lobes or simple landslides than rock glaciers.

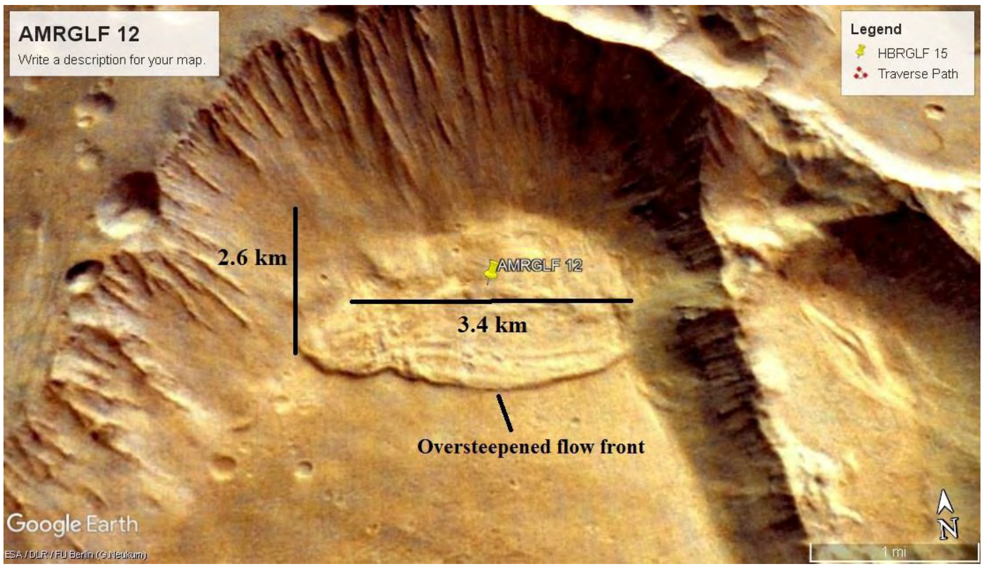

Figure 30: A debris deposit nearby AMRGLF 7 on the slopes of Arsia Mons, this feature has an oversteepened front but it has a width greater than its length and lacks clear transverse ridges on its slope. As a result, it is considered to more likely be a protalus lobe or solifluction lobe than a rock glacier or debris-covered glacier.

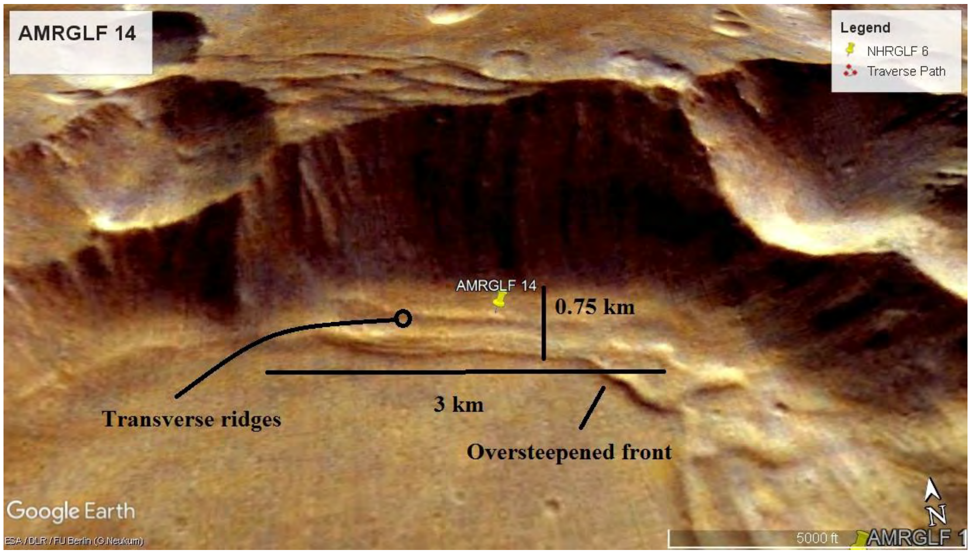

Figure 31: A debris deposit on the slope of Arsia Mons nearby AMRGLF 7 that contains features that plausibly could be characteristics of rock glaciers such as transverse flow ridges and an oversteepened front. The length however is greater than the width, so it is considered more likely to be a protalus lobe than a rock glacier.

Furthermore, features which consisted of just one bow-shaped shaped ridge (Figure 32) or contained ridges that had noticeable spacing between them were considered to more likely be moraines.

Figure 32: The large single bow-shaped ridge composing NHRGLF 4, located in the Deteronilus Mensae region, pointed out in this figure is more characteristic a moraine than a rock glacier.

Also, flow features that contained longitudinal ridges instead of transverse ridges (Figure 33, Figure 34) were considered to more likely be debris-covered glaciers because of morphological similarity to medial moraines found in Earth glaciers (Figure 35).

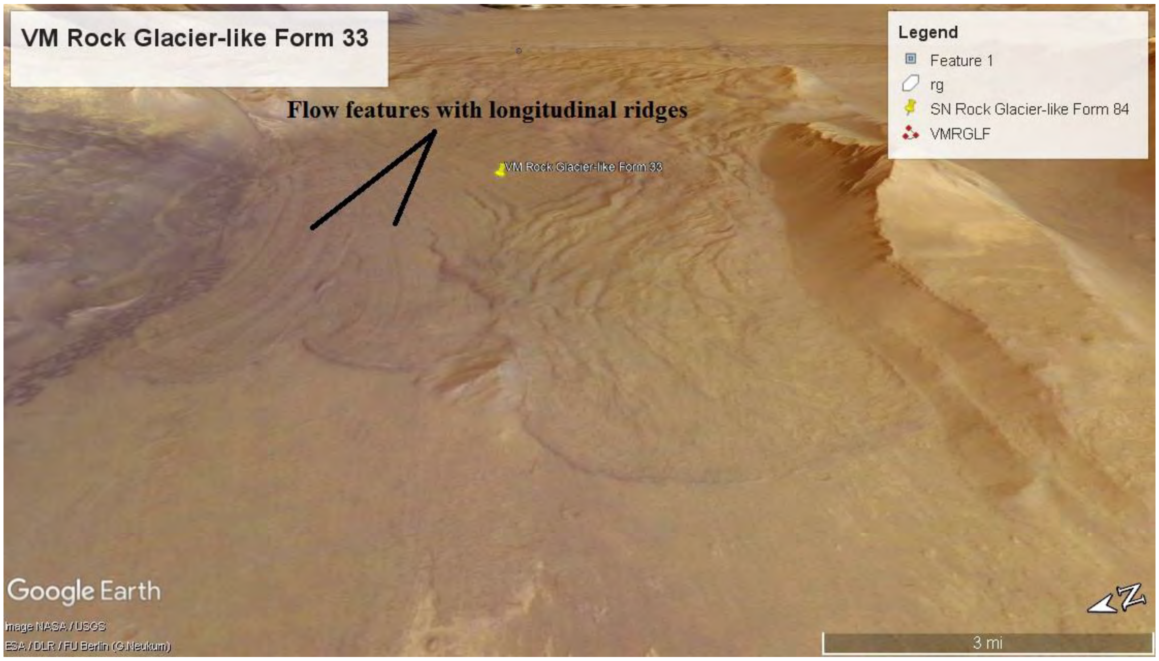

Figure 33: A flow feature (VMRGLF 33) in southern Valles Marineris, the left part of the image shows parts of the feature that have longitudinal ridges that resemble the lineations and medial moraines created by Earth glaciers. This suggests that it is a debris covered glacier rather than a rock glacier.

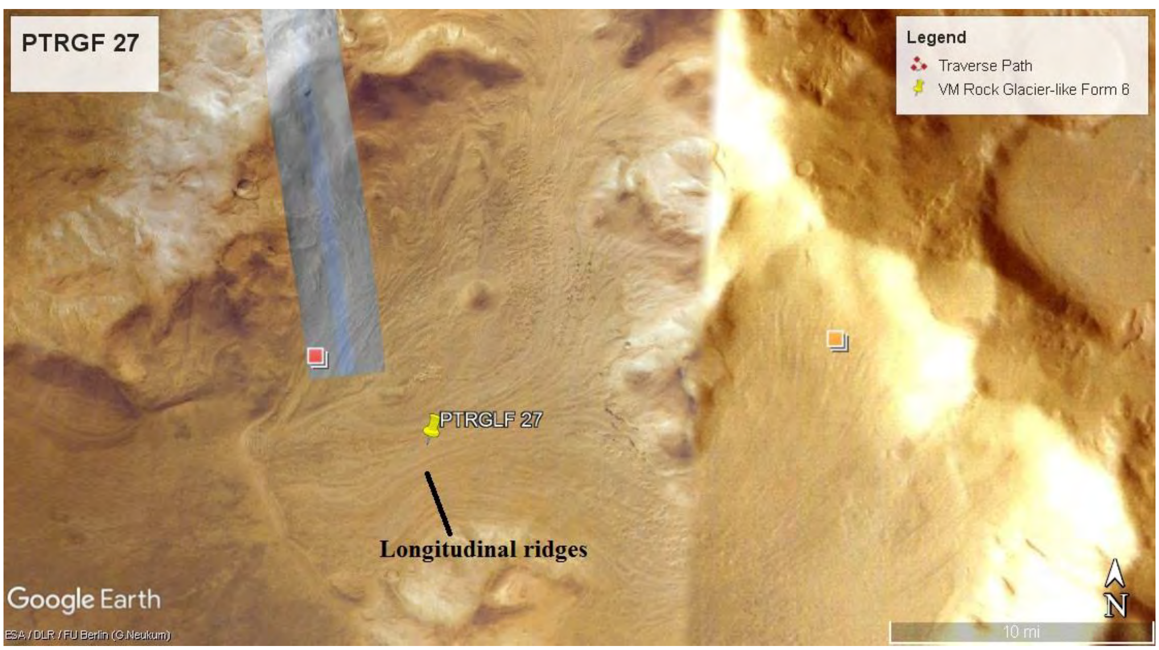

Figure 34: a flow feature (PTRGLF 27) to the east of Hellas Basin which has longitudinal ridges characteristic of debris covered glaciers but not rock glaciers.

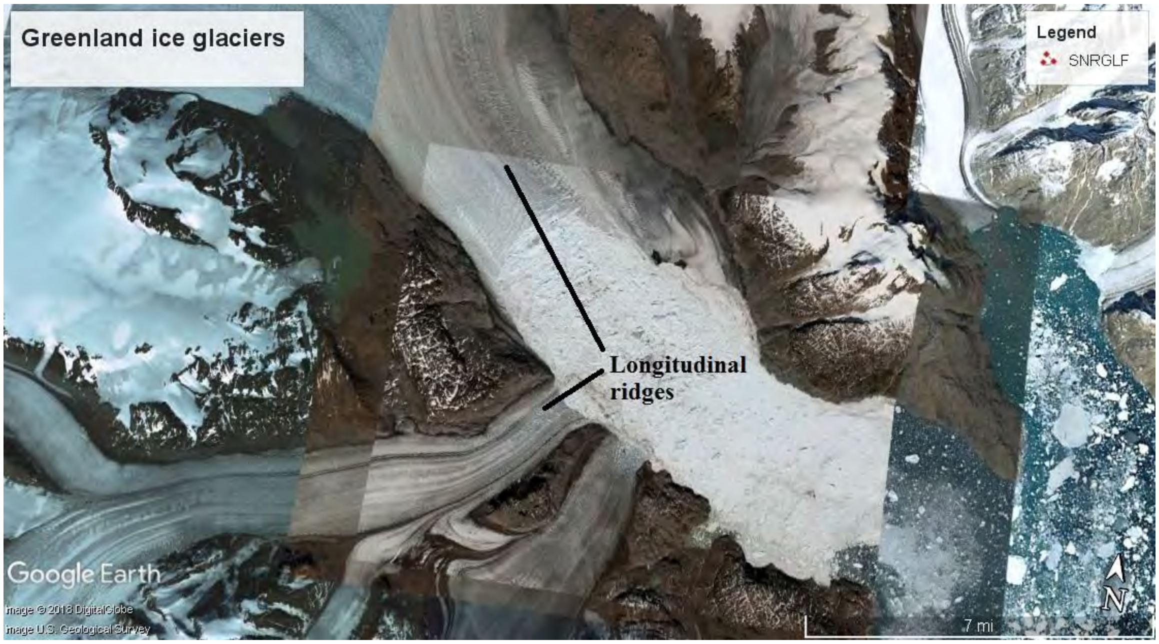

Figure 35: Earth ice glaciers on the coast of eastern Greenland with noticeable longitudinal ridges are shown for comparison to the Martian features resembling debris-covered glaciers**.**

Rock-ice features which could be rock glaciers, debris covered glaciers, or ice-rich landslides were counted in the quantitative study. Martian debris covered glaciers and ice rich landslides are very similar to rock glaciers and, based on attempts by previous researchers to discern the identity of Martian glacier-like forms (e.g., Pierce and Crown, 2003), it may not be possible to distinguish them without visiting the surface.

Geographically, rock-ice features were considered more likely to be rock glaciers that could be included for quantitative analysis if they were found in regions where other rock-ice features had been found by previous studies. Additionally, features found in regions likely to have other flow features unrelated to rock-ice flows but similar in appearance were also considered less likely to be true rock-ice features. Features in regions with extensive volcanism in the past would be considered less likely to be rock-ice features because lava flows can also resemble rock glaciers morphologically. This is unless another factor increased the likelihood of the feature being glacial, such as existing at high elevation in a region which had been glaciated during a period of high obliquity. One such example would be Olympus Mons. Potential rock glacier-like features were given the most credence if they occurred either at mid-latitudes 45 degrees north or south or at high elevation such as the volcanic mountains Olympus Mons and Arsia Mons.

<table>
<tr><th colspan="2">Morphological criteria for inclusion of Martian rock-ice feature in quantitative analysis</th></tr>
<tr><th>Primary criteria</th><th>Secondary criteria</th></tr>
<tr><td><u>At least two of the following:</u>
■ Oversteepened front
■ Transverse or “wrinkle ridges”
■ Tongue-like shape</td><td>■ Length/width ratio greater than 1</td></tr>
</table>

Table 2: The table above organizes the morphological criteria for including Martian rock-ice features in the quantitative part of the analysis. The primary criteria are at least two of the three main features that define a classic rock glacier, an oversteepened front, transverse ridges, and a tongue-like shape. The secondary criteria are used if a flow feature is found that has some characteristics of a rock glacier but is still ambiguous. A larger length/width ratio makes it more likely that a rock-ice feature is a rock glacier.

Data collection

Of the 50-rock glacier-like forms and rock-ice features identified, 18 were chosen,on the basis of meeting the primary and secondary criteria as well as being high enough resolution for the required details to be clearly discerned. They were chosen to be quantitatively analyzed using ArcGIS and a MOLA-derived DEM. Polygons were made around each rock-ice feature chosen for quantitative analysis. After this was done, spatial analysis and zoning statistics tools were used to find the rock-ice feature height, length, body slope steepness, aspect, and headwall steepness with the MOLA data.

Nature of the MOLA DEM

The MOLA DEM was based on altimetry data collected by the Mars Global Surveyor (MGS) spacecraft using the MOLA instrument between 1999 and 2001. Using MOLA, the spacecraft made elevation measurements of the surface in thousands of successive orbits around the planet. Spacing between the tracks created by the individual orbits of MGS create varying areas of data points so that some parts of Mars contain abundant individual data points while others contain large areas where the elevation data is mostly interpolated. The average along track spacing is 300 m, but the average cross-track spacing is about 1.2 to 4 km (Anderson *et al*, 2003; Kreslavsky and Head, 2000). As a result, features that are oriented roughly east-west are likely to be subject to more interpolation than features with a more north-south orientation. Rock ice features with a rough north-south orientation would be more likely to be along actual orbital tracks and thus have a resolution of 300 m instead of 4 km.

To account for this, for quantitative analysis, preference was given to rock-ice features that occurred in regions with noticeable surface roughness indicated by a hillshade map (Figure 36). Uneven areas that showed details of cliffs and rough terrain were favored over uneven smooth areas, as opposed to smooth areas that were just naturally flat. Because MOLA track location data was not available in a readily usable format, Rougher, more detailed terrain was assumed to be more likely along an MGS orbital track, and thus higher resolution, than terrain that was smoothed over. This is illustrated in figure 36.

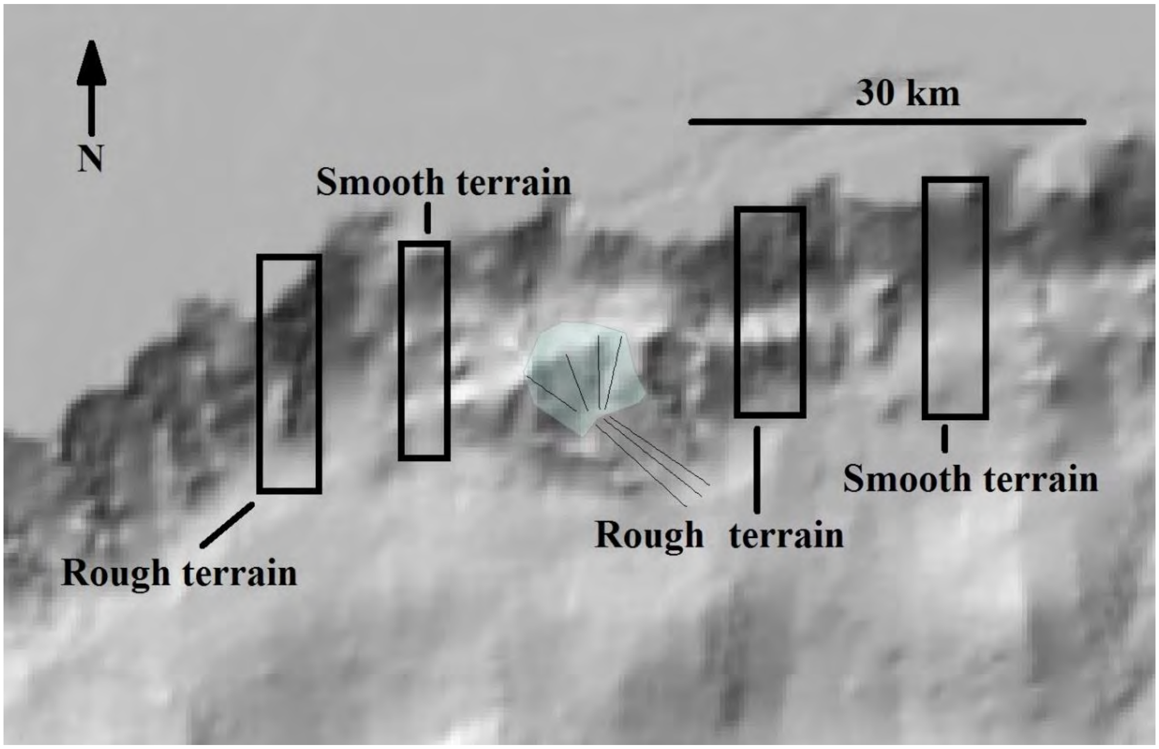

Figure 36: The above is a hillshade terrain map of a rock glacier-like feature in Valles Marineris (VMRGLF 27). the rough terrain is considered to contain a high density of data points while the smooth terrain is considered to have a low density of data points and be mostly interpolation. More credence was given to the measurements made in rough areas. The white polygons and thin black lines are from measurements of the rock glacier-like feature.

For each rock-ice feature that I intended to quantitatively analyze, I created elevation profiles using lines (Figure 38) created by the 3D analysis tool in ArcGIS to determine the data resolution for that spot. For this study, a profile with a curved or uneven line was considered relatively high resolution (Figure 39) while a profile showing a straight line was considered low resolution. Rock-ice features with high-resolution data and low-resolution data were both considered to avoid bias.

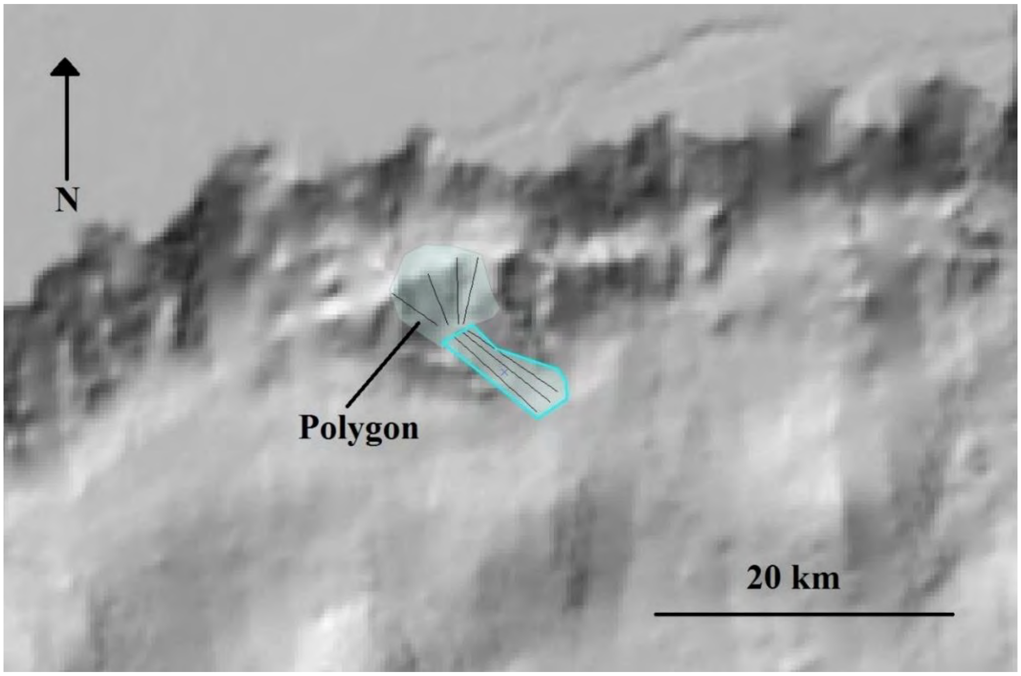

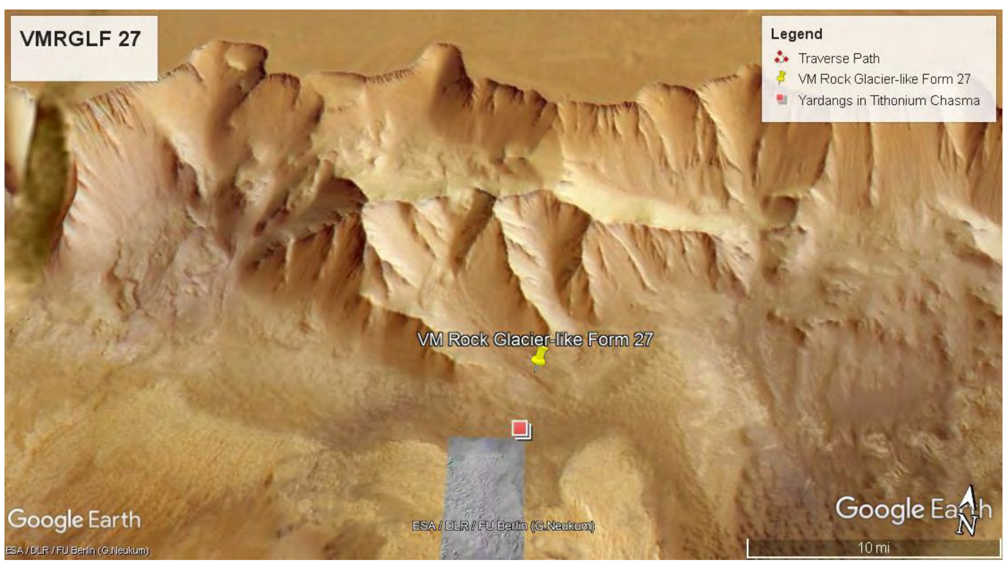

Figure 37: In the Hillshade map of feature VMRGLF 27 (above), the light blue polygons in the image were used to quantitatively analyze the altimetry data. The black lines within the polygons are the 3D lines used to create the elevation profiles both for the rock-ice features themselves and for their headwalls. A minimum of 3 lines were used to construct each profile. A google Earth (Mars mode) Image is shown for context (below).

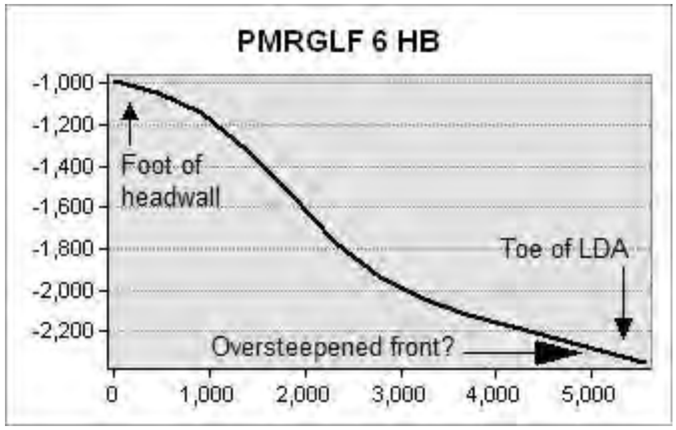

Figure 38: Example of a relatively high-resolution profile of PMRGLF 6, the vertical and horizontal axes are the elevation and horizontal length, respectively, in meters. The locations of important features such as the foot of the headwall and over-steepened front are pointed out with arrows.

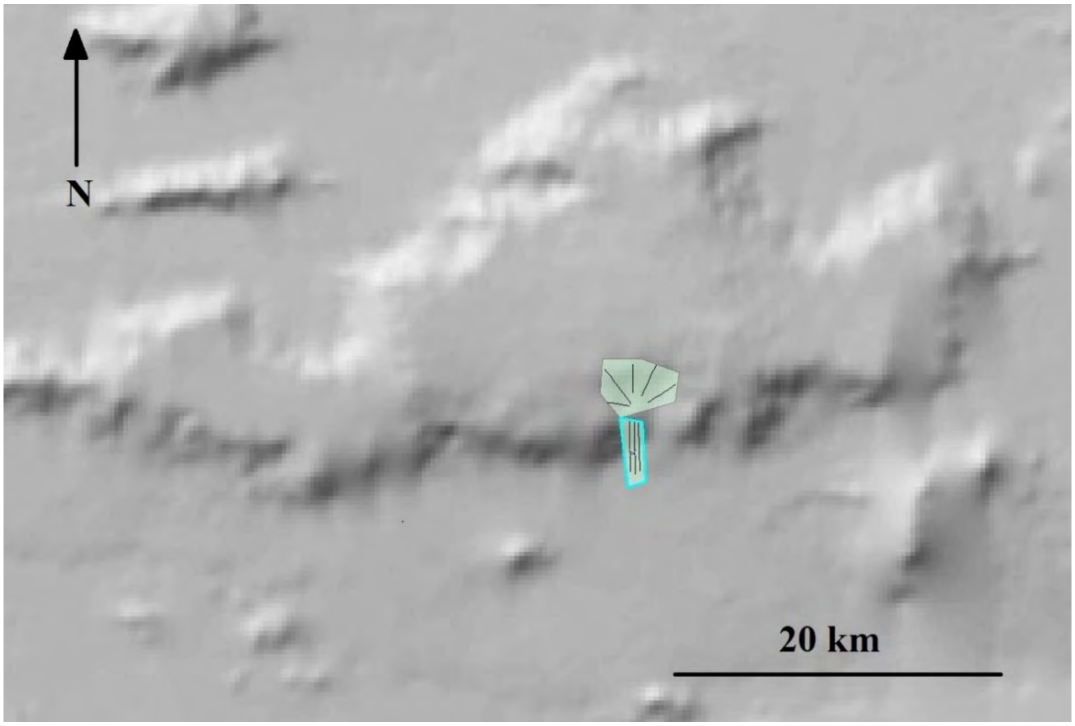

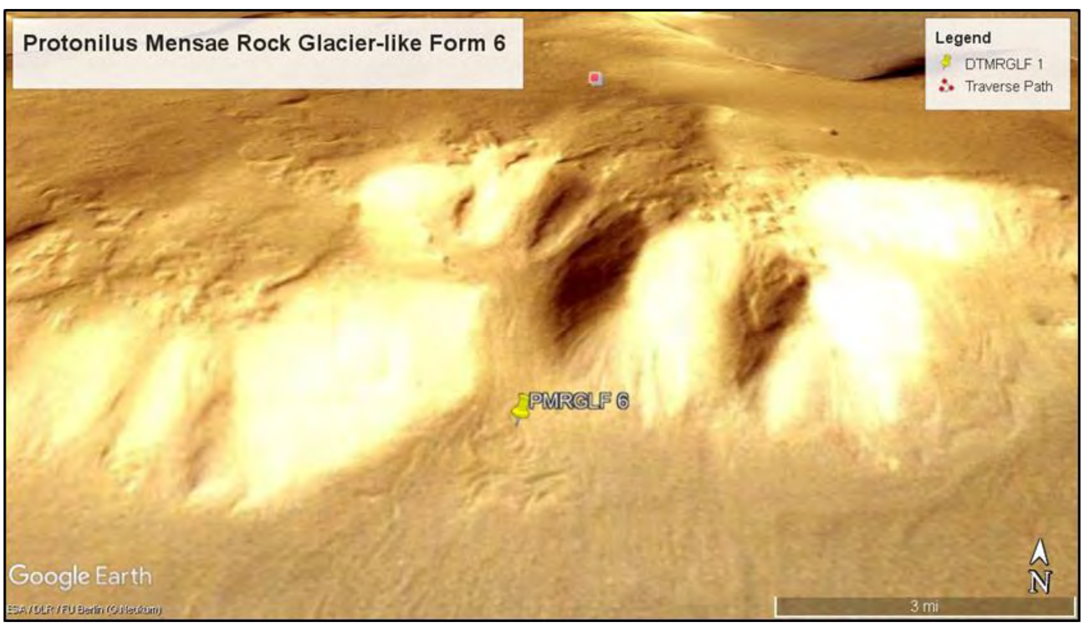

Figure 39: For each profile, the hillshade map (top) and Google Earth image (bottom) of the rock-ice feature are also included for context.

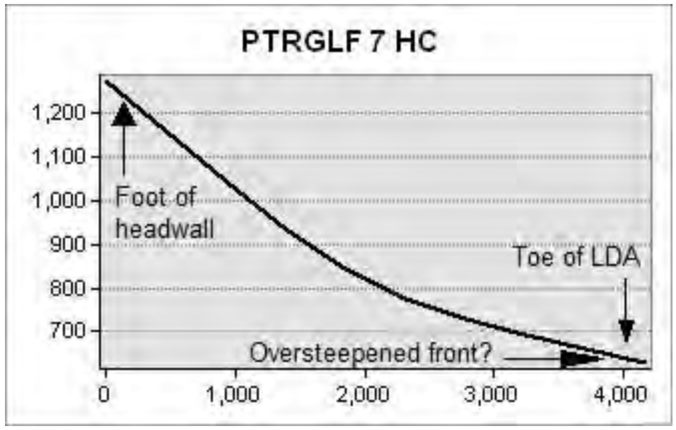

Figure 40: Example of a moderately high-resolution profile of PTRGLF 7, the vertical and horizontal axes are the elevation and horizontal length, respectively, in meters. The locations of important features such as the foot of the headwall and over-steepened front are pointed out with arrows.

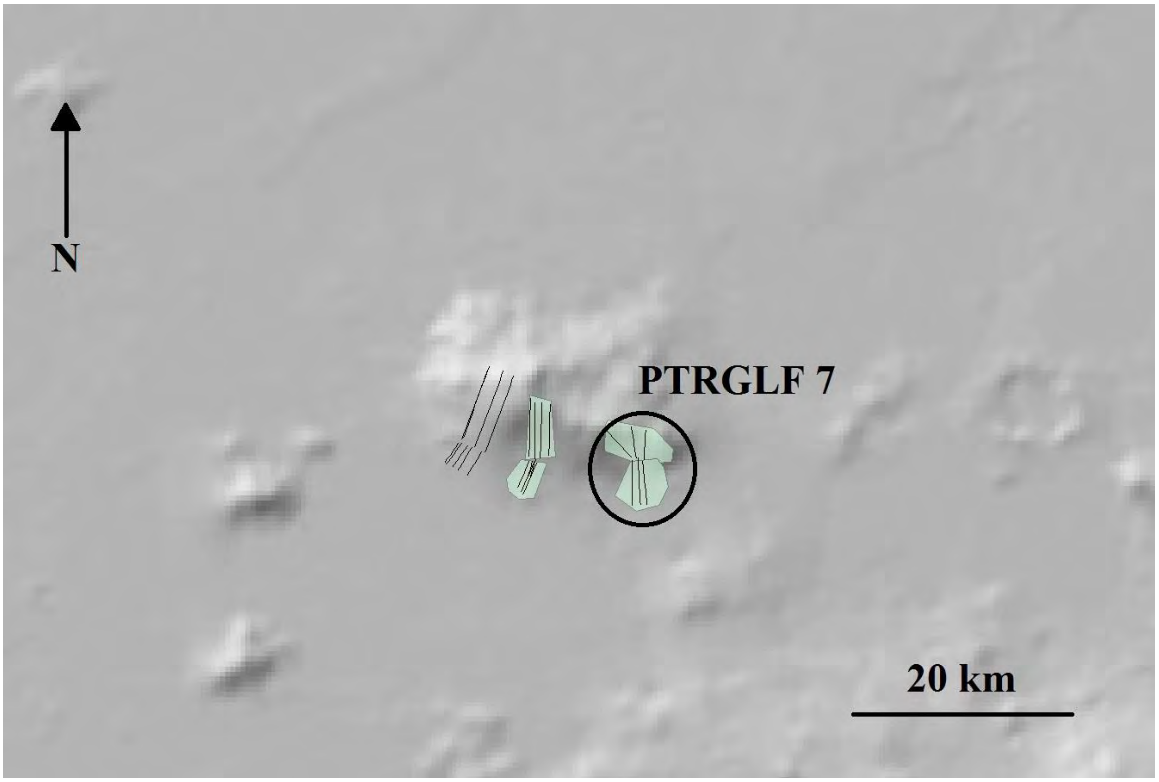

Figure 41: For each profile, the hillshade map (top) and Google Earth image (bottom) of the rock-ice feature are also included for context.

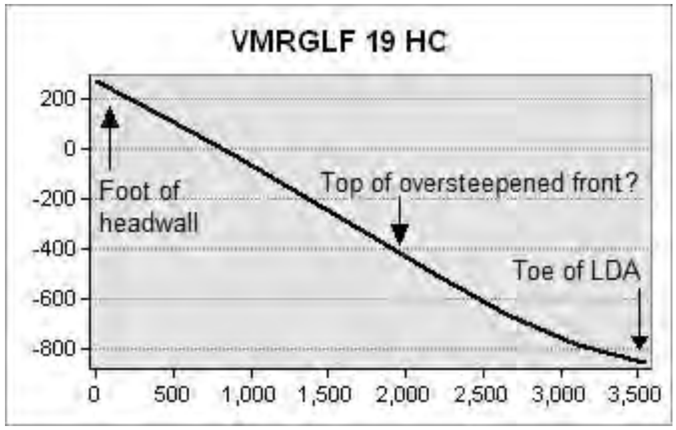

Figure 42: Example of a low-resolution profile of VMRGLF 19, the vertical and horizontal axes are the elevation and horizontal length, respectively, in meters. The locations of important features such as the foot of the headwall and over-steepened front are pointed out with arrows.

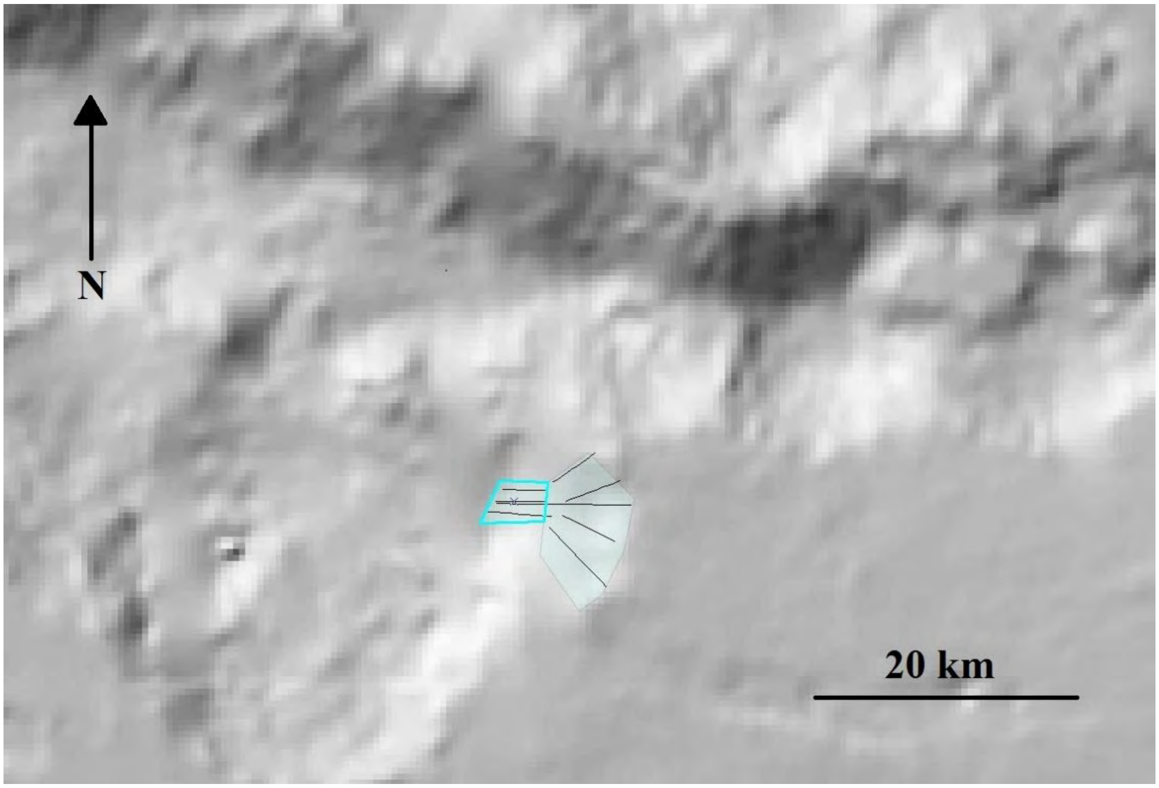

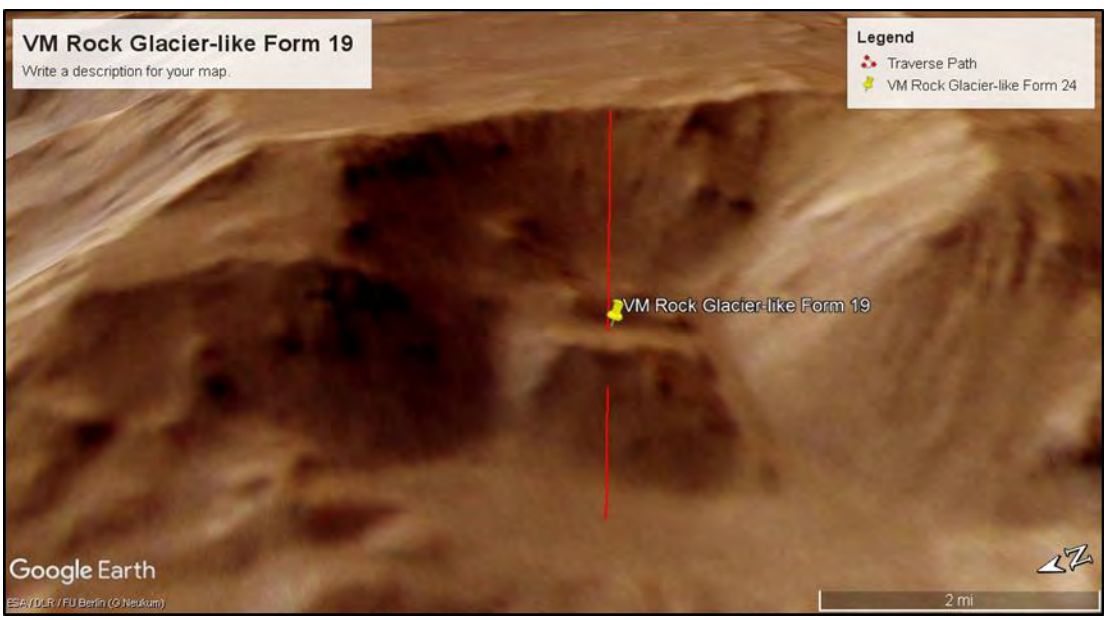

Figure 43: For each profile, the hillshade map (top) and Google Earth image (bottom) of the rock-ice feature are also included for context.

Analysis

After making all the measurements and recording all the data, I made scatter plots comparing the headwall steepness with the rock glacier height, length, and latitude. For Mars, I also plotted the headwall steepness against aspect. In each case, I looked for any correlation between headwall steepness and the other participating factor. After making figures and identifying possible correlations, I used linear regression analysis to test the likelihood that the correlations found between headwall steepness and the other parameters were real correlations. For this statistical test I made the p-value less than or equal to 0.01. In this case, the p-value being less than or equal to 0.01 would mean that the hypothesis that there is a correlation is likely enough that it cannot be assumed to be false. A value greater than 0.01 would mean that the null hypothesis, that there is no correlation and that any association between the factors is by chance, is more than 1% likely to be correct.

RESULTS

Earth

The main rock-ice features identified on Earth were rock glaciers (See Figure 10), protalus lobes or ramparts, and debris covered glaciers. Possible debris covered glaciers were identified in the Himalaya and New Zealand. Protalus lobes and ramparts were found in the Alps and the Sierra Nevada. In the Sierra Nevada, the most common rock-ice features observed were rock glaciers. Protalus lobes and ramparts were comparatively rare. The mountain range with the second highest number of rock glaciers identified in this quick survey was the European Alps. A total of 20 Alpine rock glaciers were identified mostly in the Swiss and Austrian Alps with a few rock glaciers identified in the Italian Alps. The observed Andean rock-ice features were also predominantly rock glaciers. All the rock glaciers studied occurred in the same high elevation alpine environment.

Figure 44: A rock glacier (SNRGLF 92) in the high Sierra Nevada

Although some rock glaciers and other rock-ice features were noted in the Alps, the Andes, the Himalaya, and the Southern Alps of New Zealand, all terrestrial rock glaciers studied quantitatively were in the Sierra Nevada.

Rock glacier characteristic	Measurement
Rock glacier length	150-1600 m
Rock glacier height	50-300 m
Rock glacier slope steepness	5-30 deg.
Rock glacier headwall steepness	25-40 deg.
Latitude	36.4-38 deg.
Elevation	3000-4000 m
Average maximum elevation of the beginnings of accumulation zones	3627 m
Average minimum elevation of the edges of ablation zones	3463 m

Table 3: Of the 101 rock glaciers measured, they all occurred within a latitude of 38 degrees and 36.4 degrees north. They were found to be within an elevation of 3000-4000 meters. The lengths of the rock glaciers varied between 150 and 1600 meters. The average head wall steepness for the Sierra Nevada rock glaciers observed varied between 25 and 40 degrees. The average glacier slope steepness has much broader range, varying from 5 degrees to about 30 degrees. The rock glacier height varies from 50 meters to as high as 300 meters. On average, the maximum elevation where rock glaciers accumulate debris in the cirque was

3627 meters and the average minimum elevation at the toe of the rock glacier was 3463 meters. This reflects the typical scale of rock glaciers in Terrestrial mountain ranges.

A very weak inverse correlation was found between headwall steepness and the rock glacier length for Sierra Nevada rock glaciers (Figure 47). Length slightly decreases with increasing steepness. No other correlations related to headwall steepness were found. This implies that the headwall steepness is not a significant factor in determining rock glacier growth or behavior in the Sierra Nevada.

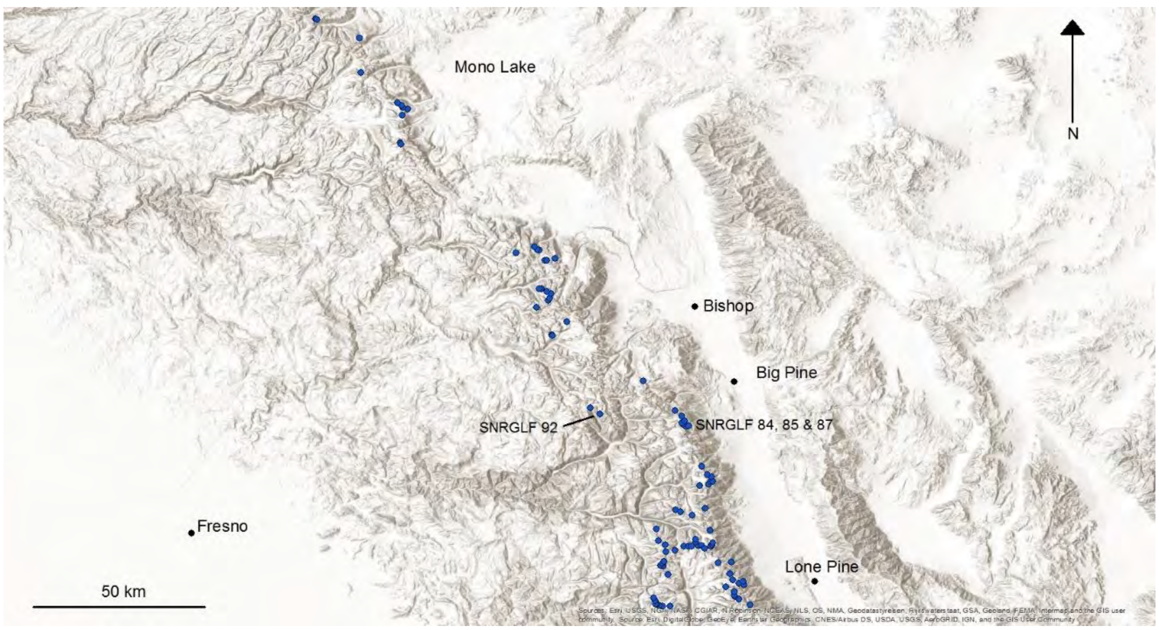

Figure 45: The above image is a satellite overview of the region in the Sierra Nevada across which the terrestrial rock glaciers were mapped and identified. The blue dots represent the rock glacier-like features identified in the study. (Map data source: USGS).

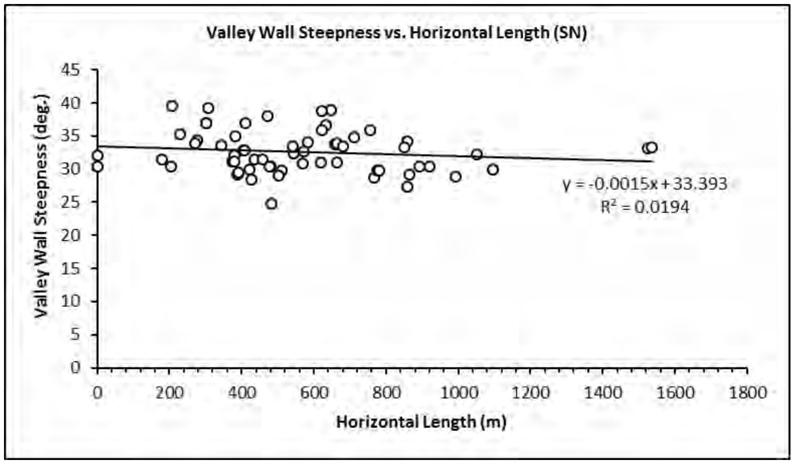

Figure 46: This graph shows a very weak correlation between headwall steepness and rock glacier length on Earth. The circular symbols represent rock glaciers used in the quantitative measurements.

Mars

Quantitative assessment of glacial features

Features that were likely rock glaciers or debris covered glaciers were found mainly in the regions of Promethei Terra, Valles Marineris, Protonilus Mensae, Deuteronilus Mensae, and Argyre Basin. In analysis of the data, two possible correlations were found related to head wall steepness, a weak correlation with height (Figure 48) and a moderate correlation with length (Figure 49). After doing the linear regression analysis, the p-value for height was found to be 0.047383 while the p-value for the length was 0.000333 which implies that the correlation with length is significant while it is not certain that the correlation with height is significant. This suggests that headwall steepness does play a significant role in the behavior of Martian rock glaciers and other rock ice features.

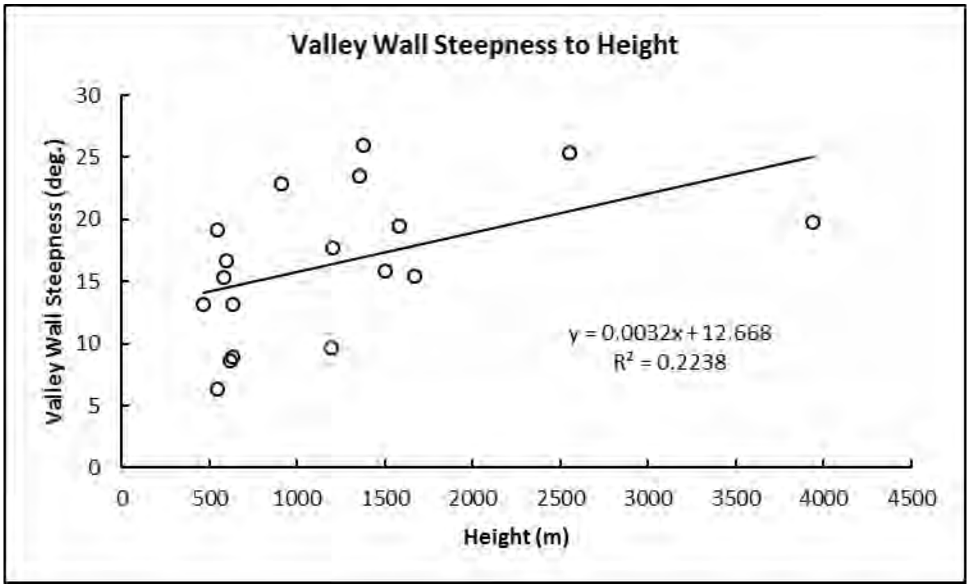

Figures 47: The above graph shows the distribution of the height values for the measured glacial features plotted against headwall steepness. The R^2 value suggests a weak correlation but linear regression analysis yielded results that make it unlikely that there is any correlation.

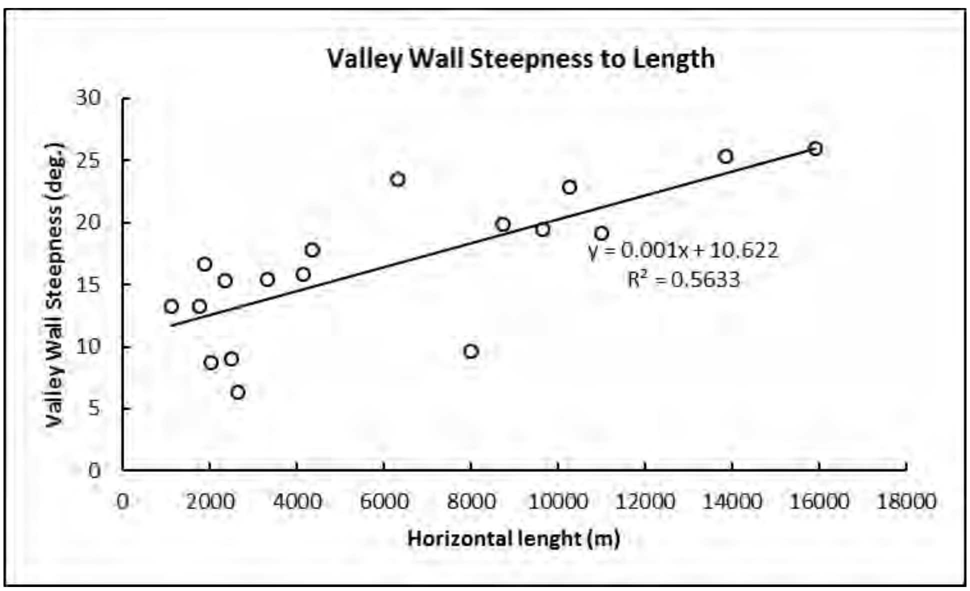

Figures 48: The above graph shows the distribution of the length values for the measured glacial features plotted against valley wall steepness. The R^2 value suggests a moderate correlation and linear regression analysis yielded results that make it plausible that there is a correlation.

After finding the correlation, I compared the values for different regions on Mars to see how this potential correlation was reflected regionally. Valles Marineris contained the largest rock glaciers found.

The average rock glacier length in Valles Marineris was 10 kilometers, greatest of all the regions. The Valles Marineris (VM) rock glaciers also had the highest average head wall steepness angle at 21 degrees. Deuteronilus Mensae had the lowest average headwall steepness which was 10 degrees. Deuteronilus Mensae (DM) also had shortest rock glaciers at 577.8 meters. Promethei Terra (PT) was between DM and VM in both size and head wall steepness. Protonilus Mensae (PM), on the other hand, was found to have a lower average head wall steepness than PT but also greater length. This revealed that the correlation is reflected imperfectly on a regional level and is more likely a global average, if it is genuine.

Distribution of glacial features

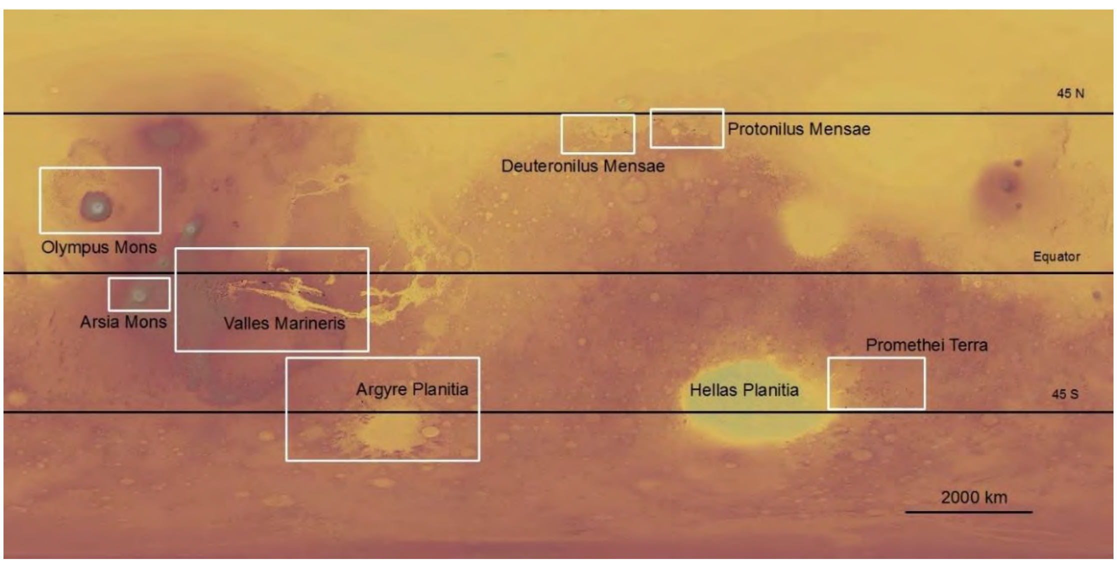

Figure 49: A global map showing the contexts of the later maps. The white boxes represent the extent of the maps for each of the regions that were studied.

Most rock glacier-like forms identified were in the equatorial regions of Mars or at mid-latitudes in the northern and southern hemispheres. A surprising number of possible remnant glacial features were identified along the equator and the tropics in the region of Valles Marineris as well as Olympus Mons and Arsia Mons. This contradicts the findings of other researchers who found the majority of rock-ice features at mid-latitudes (Pierce and Crown, 2003; Mahaney, 2007; Arfstrom and Hartmann, 2005) but is consistent with other research findings that identify rock-ice features and other evidence of glaciation in the tropical and equatorial regions of Mars (Head and Neukum, 2005; Mege and Bourgois, 2011).

Valles Marineris

Thirty potential glacier-like features were identified in Valles Marineris, though most of them were only evaluated qualitatively. Most of these features were located in the northern part of the canyon system in Candor Chasma and Tithonium Chasma (Figure 51, Figure 52). Some of the features, initially thought to be glacially related, upon closer examination turned out to more likely be landslides. This is to be expected in Valles Marineris. Most glacial features, unless they have thick debris mantles (Colaprete and Jakoski, 1998), would likely be ancient relicts because of the direct sunlight near the equator. Any fresh-looking features in Valles Marineris are more likely to be landslides or other non-ice related features.

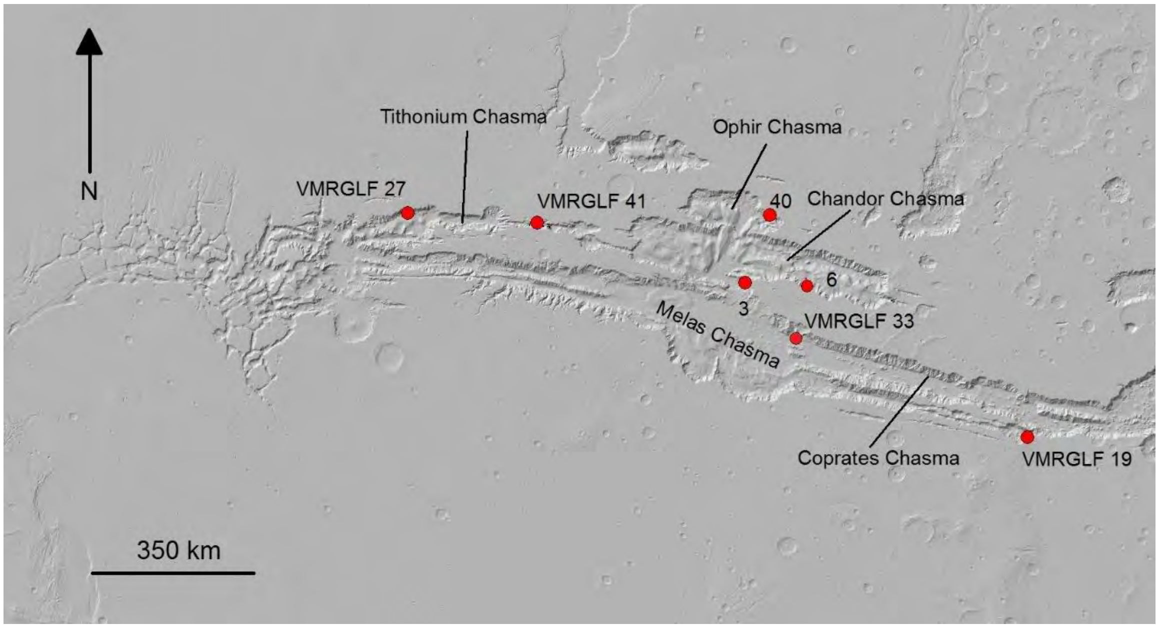

Figure 50: A feature map of Valles Marineris. The red circles represent clusters of glacier-like forms

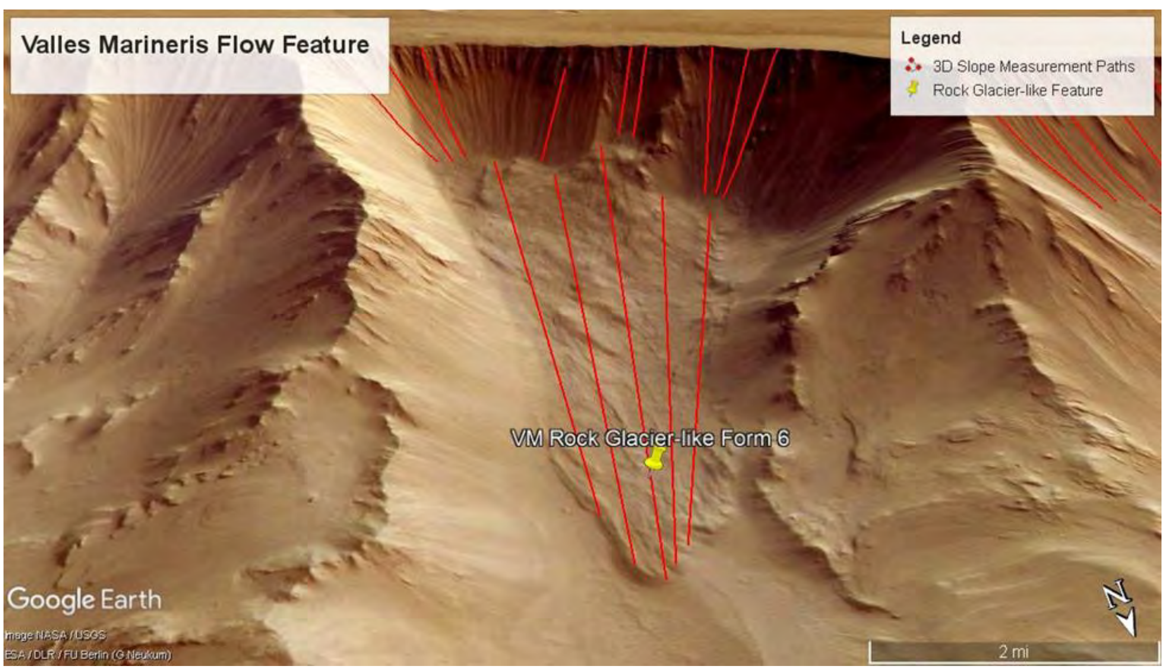

Figure 51: A lobate feature of unknown designation in Candor Chasma of Valles Marineris. It could be a rock-ice feature, or it just could be a landslide.

Olympus Mons

Some researchers have reported evidence of ancient tropical mountain glaciers adjacent to Olympus Mons (e.g., Head and Neukum, 2005). During this survey of glacier-like forms on Mars, enormous moraine-like features were identified at the foothills of Olympus Mons (Figure 53, Figure 54). These features are of immense size (average, 60 km in length), and have an extremely low gradient, and their flat spread out shape.

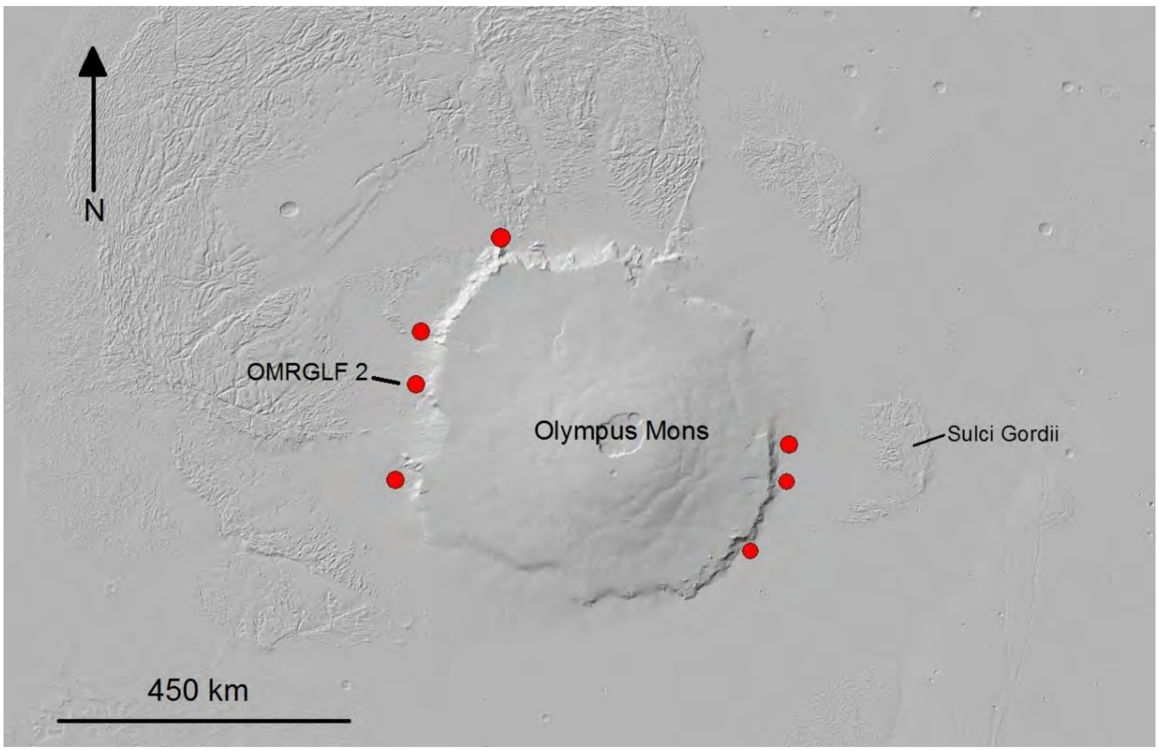

Figure 52: A map of Olympus Mons with rock glacier-like features represented by red circles

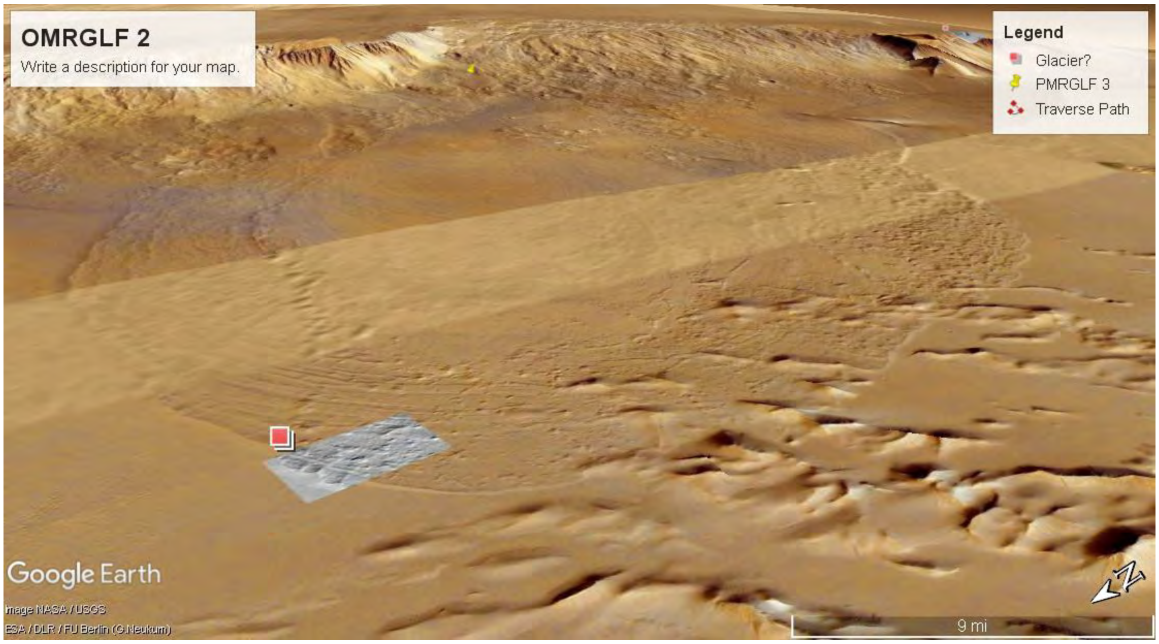

Figure 53: A Glacier-like form near Olympus mons, likely a moraine if genuinely glacial

Promethei Terra

Abundant glacial features were found in the region east of Hellas Basin near Reull Vallis and Greg Crater (Figure 55). Promethei Terra is an ancient region of Mars scarred by craters where a few younger volcanic features have cut through the ancient cratered highlands. Numerous craters, particularly Greg Crater, contain glacial moraines and mantled rock-ice deposits. One particular massif to the east of Greg Crater contains at least three well-defined lobate features with transverse ridges which have all the features associated with classic rock glaciers. One of the features is shown in Figure 20. Additionally, several nearby features within the region resemble debris-covered glaciers including one that is adjacent to a massif to the south of Reull and Harmakhis Vallis.

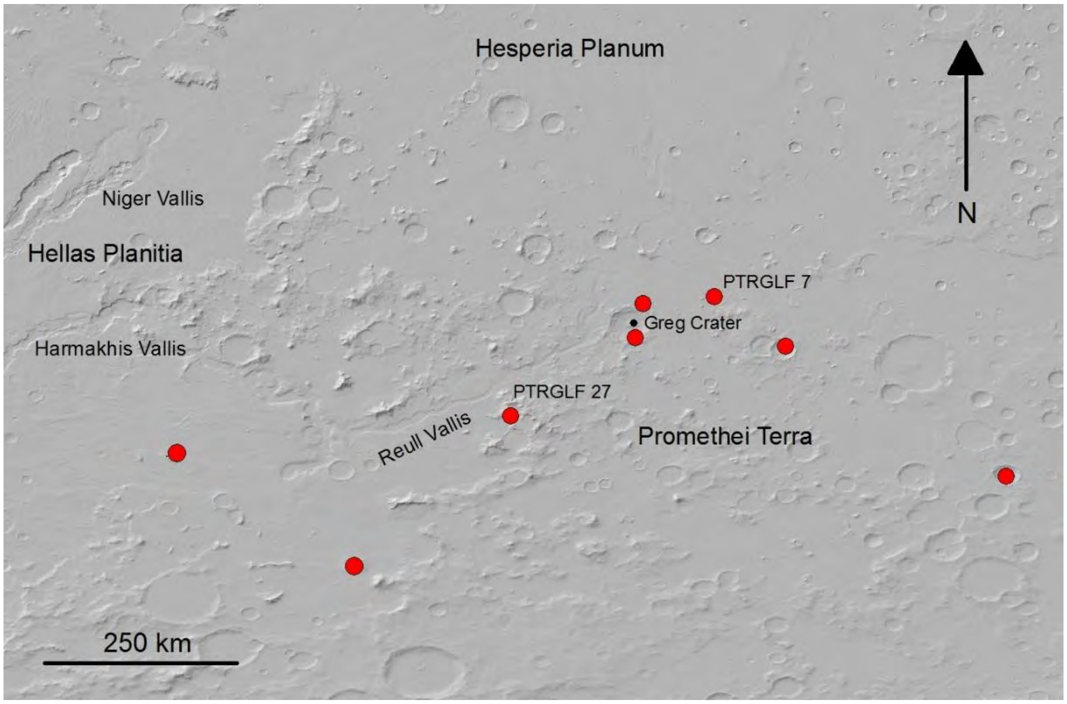

Figure 54: Feature map of Promethei Terra and the surrounding regions. Glacier-like features are represented with red circles.

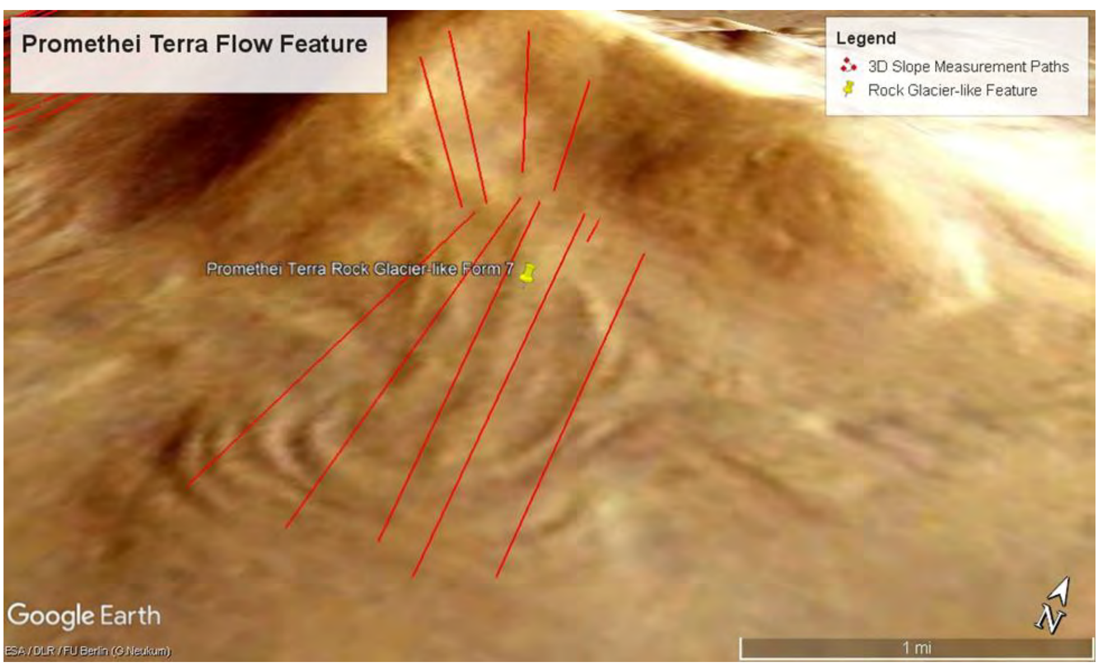

Figure 55: A rock glacier like form (PTRGLRF 7) near Promethei Terra in the vicinity of Greg Crater displaying transverse ridges and a tongue-like shape.

Argyre Basin

Argyre Planitia (Figure 57) is at the southern latitude where glacial features are well known on Mars, about 40 degrees. It is also one of the prime regions where past researchers have found glacial features (e.g., Pierce and Crown, 2003) In my survey of Argyre Planitia, findings were scant. Only one rock glacier-like feature was identified. It is made up of one or two lobate structures which could be rock glaciers, debris covered glaciers, or possibly moraines.

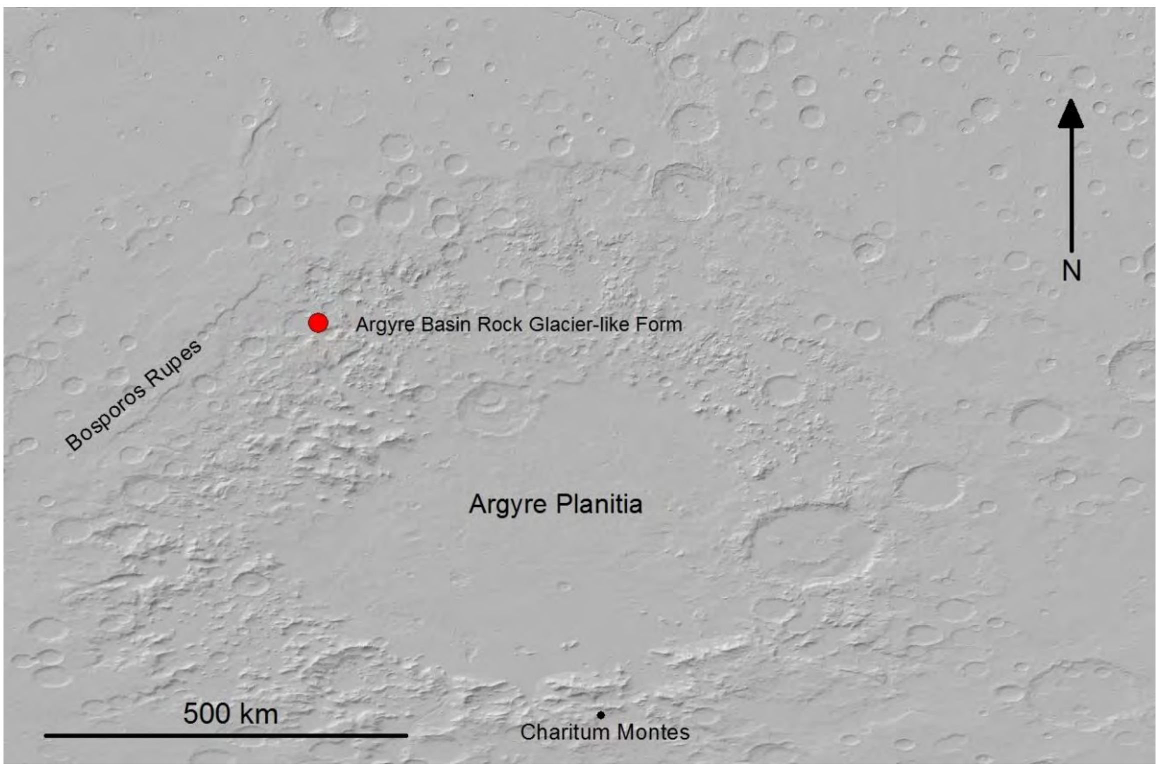

Figure 56: Argyre Basin Feature Map. Red circles represent rock-ice features.

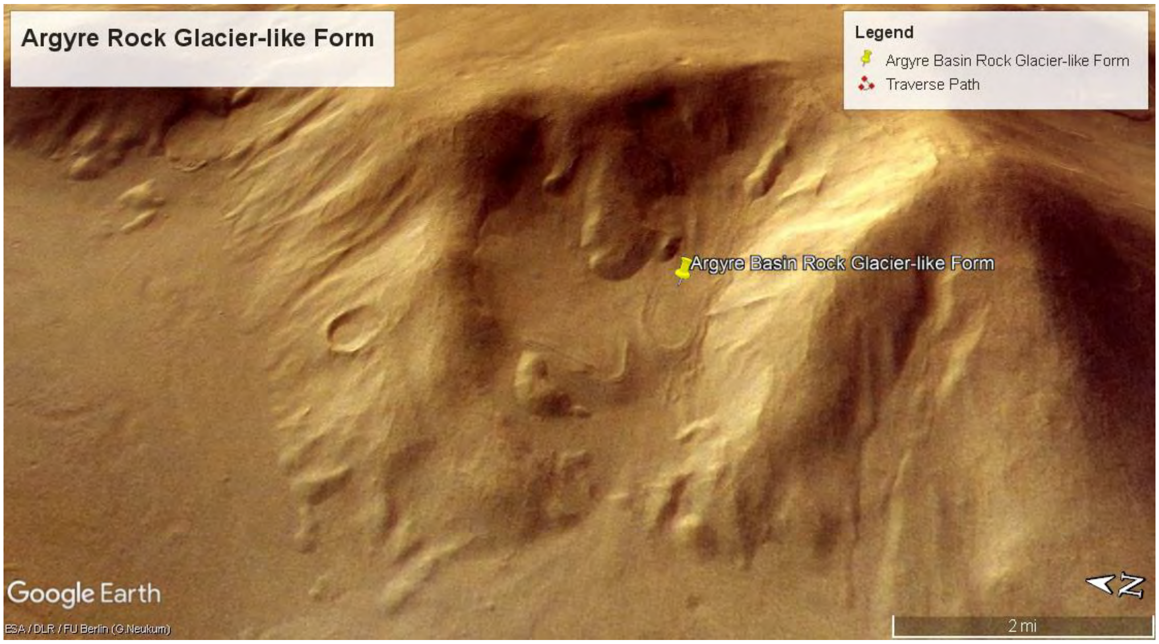

Figure 57: Two lobate features in Argyre Basin which may be glacial in origin.

Deuteronilus Mensae and Protonilus Mensae

At about 40 degrees latitude in the northern hemisphere of Mars is a terrain called fretted terrain (Pierce and Crown, 2003). This region is a boundary between the southern highlands and the northern lowlands. Deuteronius Mensae (Figure 59, Figure 60) and Protonilus Mensae (Figure 61, Figure 62) contain significant amounts of badlands-like terrain referred to as "fretted" terrain. valley floors in between the massifs strongly suggest the existence flowing subsurface ice. Terrain containing lineations resembling the flowlines in glacial terrain are probably debris covered ice flows. In many parts of the fretted terrain, these flow features are severely ablated with abundant sublimation pits and ablation lag. This material has been noted by previous authors and was referred to as lineated valley fill (Head *et al*, 2010; Pierce and Crown, 2003).

Lobate debris aprons are also adjacent to the massifs and some of the observed aprons have features diagnostic of rock glaciers such as wrinkle ridges (Figure 20).

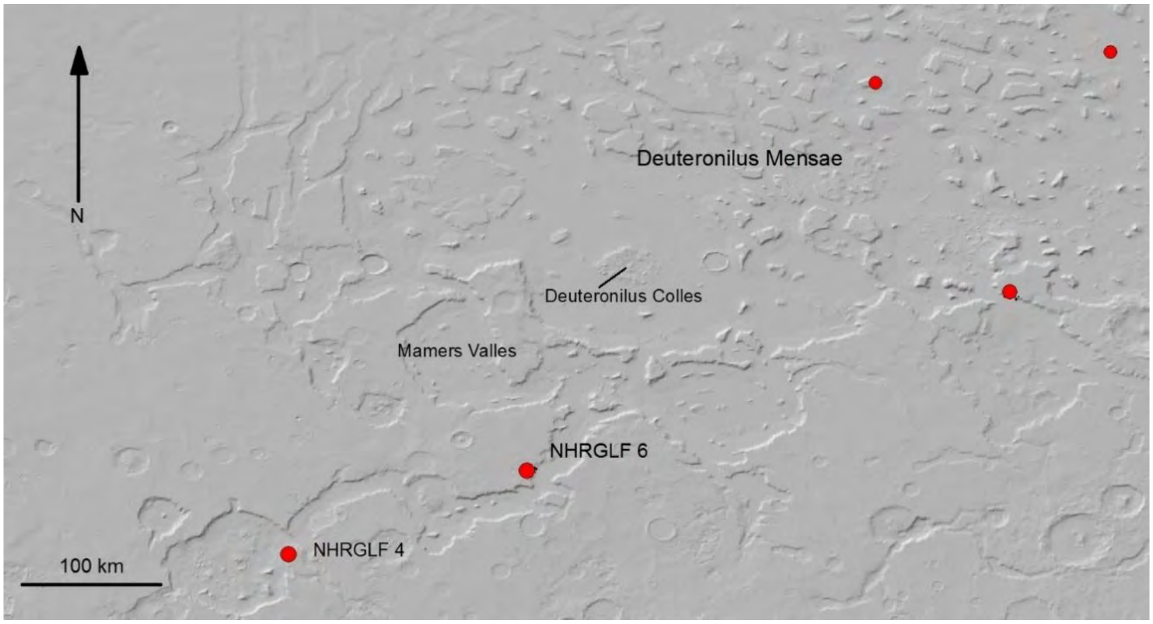

Figure 58: A feature map of the Deuteronilus Mensae region. The red circles represent clusters of rock glacier-like features.

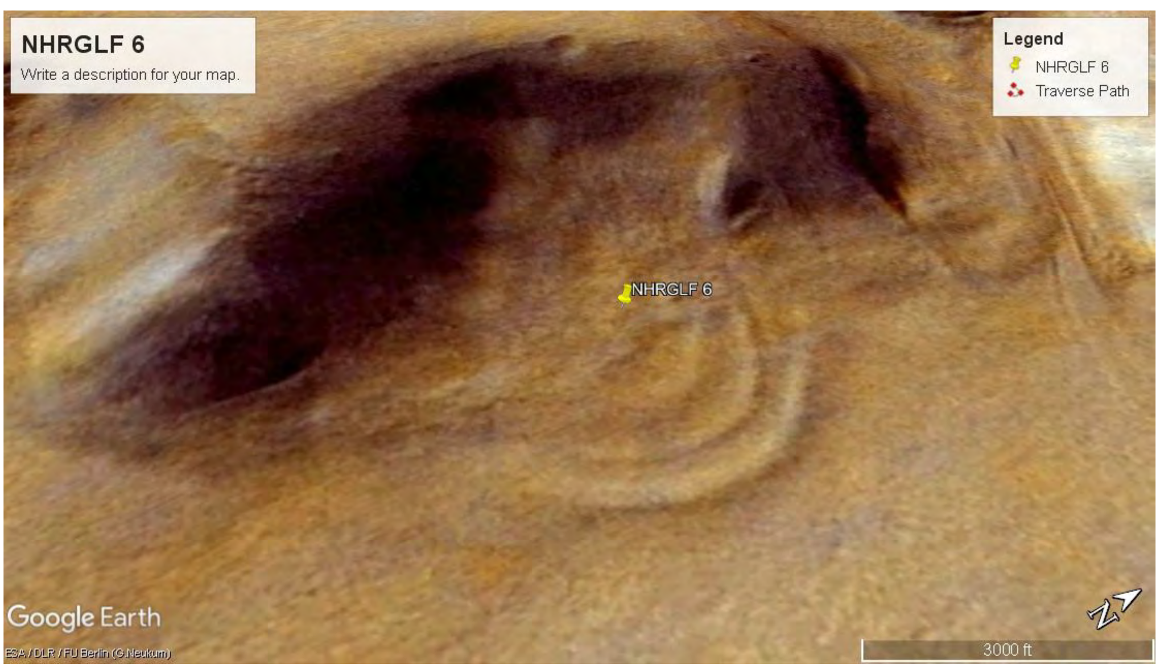

Figure 59: A series of ridges which could be a rock glacier or a series of moraines

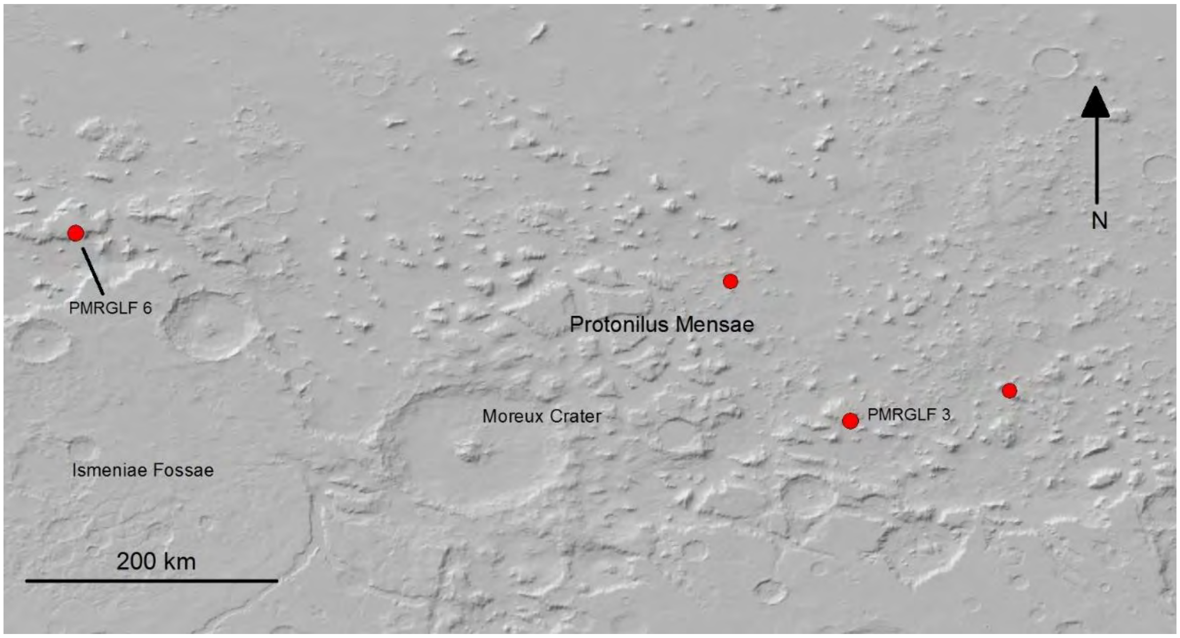

Figure 60: Feature map of the Potonilus Mensae region, the red circles represent clusters of rock glaciers.

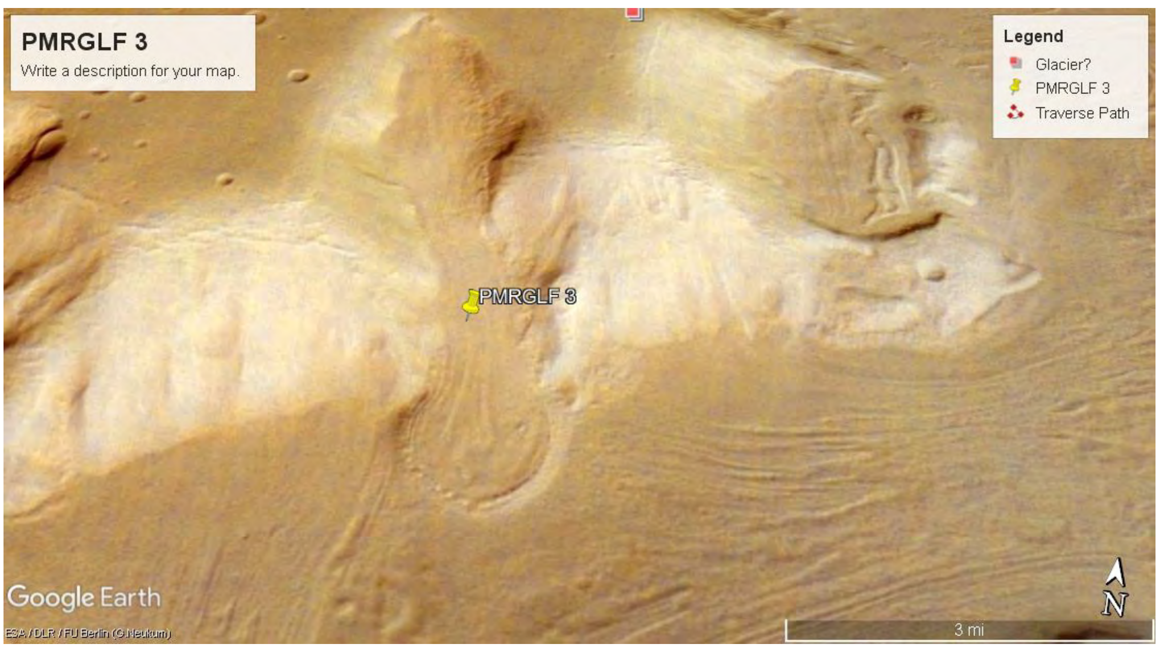

Figure 61: A glacier-like feature in the Protonilus Mensae region. The circular shape gives it the appearance of a piedmont glacier. It is most likely a debris covered glacier.

Arsia Mons

Arsia Mons contains numerous volcanic features such as collapsed lava tubes which have created larger chambers and depressions (Figure 24). Within the depressions are flow features which appear to be ice rich landslides, solifluction lobes, protalus lobes, and protalus ramparts (Figure 25). The equatorial location of these features and their lack of obvious recent flow suggests that they are fossil structures. There are also some features that may be rock glaciers.

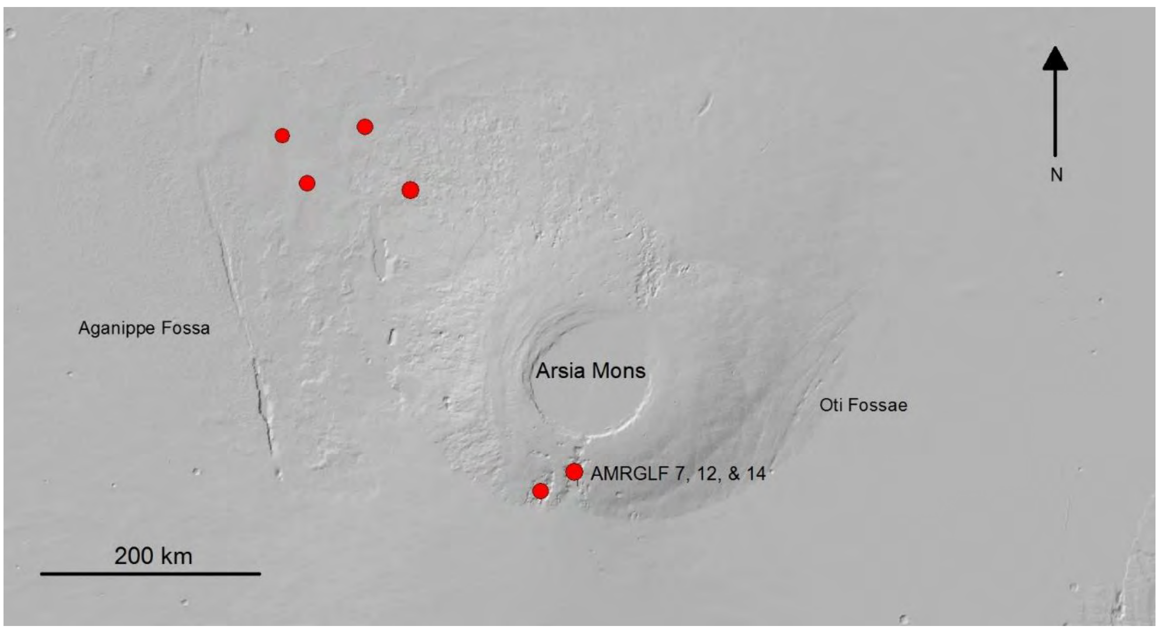

Figure 62: Arsia Mons Feature Map. Red Circles Represent clusters of rock-ice features

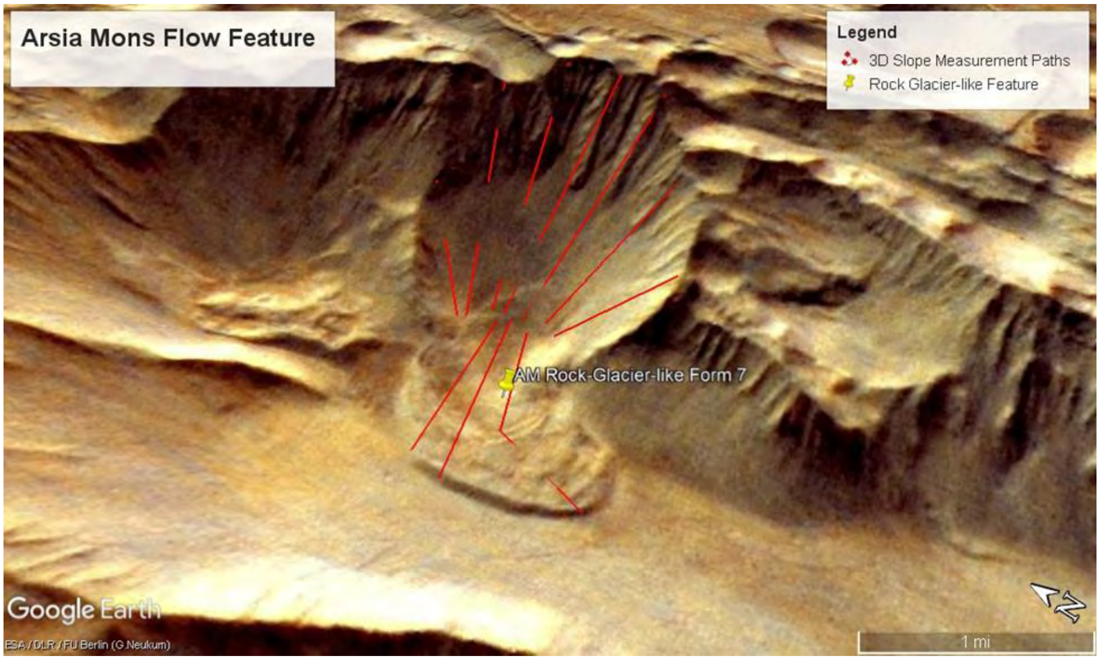

Figure 63: The image above shows a flow feature which could be ice related on the slopes of Arsia Mons at an elevation of 13,215 meters.

DISCUSSION

Diversity in rock glacier behavior across Earth and Mars

Unlike Mars, no correlations were found for Earth in this study between headwall steepness and other factors. Although rock glaciers occur on both planets, they follow slightly different patterns. Terrestrial rock glaciers, for example, have been used in studies related to permafrost (Jakob, 1992; Brazier *et al*, 1998; Brenning, 2005), aridity (Owen and England, 1998; McGregor, 1967; Azocar and Brenning, 2010), and paleoclimate (Kerschner, 1978; McGregor, 1967). These studies demonstrate that rock glaciers can be used to infer past and present terrestrial climate. Also, from the aforementioned studies, it can be concluded that terrestrial rock glaciers, in general, indicate arid conditions with regular subzero temperatures which are most common at very high elevations on Earth. Rock glaciers will often form where precipitation rates are too low for enough accumulation of ice to form true glaciers (Owen and England, 1998; McGregor, 1967). Rock glaciers can also indicate permafrost conditions (Brenning, 2005; Brazier *et al*, 1998; Whalley and Azizi, 2003). Although terrestrial rock glaciers exist at a variety of latitudes, they commonly occur in high elevation mountain areas (Whalley and Azizi, 2003; Giardino and Vitek, 1988) that are usually part of mountain ranges produced through tectonic processes that are currently unique to Earth. Martian rock-ice features are similar but do not follow the exact same patterns of behavior and distribution. This fact, along with the findings of this study, are significant for comparing the distribution and behavior of rock glaciers on Earth with their distribution and behavior on Mars and other planets.

Most of the Martian rock glaciers observed in the study were found either at mid-latitudes around 45 degrees north or south, or near the equator. This finding is consistent with the findings of other researchers who found such features in some or all of these locations (Arfstrom and Hartmann, 2005; Mege and Bourgois, 2011; Head and Neukum, 2005; Pierce and Crown, 2003). There is little association between the presence of glacial features and aspect, except in the northern hemisphere, which contradicts findings of other researchers that glacial features tended to be pole facing in both hemispheres (Arfstrom and Hartmann, 2005). The reason for this is could be small sample size since some rock glaciers will not always fit the pattern. For the factors most considered in this study, the association between headwall steepness and rock glacier length is also regionally consistent in some cases. Valles Marineris has both the highest head wall steepness and the largest rock glacier-like features. The regions of Promethei Terra and Deuteronilus Mensae follow this pattern as well. Protonilus Mensae does not follow the pattern, since it has the third-highest headwall steepness but the second-largest rock glacier size. The number of glacial features per region, however, is very small, and caution should be taken in reading too much into this pattern. The possible correlation is clearest on a global scale. Thus, if there is a real correlation, the correlation is likely due to factors that affect all of Mars rather than local factors particular to part of the planet's surface.

Possible causes of the correlation between size and headwall steepness

If there is a correlation between rock glacier size and head wall steepness, one reason for it might be the relation between slope and rockfall. Accumulation of rocky debris is greatest at a certain optimal steepness that depends on the local lithology (Marquinez *et* *al*, 2003; Dorren *et al*, 2004). For example, calcareous cliffs tend to have high rockfall activity between 50 degrees and 60 degrees while the rockfall tends to decrease with increasing slope steepness above 60 degrees (Marquinez *et al*, 2003). The authors of the study do not discuss the reasons, but a possible explanation will be discussed in the section on rock strength.

Defining optimal slope steepness for maximum rockfall and influencing factors

In the studies reviewed, the idea of a slope value where rockfall is most frequent for specific rock types, referred to as "optimal slope steepness" in this volume, was assumed rather than explained. The reason why different lithological types would have an optimal slope steepness could be related to rock strength and the angle of repose.

Rock strength

Studies on rock strength suggest that slope steepness increases with rock strength at least for sedimentary rocks (Burnett and Meyer *et al*, 2008). The relationship is complicated, but some possible inferences can be made. For example, the reason that rockfall declines above a certain maximum steepness could be that below that maximum steepness, loose debris builds up on the slope which can eventually cause rockfall events. For rockfaces above that steepness, the slope might be too steep for rockfall to accumulate in large amounts on the slope before a rockfall event occurs. Above the optimal steepness angle, the amount of rockfall might be more dependent on rock strength. Cliffs composed of relatively weak rock would have more rockfall because they crumble more easily, whereas cliffs of stronger rock types would have less rockfall since they would not produce as much debris. In this scenario, slope steepness would become a significant factor because slopes below the optimal steepness would be shallow enough that the debris could gradually accumulate along the slopes leading to regular rockfall events in both stronger and weaker rocks. Above the optimal steepness angle however, any debris that forms would immediately result in rockfall meaning that the frequency of rockfall would depend more on how much debris is accumulated and thus the rock strength.

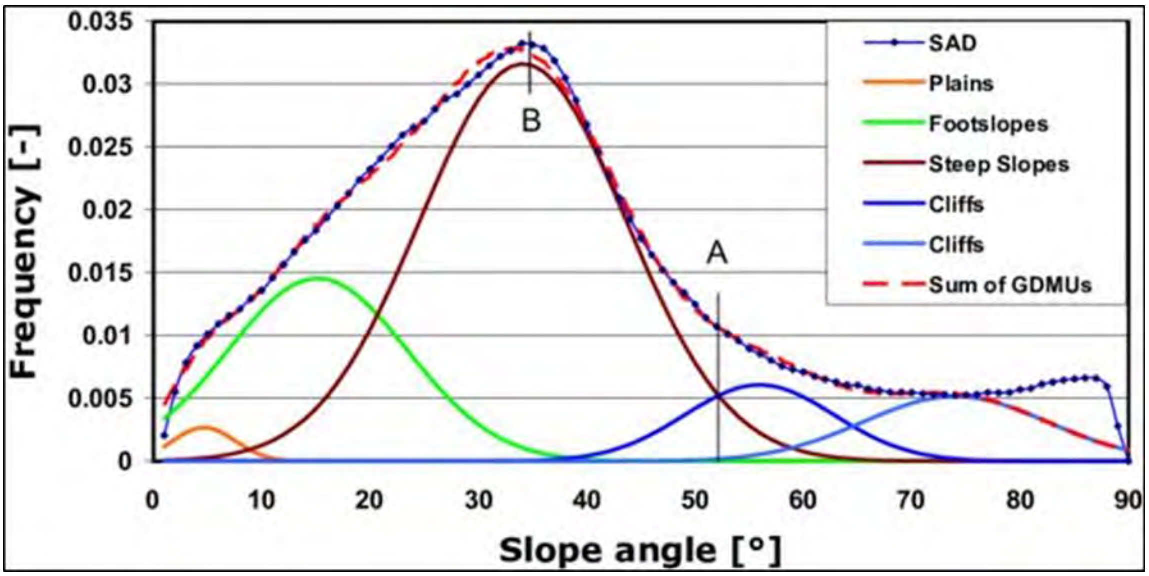

Figure 64: This figure from a study in the Swiss Alps demonstrates that, for different types of terrain in the region, the frequency of rockfall is greatest at a particular slope steepness which appears to be 35 degrees for this particular region. The slope steepness where rockfall events are most frequent is the optimal slope steepness (adapted from Loye and Jaboyedoff *et al*, 2009).

Angle of repose and coefficient of static friction

The angle of repose tends to increase with the coefficients of rolling and sliding friction of a material (Zhou and Xu *et al*, 2002). A material with a higher coefficient of rolling or static friction will tend to have a higher angle of repose, in general. As a result, a lithological type with a high coefficient of rolling or static friction would require a steeper angle for rockfall events to occur. A rock type with a lower coefficient of rolling or sliding friction would not need as steep of slopes to produce the same rockfall events also because of its angle of repose. This would explain why slope steepness plays a role in the frequency of rockfall events. Rockfall events occur when a build up of debris reaches a steepness that exceeds the angle of repose for the material composing it. In light of this explanation, the reason for a positive correlation between headwall steepness and the size of rock glaciers on Mars, could be related to the angle of repose of Martian rock material. If Martian material tends to have a certain angle of repose that happens to be steep compared to other types of material, it would explain why higher headwall steepness values are associated with greater rock glacier size since high slope values, close to that particular angle of repose, would mean high debris accumulation at the base of a slope.

Greater debris accumulation allows for more insulation of the glacial ice that is flowing beneath it (Colaprete and Jakoski, 1998). Because of greater insulation, the rock glacier or debris-covered glacier would last longer and be able to flow farther, thus increasing its length.

<u>Why Mars and Earth data differ in correlation</u>

If this is a real correlation between slope steepness and rock glacier length, the fact that it was not also found for Earth requires an explanation. One possible reason for this might be related to the fact that optimal slope steepness depends on the lithology of the local rocks (Marquinez *et al*, 2003; Dorren *et al*, 2004). It is possible that while steeper slopes are most optimal for the occurrence of rockfall in Martian rocks, this may not be the case for the rocks that compose the Sierra Nevada. This could be because of differences in the rock strength or the angle of repose in Sierra Nevada rocks versus Martian rocks.

For example, it could be that the steepest slopes in the Sierra Nevada tend to occur in the areas with the strongest rock so that rock debris will not vary significantly across the Sierra Nevada in regard to slope.

Earth also is probably not as uniform in rock type, and thus rock strength, as Mars, meaning that there will not be as discernible a pattern with respect to headwall steepness and rockfall on Earth as Mars where the rock type tends to be more uniform resulting in a more uniform pattern across the planet with respect to headwall steepness and rockfall.

Furthermore, if Earth has much steeper headwalls than Mars, especially in the Sierra Nevada, it may be that the slopes of the Sierra Nevada are above the optimal slope steepness so that rockfall depends more on rock strength than slope steepness, resulting in little or no correlation between headwall steepness and the size of rock glaciers in the Sierra Nevada.

Other differences in Earth results and Mars results

Parameter	Earth (Sierra Nevada)	Mars
Average rock-ice feature length (m)	640	6100
Average rock-ice feature height (m)	160	1200
Average headwall steepness (deg.)	31	17
Average rock-ice feature steepness (deg.)	17	11

Table 4: Martian glacial features in general have gentler slopes and are larger in scale than terrestrial features. The average head wall steepness results for Mars are 17 degrees while the terrestrial average gained for the Sierra Nevada is 31 degrees. The average rock glacier slope for Mars is 11 degrees which is 6 degrees lower than the average for the Sierra Nevada. The average rock glacier length for the Sierra Nevada is about 640 meters and the average rock glacier height is 160 m. The average values for Mars are 6100 m and 1200 m respectively.

Why are Martian rock glaciers larger than Earth rock glaciers?

Although this study suggests that steeper slopes result in larger rock glaciers, Martian rock glaciers tend to be much larger than rock glaciers on Earth despite having gentler headwall slopes. The reason for this is likely due to the scale of the surrounding terrain from which debris is derived. The alcoves and cirques in which Martian rock glaciers are found are often significantly larger than their terrestrial counterparts. This provides more surface area increasing the amount of debris that can be produced from weathering and erosion of the headwalls and cirque walls. Martian rock glaciers with alcoves that were the same size as the cirques of Earth rock glaciers might indeed be smaller than their Earth counterparts. Since Martian rock glaciers have such larger cirques, however, they tend to be much larger than their Earth equivalents.

Additionally, another reason that rock glaciers on Mars might be larger is the lack of regular ice glaciers. Glaciers on Earth tend to be much larger than rock glaciers. It is possible that in the dry Martian climate where exposed ice tends to sublimate, giant rock glaciers take the place of ice glaciers in areas which would have true ice glaciers in a more Earth-like environment.

Headwall steepness and rock glacier morphology on Earth and Mars

There are several possible reasons for the difference in headwall steepness between Earth and Mars noted above. These include the tectonic environment, temperature range, timescale, glaciation, and aspect.

Furthermore, if headwall steepness is a control on the distribution and size of rock-ice features, the factors that control headwall steepness are also important for the difference in size and distribution of rock glaciers and similar features on Earth, Mars, and other terrestrial planets.

Plate tectonics

I. Plate tectonics and headwall steepness

Tectonic processes on a planet can determine the kind of slopes which will exist in a region. On Earth, very steep slopes can be created at plate collision zones in the formation of oceanic trenches and mountains. Other parts of Earth's surface, such as the middle of the Pacific plate where the Hawaiian Islands are forming due to hotspot volcanism do not generally have steep slopes because the shield volcanoes formed in the process tend to have fairly gentle slopes. Even on Earth's surface, different tectonic environments can produce very different slopes.

Similar mountain ranges to those formed by plate collisions are typically not found on Mars today. The most common large Earth-like features on Mars that could be called mountains are shield volcanoes (Carr, 1976; Xiao *et al*, 2012) which generally produce relatively gentle slopes compared to mountain building involving plate collisions. The reason that Earth-like mountain ranges do not currently form on Mars is probably because Mars lacks Earth-like plate tectonics, though it may have briefly had such plate tectonics in the distant past (Breuer and Spohn, 2003).

II. Plate tectonics and rock glacier morphology

Furthermore, if the global tectonic environment affects slope steepness, it may also affect the size and growth of rock glaciers that form beneath those slopes. If the optimal steepness for the rock type dominant on a planetary surface is rare because local tectonic processes just don't produce slopes of that particular steepness, large rock glaciers may be rare on that planet.

Thermal weathering and erosion

Another factor affecting the differences in headwall steepness on Earth and Mars is thermal weathering, On Mars, the daily atmospheric temperature varies by as much as 60-90 degrees Celsius, whereas the temperature range for Earth is only 30-50 degrees

Celsius (Leovy, 2001). Greater temperature extremes on Mars may significantly increase thermal weathering, damaging the minerals within (Molaro and Byrne, 2012).

As temperatures change from throughout the day-night cycle, rocks will expand and contract. This gradually weakens the rock causing it to fragment into debris (Molaro an Byrne, 2012). Since the differences in night time and day time temperature on Mars tend to be much greater than on Earth, thermal weathering is likely to play a more important role not only in the creation of debris, but also the erosion of slopes, on Mars. This is because cliffs that are more fragmented from physical weathering will be more likely to erode. Greater thermal weathering could also result in more debris accumulation and larger rock glaciers because rock weakened by thermal weathering is more likely to crumble.

Past glaciation and headwall steepness

An additional factor that influences the local slope steepness is the presence of past glaciation. On Earth, particularly in the Sierra Nevada, many steep slopes have been created by ice glaciers as they have carved glacial valleys through mountain areas. On Mars, on the other hand, it is unclear that true ice glaciers were ever stable at the surface, making it less likely that the canyons on Mars were carved by glaciers. Since glaciers are known to create very steep slopes (Dorren *et al*, 2004), the lack of steep slopes on Mars may be partly because true ice glaciers are historically unusual, if not absent, on Mars.

Temperature and rock glacier morphology

Surface temperature is also a factor in the distribution of rock glaciers. Rock glaciers on Earth form at high elevations, often because these are the elevations at which rock ice-features can exist without the ice melting (Kerschner, 1978; Azocar and Brenning, 2010; Owen and England, 1998). The relative rarity of these high elevation areas on Earth, compared to areas of lower elevation, might be one reason why Earth rock glaciers tend to be smaller since limited suitably high elevation land area would mean less potential area over which ice and rock debris can accumulate to feed rock glaciers. On Mars, surface temperature also plays a role in the distribution of rock glaciers and other rock ice features. This may be one reason why rock-ice features occur in bands at the equator (Head and Neukum, 2005) and the mid-latitudes (Head *et al*, 2010; Pierce and Crown, 2003). The two bands are likely caused by changes in obliquity over time, causing ice to shift between lower latitudes and the poles periodically (Head and Neukum, 2005; Head *et al*, 2010). The low temperatures on Mars also affect the flow rate and shape of the rock glaciers. Martian rock glaciers are predicted to flow much more slowly (Mahaney, 2007; Colaprete and Jakosky, 1998).

Timescale

I. Timescale and headwall steepness

Another influence on headwall steepness is timescale. One Earth, plate tectonics happens rapidly enough that there are probably slopes that are only tens of thousands to millions of years old. These young slopes would have had less time to be subject to erosion and weathering from wind and water. The headwall slopes on Mars are likely much older, tens of millions if not billions of years old, because most of the slopes on Mars probably formed when the planet was more tectonically active (e.g., Carr and Head, 2010). This would mean that slopes on Mars would have much more time to be subject to erosion and weathering. In this way, timescale may also influence the difference in slope steepness between Earth and Mars.

II. Timescale and rock glacier morphology

The larger timescale on Mars also gives more time for debris to accumulate. It is possible that the reason that rock glaciers are on such a large scale on Mars is because they are old. Certain rock glaciers may have thicker debris mantles just because they are older and have had much more time to accumulate debris rather than having an optimal steepness for rockfall.

Aspect

I. Aspect and headwall steepness

Finally, aspect can also indirectly impact the steepness of slopes. Shadows can affect the amount of solar radiation slopes receive as well as the variation in solar radiation throughout the day and year (Molaro and Byrne, 2012). If a slope is regularly in shadow from topographic features at different parts of the day and year, it will have a different temperature pattern, and thus a different thermal weathering pattern, compared to regions which are not regularly in shadow. This is probably especially true on planetary bodies with little or no atmospheres where temperature differences are especially extreme. It is unclear whether shadowing would increase or decrease thermal weathering on slopes, but the effects of aspect should be taken into account since shadowing may significantly affect thermal weathering patterns. On Earth, it is known that ice preferentially accumulates on north-facing slopes because of shadows. On Earth this can result in the formation of ice glaciers which will steepen on Earth. It is uncertain that this ever happened on Mars, however.

II. Aspect and rock glacier morphology

Rock-ice features on Mars, especially in the southern hemisphere tend to be pole-facing (Arfstrom and Hartmann, 2005). Furthermore, deeper shadows tend to be associated with a higher density of rock glaciers (Brazier *et al*, 1998). This makes slopes with significant shadows more optimal for the formation and growth of rock-ice features. Shadow length is also affected by slope steepness which may represent another indirect way that headwall steepness may influence the behavior of rock glaciers and similar features.

Gravity

I. Gravity and headwall steepness

Another factor relevant to interplanetary differences in headwall steepness is gravity. There is a debate among planetary scientists over how higher gravity would affect plate tectonics. Some believe that, as gravity increases, the movement of tectonic plates would be inhibited slowing down or preventing Earth-like plate tectonics (O'Neill and Lenardic, 2007). Others disagree and believe that, below a certain threshold, larger gravity would accelerate plate tectonics or at least not affect it (Van Heck and Tackley, 2011; Valencia *et al*, 2007). If gravity is a control on plate tectonics, then gravity would also be a factor in slope steepness variations from planet to planet. The acceleration due to gravity on Mars is only 3.7 m/s^2 in contrast to 9.8 m/s^2 on Earth. This suggests that gravity is may be an important factor in tectonic differences between Earth and Mars and, as a result, a significant factor in differences in headwall steepness between the two planets.

II. Gravity and rock glacier morphology

Gravity also plays a role in rock glacier morphology. It has been suggested that rock glaciers will be also be proportionately thicker and less mobile on Mars due to gravity because the buildup of debris is what provides the gravitational driving force that leads to the deformation of the ice within the rock glacier (Mahaney *et al*, 2007). Lower gravity of Mars would lead to a lower driving force than on Earth and thus rock glaciers that flow more slowly. Earth rock glaciers on the other hand, would flow faster and be thinner because of higher gravity (Mahaney *et al,* 2007). If a Martian rock glacier and Earth rock glacier of the same scale and temperature were compared, the Martian rock glacier would be shorter and thicker because of gravity (Mahaney *et al*, 2007).

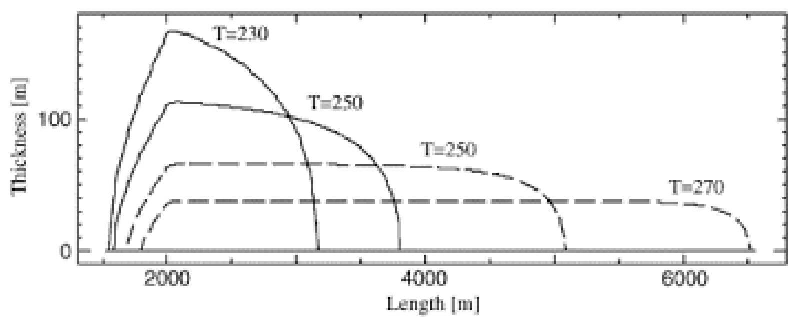

Figure 65: a diagram showing the difference in thickness of a rock glacier with temperature, the solid line is for Mars conditions and the dotted line is for Earth conditions. Low temperature conditions make the rock glacier shorter and thicker. At the same ice temperature, rock glaciers on Earth would be longer and thinner because of gravity (adapted from Mahaney *et al*, 2007).

Headwall steepness and planetary variations in gravity, temperature, and physical scale

The principle of the interplay between gravity and temperature and its effects on rock-ice flow features can also be applied to planets beyond Earth and Mars. While rock glaciers on Mars are likely to flow more slowly and be thicker and shorter than rock glaciers on

Earth of the same scale and temperature because of gravity (Mahaney *et al*, 2007), rock glaciers on super-earths, terrestrial planets more massive than Earth, are likely to flow faster and be thinner and longer than Earth rock glaciers of the same scale and temperature. This is because of a higher acceleration due to gravity on the super-earth. Less debris accumulation would be required to build up a driving force for the deformation of subsurface ice on a super-earth compared to the driving for needed for an equivalent deformation on Earth. As a result, a rock glacier on a super-earth with the same crust lithology would not need as much debris accumulation to reach a length equivalent to an Earth rock glacier of the same scale and temperature.

The influence of gravity on the driving force of the deformation of ice within a rock glacier is important because the deformation rate determines the flow rate. The flow rate, in turn, determines the resulting length of the rock glacier after a given period of time. Suppose that three rock glaciers, one on Earth, one on Mars, and one on a hypothetical super-earth, that are of the same size scale and temperature are compared. If they are to reach the same length in the same amount of time, the Martian rock glacier would require more debris accumulation than the Earth rock glacier while the super-earth rock glacier would require less.

This simple scenario is made a lot more complicated if headwall steepness is also a control on debris accumulation since it means that tectonics as well as other factors affecting slope steepness, such as timescale, temperature, aspect, and weathering styles, all have to be taken into account when studying rock glacier morphology and behavior. This is especially true if rock glaciers are being used to predict past climate changes in situations where the factors are not all uniform, such as when studying paleoclimate on multiple planets. For this reason, it is worth considering the influence of headwall or slope steepness on rock glacier morphology.

Interplay of all factors

Some factors seem to have a stronger influence on the behavior of Martian rock-ice features on others. The findings of this study are generally consistent with what would be expected of slopes on Mars based on plate tectonics. The slopes on Mars tend to be less steep than those on Earth because Mars lacks the mountain-building mechanisms which have created especially steep slopes on Earth.

Surface temperature may play an important role especially along the equator. Rock-ice features are rare along the equator, except for potential fossil forms in Valles Marineris. On the other hand, more rock ice features are found in the vicinity of Arsia Mons and Olympus Mons. On the other hand, the rock-ice features on Arsia Mons and Olympus Mons may also be fossils. Surface temperature does play an important role latitudinally, since rock-ice features for the most part restricted to the mid-latitudes and the equator appears to currently be too warm.

Furthermore, it is unclear how significant aspect is in the formation of rock-ice features on Mars. The results of this study do not give conclusive results which may be due to a small sample size.

Another factor that was discussed is the lack of ice glaciers since ice glaciers are known for producing steep slopes. Overall, the findings of this study are consistent with a lack of ice glaciers carving steep canyons in the Martian past. The steep slopes associated with ice glaciers on Mars are not found. On the other hand, possible debris covered glaciers have been found which suggests that a lack of steep slopes is not inconsistent with the presence of ice glaciers. In this case, the presence or lack of ice glaciers would not explain the slope steepness of Mars since ice glaciers may have been present on Mars in the form of debris covered glaciers and steep slopes associated with Earth glaciers are still not found.

Ice temperature and gravity would both suggest that Martian rock glaciers would be shorter and thicker than those on Earth, but Martian rock-ice features in this study were on average larger than Earth rock glaciers. One possibility is that timescale, and perhaps thermal weathering, is a stronger factor in some cases since rock-ice features are likely to be much older than rock-ice features on Earth and thermal weathering may result in more debris necessary for large rock glaciers.

Implications for paleoclimate studies of Mars

If headwall steepness is a non-climatic factor that effects the size and behavior of rock glaciers and similar flow-features, the tentative correlation between rock glacier length and headwall steepness found in this study for Mars has implications for any paleoclimate studies on Mars using rock glaciers an other rock-ice features to study the climate history of the planet.

The reigning paradigm to understand glacial phenomena on Mars is the Martian obliquity cycle (Head and Neukum, 2005; Head *et al*, 2010). The presence and behavior of rock-ice features can be used to test this explanation for variations in Martian climate. At maximum obliquity, the angle of insolation would be greater at the polar regions causing the ice to migrate to lower latitudes (Head *et al*, 2010). As this cycle repeats, a record should have gradually built up of glacial features waxing, reaching a maximum, and then waning as the obliquity changes to a value that is suboptimal for glaciers at that latitude.

Evaluating this hypothesis is beyond the scope of this study, but the results of this study have implications for such a hypothesis. Testing this hypothesis would require examining the Martian geologic record and looking for signatures of this cycle. One of these signatures would be a series of glaciations recorded in the geologic record that fits the pattern predicted by the hypothesis. Identifying these glaciations requires knowing the relative age of the related features, such as rock glaciers and debris covered glaciers.

It has been suggested that the presence of ice indicates an active rock glacier while the absence of ice indicates that it is fossil or extinct (Giardino and Vitek, 1988). On Mars, this probably works as long as the rock ice feature flows. As a result, the presence of residual ice would indicate that it is relatively young while a lack of ice, or even very little ice, may indicate that a feature is a fossil and quite old. Thus, a rock glacier with residual ice might belong to the most recent obliquity period while one that no longer contains ice but still has some of the morphological features of a rock glacier might belong to the one before that.

One problem with this simple approach, however, is that it assumes that the ice from a cycle before the last one will always melt or sublimate completely. If there is an extraneous factor, such as an unusually thick debris mantle, then the age results might be skewed. Researchers might think that a glacial feature is from a later period when in fact it is much older, and the ice has just been more well preserved than in other rock-ice features of similar age.

If a thicker debris mantle has this effect, then knowing that these thicker mantles form may allow future workers in the field to develop a correction factor. This correction factor could be used to adjust for the offset in age caused by non-climatic factors such as steep slopes that result in higher-than-expected debris accumulation.

Future work

The relationship between slope value and rockfall as an explanation for the correlation observed in this study fits with the predicted flow behavior of Martian rock glaciers and the predicted flow behavior of rock glaciers on Earth (Mahaney, 2007) as well as super-earths, but how could it be tested? One way to test this explanation, without going to Mars, would be to find terrestrial cliffs with lithologies very similar to Martian rocks and determine the slope steepness for the local rock type most optimal for producing significant amounts rockfall. Once this slope value is found, it could be compared to the average slope values found on Mars associated with the valley walls adjacent to the longest glacial features.

This could not be done in this study due to time constraints, but another follow up investigation that could be done would be to use structure from motion techniques to analyze high resolution images of the Martian rock-ice features that can be detected on the surface. This could be done to more accurately determine the 3-dimensional structure of rock-ice features and further constrain whether they are in fact rock glaciers or similar rock-ice features.

CONCLUSION

The purpose of this study has been to determine if there is a correlation between head wall steepness and any aspects of rock glacier behavior and structure that might have implications for paleoclimate studies on planets with water-ice cryospheres, such as Earth and Mars. For Mars, such a correlation has been found between head wall steepness and rock glacier length.

One possible explanation for this positive correlation between headwall steepness and rock glacier size is the existence of an optimal slope steepness angle on Mars where rock glaciers with headwalls with steepness closest to the steepness angle produce the most rockfall allowing for the formation of larger rock glaciers. This optimal slope steepness appears to be related to rock strength and the angle of repose and is probably determined by lithology as well as tectonics. It is thus a non-climatic factor in the morphology and behavior of rock glaciers.

The reason that the correlation does not occur on Earth may be because of the difference in the optimal slope steepness for the lithologies that make up the Sierra Nevada. The slopes in the Sierra Nevada probably also differ from the average slopes on Mars because of differences in tectonic processes. Earth-like plate tectonics tends to produce steeper slopes than the tectonic and mountain-building processes common on Mars.

In addition to lithology and tectonics, other factors influencing headwall steepness and rock glacier morphology may include tectonics, surface temperature, thermal weathering, aspect, absence of past glaciers, and an interplay of ice temperature and gravity.

This phenomenon of a correlation between slope and increasing occurrence of rock fall, if it is accurate, has implications for paleoclimate studies since it may result in some rock glaciers looking younger than their true age on account of greater amounts of preserved ice. This could skew the reconstruction of past glaciations on Mars.

Additionally, since rock glaciers are reservoirs of water ice (Azocar and Brenning, 2010; Miller and Westfall, 2008), mapping of rock glaciers will also be important for identifying water resources. On Earth, significant amounts of water are contained in rock glaciers in some mountain ranges (Azocar and Brenning, 2010; Brenning, 2005; Miller and Westfall, 2008). On Mars, it will be important for future explorers who need to replenish their water supplies while living off the land. Knowing that steeper valley walls generally result in larger rock glaciers with more insulation, and thus more preserved ice, would be helpful in identifying which regions on which to focus for finding glacial features that might still contain significant amounts of ice.

Because of the implications of the tentative results of this study, there is good reason for a more in-depth study of the relation between headwall steepness and rock glacier size and its implications for the occurrence of rockfall.

REFERENCES

Anderson, F. Scott, Albert FC Haldemann, Nathan T. Bridges, Matthew P. Golombek, Timothy J. Parker, and Gregory Neumann. "Analysis of MOLA data for the Mars Exploration Rover landing sites." *Journal of Geophysical Research: Planets* 108, no. E12 (2003).

Angillieri, María Yanina Esper. "Application of frequency ratio and logistic regression to active rock glacier occurrence in the Andes of San Juan, Argentina." *Geomorphology* 114, no. 3 (2010): 396-405

Arfstrom, John, and William K. Hartmann. "Martian flow features, moraine-like ridges, and gullies: Terrestrial analogs and interrelationships." *Icarus* 174, no. 2 (2005): 321-335.

Azócar, G. F., and A. Brenning. "Hydrological and geomorphological significance of rock glaciers in the dry Andes, Chile (27–33 S)." *Permafrost and Periglacial Processes* 21, no. 1 (2010): 42-53.

Batalha, Natalie M., Jason F. Rowe, Stephen T. Bryson, Thomas Barclay, Christopher J. Burke, Douglas A. Caldwell, Jessie L. Christiansen et al. "Planetary candidates observed by Kepler. III. Analysis of the first 16 months of data." *The Astrophysical Journal Supplement Series* 204, no. 2 (2013): 24.

Batygin, Konstantin, and Michael E. Brown. "Evidence for a distant giant planet in the solar system." *The Astronomical Journal* 151, no. 2 (2016): 22.

Bowerman, Nicole D., and Douglas H. Clark. "Holocene glaciation of the central Sierra Nevada, California." *Quaternary Science Reviews* 30, no. 9-10 (2011): 1067-1085.

Brazier, Vanessa, Martin P. Kirkbride, and Ian F. Owens. "The relationship between climate and rock glacier distribution in the Ben Ohau Range, New Zealand." *Geografiska Annaler: Series A, Physical Geography* 80, no. 3-4 (1998): 193-207.

Brenning, Alexander. "Geomorphological, hydrological and climatic significance of rock glaciers in the Andes of Central Chile (33–35 S)." *Permafrost and Periglacial Processes* 16, no. 3 (2005): 231-240.

Breuer, D., and T. Spohn. "Early plate tectonics versus single-plate tectonics on Mars: Evidence from magnetic field history and crust evolution." *Journal of Geophysical Research: Planets* 108, no. E7 (2003).

Burnett, Benjamin N., Grant A. Meyer, and Leslie D. McFadden. "Aspect-related microclimatic influences on slope forms and processes, northeastern Arizona." *Journal of Geophysical Research: Earth Surface* 113, no. F3 (2008).

Carr, Michael H. "The volcanoes of Mars." *Scientific American* 234, no. 1 (1976): 32-43.

Carr, Michael H., and James W. Head III. "Geologic history of Mars." *Earth and*

Planetary Science Letters 294, no. 3-4 (2010): 185-203.

Carter, John, Damien Loizeau, Nicolas Mangold, François Poulet, and Jean-Pierre Bibring. "Widespread surface weathering on early Mars: A case for a warmer and wetter climate." *Icarus* 248 (2015): 373-382.

Colaprete, Anthony, and Bruce M. Jakosky. "Ice flow and rock glaciers on Mars." *Journal of Geophysical Research: Planets*103, no. E3 (1998): 5897-5909.

Dorren, Luuk KA, Bernhard Maier, Uif S. Putters, and Arie C. Seijmonsbergen. "Combining field and modelling techniques to assess rockfall dynamics on a protection forest hillslope in the European Alps." *Geomorphology* 57, no. 3-4 (2004): 151-167.

Grotzinger, John P., Do Y. Sumner, L. C. Kah, K. Stack, S. Gupta, L. Edgar, D. Rubin et al. "A habitable fluvio-lacustrine environment at Yellowknife Bay, Gale Crater, Mars." *Science.* 343, no. 6169 (2014): 1242777.

Giardino, John R., and John D. Vitek. "The significance of rock glaciers in the glacial-periglacial landscape continuum." *Journal of Quaternary Science* 3, no. 1 (1988): 97-103.

Head, James W., David R. Marchant, James L. Dickson, Ailish M. Kress, and David M. Baker. "Northern mid-latitude glaciation in the Late Amazonian period of Mars: Criteria for the recognition of debris-covered glacier and valley glacier landsystem deposits." *Earth and Planetary Science Letters*294, no. 3-4 (2010): 306-320

Head, James W., and David R. Marchant. "The climate history of early Mars: insights from the Antarctic McMurdo Dry Valleys hydrologic system." *Antarctic Science* 26, no. 6 (2014): 774-800.

Head, J. W., G. Neukum, R. Jaumann, H. Hiesinger, E. Hauber, M. Carr, Ph Masson et al. "Tropical to mid-latitude snow and ice accumulation, flow and glaciation on Mars." *Nature* 434, no. 7031 (2005): 346.

Hippolyte, Jean-Claude, Didier Bourlès, Régis Braucher, Julien Carcaillet, Laëtitia Léanni, Maurice Arnold, and Georges Aumaitre. "Cosmogenic 10Be dating of a sackung and its faulted rock glaciers, in the Alps of Savoy (France)." *Geomorphology* 108, no. 3-4 (2009): 312-320.

Hubbard, Bryn, Ralph E. Milliken, Jeffrey S. Kargel, Ajay Limaye, and Colin Souness. "Geomorphological characterisation and interpretation of a mid-latitude glacier-like form: Hellas Planitia, Mars." *Icarus* 211, no. 1 (2011): 330-346.

Holt, John W., Ali Safaeinili, Jeffrey J. Plaut, James W. Head, Roger J. Phillips, Roberto Seu, Scott D. Kempf et al. "Radar sounding evidence for buried glaciers in the southern mid-latitudes of Mars." *Science* 322, no. 5905 (2008): 1235-1238.

Jakob, Matthias. "Active rock glaciers and the lower limit of discontinuous alpine permafrost, Khumbu Himalaya, Nepal." *Permafrost and Periglacial Processes* 3, no. 3 (1992): 253-256.

Johnsson, A., D. Reiss, E. Hauber, M. Zanetti, H. Hiesinger, L. Johansson, and M. Olvmo. "Periglacial mass-wasting landforms on Mars suggestive of transient liquid water in the recent past: Insights from solifluction lobes on Svalbard." *Icarus* 218, no. 1 (2012): 489-505.

Kerschner, Hanns. "Paleoclimatic inferences from Late Wurm rock glaciers, eastern central Alps, western Tyrol, Austria." *Arctic and Alpine Research* 10, no. 3 (1978): 635-644

Kreslavsky, Mikhail A., and James W. Head. "Kilometer-scale roughness of Mars: Results from MOLA data analysis." *Journal of Geophysical Research: Planets* 105, no. E11 (2000): 26695-26711.

Leovy, Conway. "Weather and climate on Mars." *Nature* 412, no. 6843 (2001): 245.

Le Deit, Laetitia, Jessica Flahaut, Cathy Quantin, Ernst Hauber, Daniel Mège, Olivier Bourgeois, Joanna Gurgurewicz, Marion Massé, and R. Jaumann. "Extensive surface pedogenic alteration of the Martian Noachian crust suggested by plateau phyllosilicates around Valles Marineris." *Journal of Geophysical Research: Planets* 117, no. E11 (2012).

Loye, A., M. Jaboyedoff, and A. Pedrazzini. "Identification of potential rockfall source areas at a regional scale using a DEM-based geomorphometric analysis." *Natural*

Hazards and Earth System Sciences 9, no. 5 (2009): 1643-1653.

Mahaney, William C., Hideaki Miyamoto, James M. Dohm, Victor R. Baker, Nathalie A. Cabrol, Edmond A. Grin, and Daniel C. Berman. "Rock glaciers on Mars: Earth-based clues to Mars' recent paleoclimatic history." *Planetary and Space Science* 55, no. 1-2 (2007): 181-192.

Marquinez, J., R. Menéndez Duarte, P. Farias, and M. Jimenez Sanchez. "Predictive GIS-based model of rockfall activity in mountain cliffs." *Natural Hazards* 30, no. 3 (2003): 341-360.

McGregor, V. R. "Holocene moraines and rock glaciers in the central Ben Ohau Range, south Canterbury, New Zealand." *Journal of glaciology* 6, no. 47 (1967): 737-748.

Mège, Daniel, and Olivier Bourgeois. "Equatorial glaciations on Mars revealed by gravitational collapse of Valles Marineris wallslopes." *Earth and Planetary Science Letters* 310, no. 3-4 (2011): 182-191.

Millar, Constance I., and Robert D. Westfall. "Rock glaciers and related periglacial landforms in the Sierra Nevada, CA, USA; inventory, distribution and climatic relationships." *Quaternary International* 188, no. 1 (2008): 90-104.

Molaro, Jamie, and Shane Byrne. "Rates of temperature change of airless landscapes and implications for thermal stress weathering." *Journal of Geophysical Research: Planets*117, no. E10 (2012).

O'neill, C., and A. Lenardic. "Geological consequences of super-sized Earths." *Geophysical Research Letters* 34, no. 19 (2007).

Owen, Lewis A., and John England. "Observations on rock glaciers in the Himalayas and Karakoram Mountains of northern Pakistan and India." *Geomorphology* 26, no. 1-3 (1998): 199-213.

Phillips, Fred M., Marek Zreda, Mitchell A. Plummer, David Elmore, and Douglas H. Clark. "Glacial geology and chronology of Bishop Creek and vicinity, eastern Sierra Nevada, California." *Geological Society of America Bulletin*121, no. 7-8 (2009): 1013-1033.

Pierce, Timothy L., and David A. Crown. "Morphologic and topographic analyses of debris aprons in the eastern Hellas region, Mars." *Icarus* 163, no. 1 (2003): 46-65.

Roach, Leah H., John F. Mustard, Gregg Swayze, Ralph E. Milliken, Janice L. Bishop, Scott L. Murchie, and Kim Lichtenberg. "Hydrated mineral stratigraphy of Ius Chasma, Valles Marineris." *Icarus* 206, no. 1 (2010): 253-268.

Roer, Isabelle, Wilfried Haeberli, Michael Avian, Viktor Kaufmann, Reynald Delaloye, Christophe Lambiel, and Andreas Kääb. "Observations and considerations on destabilizing active rock glaciers in the European Alps." In *Ninth International Conference on Permafrost*, vol. 2, pp. 1505-1510. Fairbanks, Alaska: Institute of Northen Ingeneering, University of Alaska Fairanks, 2008.

Rood, Dylan H., Douglas W. Burbank, and Robert C. Finkel. "Chronology of glaciations in the Sierra Nevada, California, from 10Be surface exposure dating." *Quaternary Science Reviews* 30, no. 5-6 (2011): 646-661.

Seu, Roberto, Roger J. Phillips, Daniela Biccari, Roberto Orosei, Arturo Masdea, Giovanni Picardi, Ali Safaeinili et al. "SHARAD sounding radar on the Mars Reconnaissance Orbiter." *Journal of Geophysical Research: Planets* 112, no. E5 (2007).

Shroder, John F., Michael P. Bishop, Luke Copland, and Valerie F. Sloan. "Debris-covered glaciers and rock glaciers in the Nanga Parbat Himalaya, Pakistan." *Geografiska Annaler: Series A, Physical Geography* 82, no. 1 (2000): 17-31.

Van Heck, H. J., and P. J. Tackley. "Plate tectonics on super-Earths: Equally or more likely than on Earth." *Earth and Planetary Science Letters* 310, no. 3-4 (2011): 252-261

Wordsworth, Robin, F. Forget, E. Millour, J. W. Head, J-B. Madeleine, and B. Charnay. "Global modelling of the early martian climate under a denser CO2 atmosphere: Water cycle and ice evolution." *Icarus* 222, no. 1 (2013): 1-19.

Whalley, W. Brian, and Fethi Azizi. "Rock glaciers and protalus landforms: Analogous forms and ice sources on Earth and Mars." *Journal of Geophysical Research: Planets* 108, no. E4 (2003).

Wilson, J. H., and J. F. Mustard. "Exposures of olivine-rich rocks in the vicinity of Ares Vallis: Implications for Noachian and Hesperian volcanism." *Journal of Geophysical Research: Planets* 118, no. 5 (2013): 916-929.

Xiao, Long, Jun Huang, Philip R. Christensen, Ronald Greeley, David A. Williams, Jiannan Zhao, and Qi He. "Ancient volcanism and its implication for thermal evolution of Mars." *Earth and Planetary Science Letters* 323 (2012): 9-18

Zhou, Y. C., Bao Hua Xu, Ai-Bing Yu, and P. Zulli. "An experimental and numerical study of the angle of repose of coarse spheres." *Powder technology* 125, no. 1 (2002): 45-54.

APPENDIX 1

Rock-ice features used in thesis and in quantitative study and illustration

Feature designation	Image	Location	Extra notes
SNRGLF 1	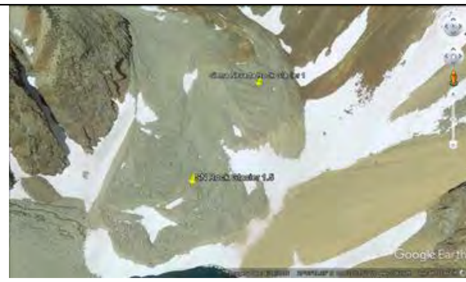	Sierra Nevada, Earth 37°53'48.42"N 119°12'11.29"W	
SNRGLF 4		Sierra Nevada, Earth 37°55'18.57"N 119°12'18.77"W	
SNRGLF 5	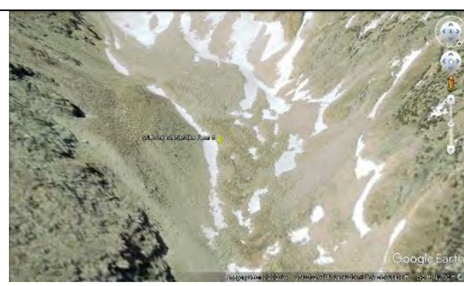	Sierra Nevada, Earth 37°55'51.20"N 119°12'55.21"W	
SNRGLF 12		Sierra Nevada, Earth 38° 9'53.86"N 119°26'33.70"W	

SNRGLF 17		Sierra Nevada, Earth 37°31'29.60"N 118°49'50.64"W	
SNRGLF 19		Sierra Nevada, Earth 37°31'20.53"N 118°49'32.15"W	
SNRGLF 24		Sierra Nevada, Earth 37°24'10.44"N 118°47'29.89"W	
SNRGLF 25		Sierra Nevada, Earth 37°24'34.58"N 118°48'13.29"W	
SNRGLF 27	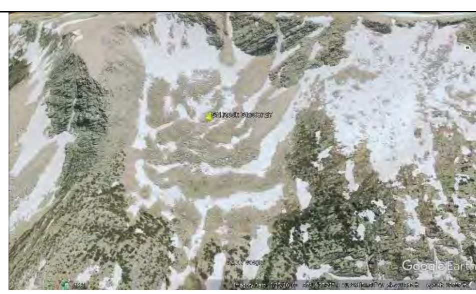	Sierra Nevada, Earth 37°19'32.89"N 118°44'52.74"W	

SNRGLF 28		Sierra Nevada, Earth 36°55'45.38"N 118°22'16.38"W	
SNRGLF 29		Sierra Nevada, Earth 36°54'13.30"N 118°21'28.65"W	
SNRGLF 30		Sierra Nevada, Earth 36°52'31.25"N 118°21'26.69"W	
SNRGLF 31		Sierra Nevada, Earth 36°52'58.25"N 118°20'39.45"W	
SNRGLF 32		Sierra Nevada, Earth 36°53'45.68"N 118°20'57.72"W	

SNRGLF 33		Sierra Nevada, Earth 36°52'59.13"N 118°20'59.89"W	
SNRGLF 34		Sierra Nevada, Earth 36°52'15.57"N 118°22'46.02"W	
SNRGLF 35		Sierra Nevada, Earth 36°47'21.38"N 118°24'14.84"W	
SNRGLF 36		Sierra Nevada, Earth 36°48'7.00"N 118°21'48.95"W	
SNRGLF 37		Sierra Nevada, Earth 36°42'9.54"N 118°25'27.56"W	

SNRGLF 38		Sierra Nevada, Earth 36°42'8.97"N 118°24'40.87"W	
SNRGLF 39		Sierra Nevada, Earth 36°42'18.82"N 118°23'8.50"W	
SNRGLF 40		Sierra Nevada, Earth 36°42'14.68"N 118°22'34.63"W	
SNRGLF 41	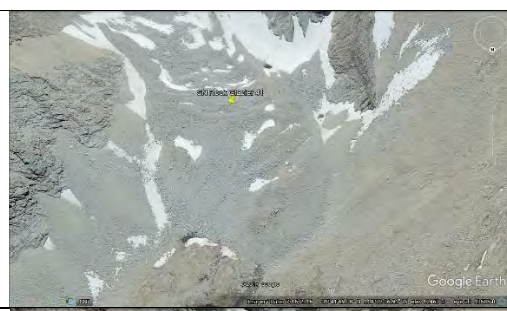	Sierra Nevada, Earth 36°41'46.32"N 118°22'5.51"W	
SNRGLF 42		Sierra Nevada, Earth 36°42'10.43"N 118°24'10.04"W	

SNRGLF 43		Sierra Nevada, Earth 36°42'50.86"N 118°23'34.58"W	
SNRGLF 44		Sierra Nevada, Earth 36°43'22.40"N 118°23'34.17"W	
SNRGLF 45		Sierra Nevada, Earth 36°41'29.98"N 118°27'0.17"W	
SNRGLF 46	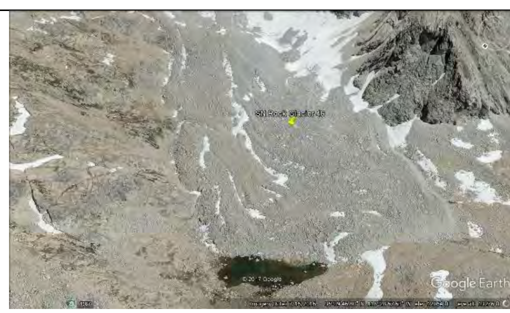	Sierra Nevada, Earth 36°39'44.00"N 118°28'57.13"W	
SNRGLF 47	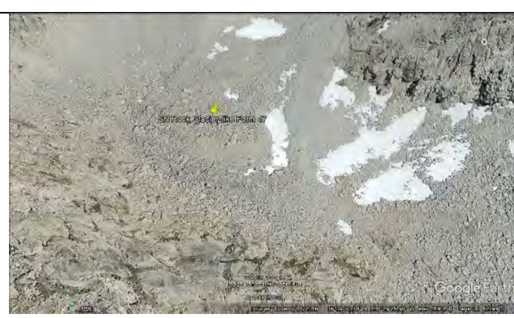	Sierra Nevada, Earth 36°39'1.07"N 118°29'24.59"W	

SNRGLF 48		Sierra Nevada, Earth 36°39'19.27"N 118°29'5.51"W	
SNRGLF 49		Sierra Nevada, Earth 36°43'9.52"N 118°29'56.03"W	
SNRGLF 50		Sierra Nevada, Earth 36°44'58.13"N 118°30'4.89"W	
SNRGLF 51		Sierra Nevada, Earth 36°42'24.53"N 118°28'28.60"W	
SNRGLF 52		Sierra Nevada, Earth 36°44'47.30"N 118°21'7.79"W	

SNRGLF 53		Sierra Nevada, Earth 36°42'16.34"N 118°21'3.71"W	
SNRGLF 54		Sierra Nevada, Earth 36°42'46.46"N 118°20'41.08"W	
SNRGLF 55		Sierra Nevada, Earth 36°42'26.66"N 118°20'49.51"W	
SNRGLF 56		Sierra Nevada, Earth 36°41'14.48"N 118°28'23.39"W	
SNRGLF 57		Sierra Nevada, Earth 36°37'30.68"N 118°17'54.92"W	

SNRGLF 58		Sierra Nevada, Earth 36°36'38.53"N 118°17'26.17"W	
SNRGLF 59		Sierra Nevada, Earth 36°35'48.75"N 118°15'38.92"W	
SNRGLF 60		Sierra Nevada, Earth 36°36'23.12"N 118°15'41.19"W	
SNRGLF 61		Sierra Nevada, Earth 36°34'37.90"N 118°17'5.25"W	

SNRGLF 62		Sierra Nevada, Earth 36°34'1.26"N 118°17'12.68"W	
SNRGLF 63		Sierra Nevada, Earth 36°33'46.53"N 118°17'3.64"W	
SNRGLF 64		Sierra Nevada, Earth 36°33'33.95"N 118°16'22.63"W	
SNRGLF 65		Sierra Nevada, Earth 36°35'25.04"N 118°18'37.15"W	

SNRGLF 66		Sierra Nevada, Earth 36°36'4.46"N 118°16'24.58"W	
SNRGLF 67		Sierra Nevada, Earth 36°39'32.73"N 118°17'39.64"W	
SNRGLF 68		Sierra Nevada, Earth 36°39'23.38"N 118°19'50.06"W	
SNRGLF 69		Sierra Nevada, Earth 36°32'23.42"N 118°14'37.42"W	

SNRGLF 71		Sierra Nevada, Earth 36°32'9.96"N 118°28'59.24"W	
SNRGLF 72	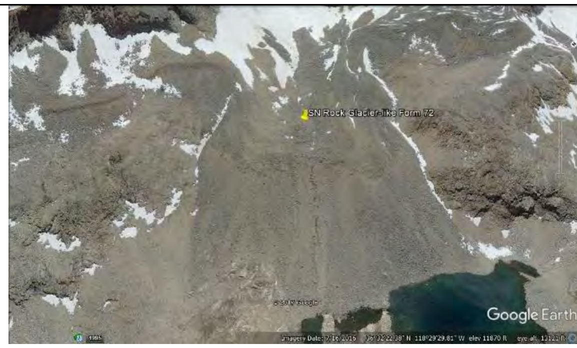	Sierra Nevada, Earth 36°32'20.09"N 118°29'33.57"W	
SNRGLF 73	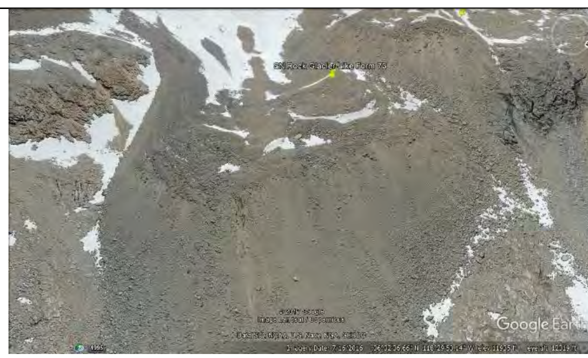	Sierra Nevada, Earth 36°32'34.94"N 118°29'59.41"W	
SNRGLF 74		Sierra Nevada, Earth 36°32'37.56"N 118°30'8.83"W	

<table>
<tr><td>SNRGLF 75</td><td>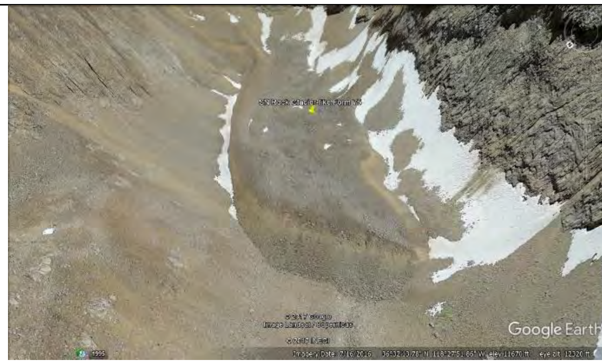
</td><td>Sierra Nevada,
Earth
36°32'9.93"N
118°27'46.37"W</td><td></td></tr>
<tr><td>SNRGLF 77</td><td>
</td><td>Sierra Nevada,
Earth
36°33'37.20"N
118°30'28.83"W</td><td></td></tr>
<tr><td>SNRGLF 78</td><td>
</td><td>Sierra Nevada,
Earth
36°33'5.02"N
118°30'10.07"W</td><td></td></tr>
<tr><td>SNRGLF 79</td><td>
</td><td>Sierra Nevada,
Earth
36°37'27.14"N
118°28'9.44"W</td><td></td></tr>
</table>

SNRGLF 80		Sierra Nevada, Earth 36°37'27.91"N 118°28'4.94"W	
SNRGLF 81		Sierra Nevada, Earth 36°38'50.07"N 118°28'55.88"W	
SNRGLF 82	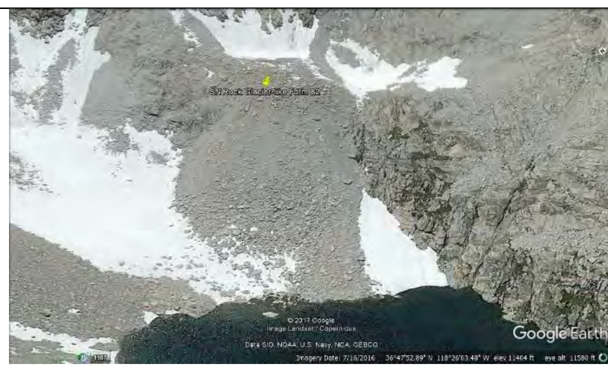	Sierra Nevada, Earth 36°47'50.28"N 118°26'4.35"W	
SNRGLF 83	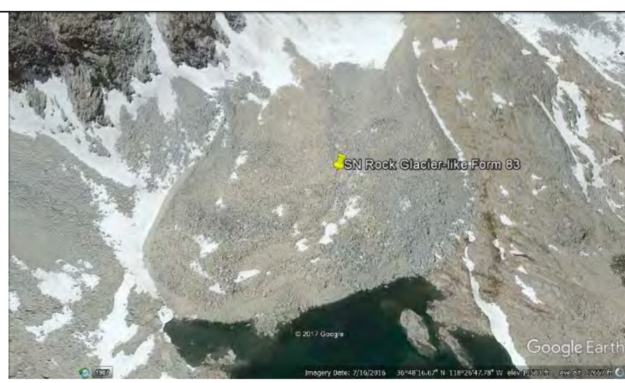	Sierra Nevada, Earth 36°48'16.38"N 118°26'49.34"W	

SNRGLF 84	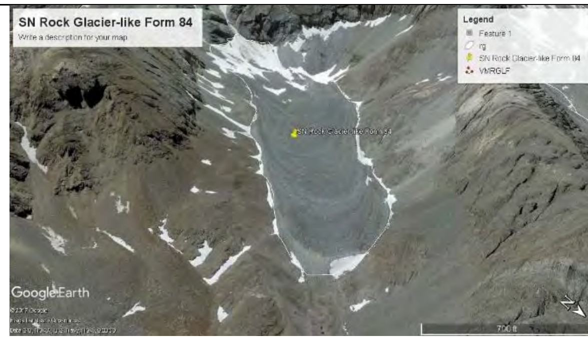	Sierra Nevada, Earth 37° 2'41.92"N 118°25'46.82"W	
SNRGLF 85	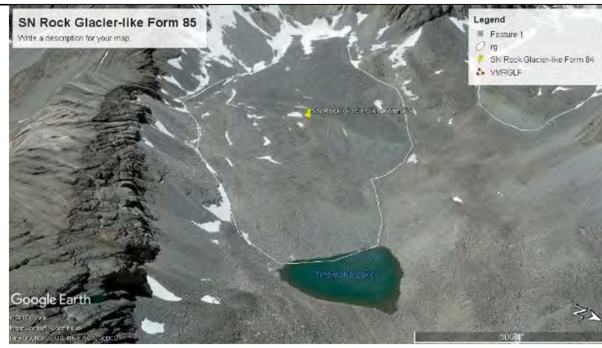	Sierra Nevada, Earth 37° 2'15.39"N 118°24'35.15"W	
SNRGLF 86		Sierra Nevada, Earth 37° 2'58.29"N 118°25'10.60"W	
SNRGLF 87		Sierra Nevada, Earth 37° 2'15.39"N 118°24'35.15"W	

SNRGLF 88		Sierra Nevada, Earth 37° 2'58.29"N 118°25'10.60"W	
SNRGLF 89		Sierra Nevada, Earth 37° 3'51.75"N 118°25'48.96"W	
SNRGLF 90		Sierra Nevada, Earth 37° 4'51.97"N 118°27'1.39"W	
SNRGLF 91		Sierra Nevada, Earth 37° 9'32.80"N 118°32'14.77"W	

SNRGLF 92		Sierra Nevada, Earth 37° 4'6.77"N 118°39'27.73"W	
SNRGLF 93		Sierra Nevada, Earth 37° 5'8.00"N 118°41'1.84"W	
SNRGLF 94		Sierra Nevada, Earth 37°17'15.02"N 118°47'16.60"W	
SNRGLF 95	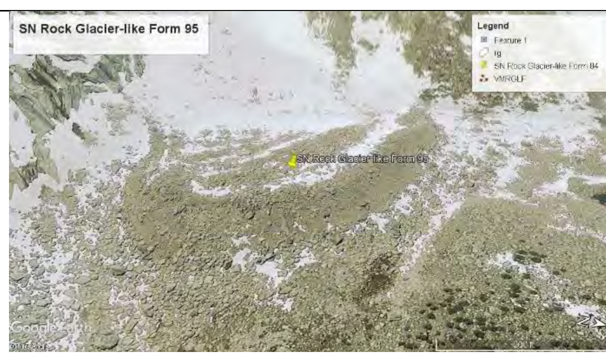	Sierra Nevada, Earth 37°17'22.39"N 118°47'22.65"W	

SNRGLF 96		Sierra Nevada, Earth 37°21'54.55"N 118°49'55.07"W	
SNRGLF 97	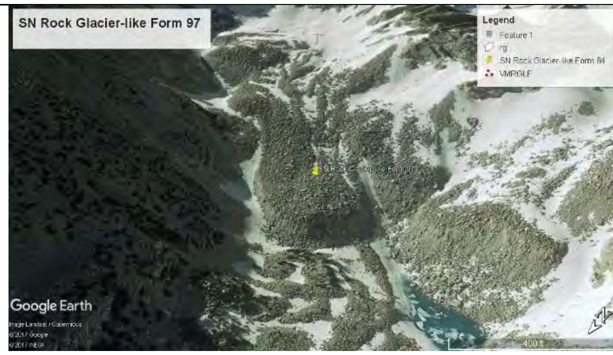	Sierra Nevada, Earth 37°25'2.33"N 118°49'13.41"W	
SNRGLF 98	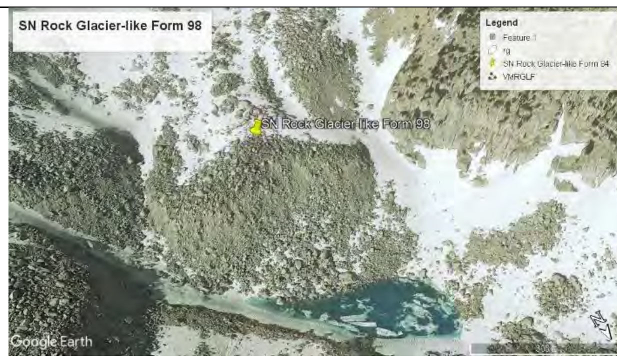	Sierra Nevada, Earth 37°25'0.44"N 118°49'22.76"W	
SNRGLF 99	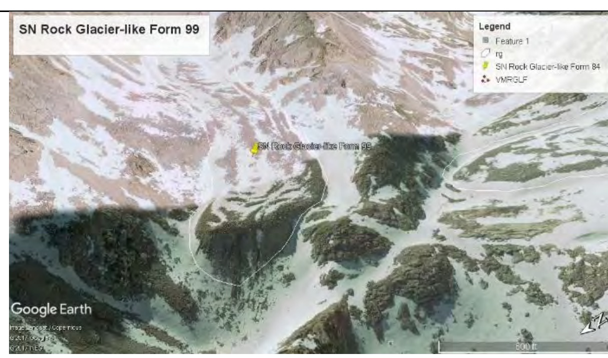	Sierra Nevada, Earth 37°23'18.63"N 118°47'40.27"W	

<table>
<tr><td>SNRGLF 100</td><td>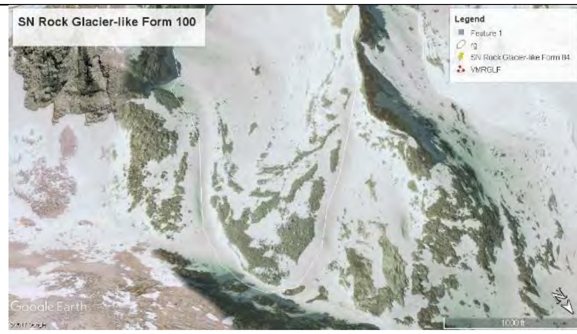
</td><td>Sierra Nevada,
Earth
37°23'1.76"N
118°47'55.00"W</td><td></td></tr>
<tr><td>SNRGLF 101</td><td>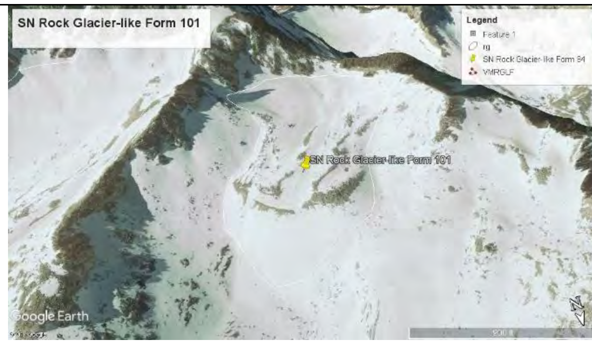
</td><td>Sierra Nevada,
Earth</td><td></td></tr>
<tr><td>SNRGLF 26</td><td>
</td><td>Sierra Nevada,
Earth
37°19'36.33"N
118°41'47.59"W</td><td></td></tr>
<tr><td>APRGLF 5</td><td>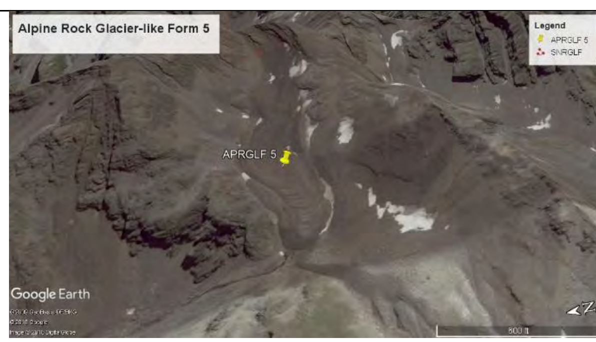
</td><td>European Alps,
Earth
37°22'57.70"N
118°48'24.23"W</td><td></td></tr>
</table>

VMRGLF 1	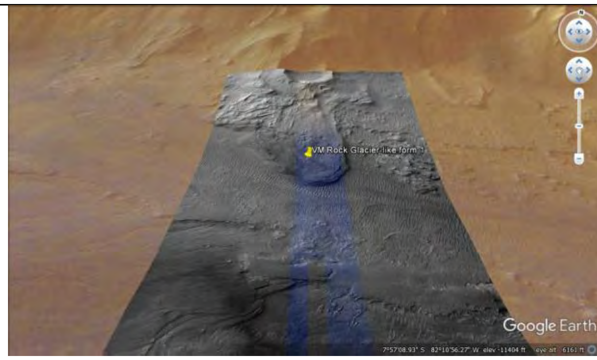	Valles Marineris, Mars 7°56'13.42"S 82°11'1.25"W	
VMRGLF 3	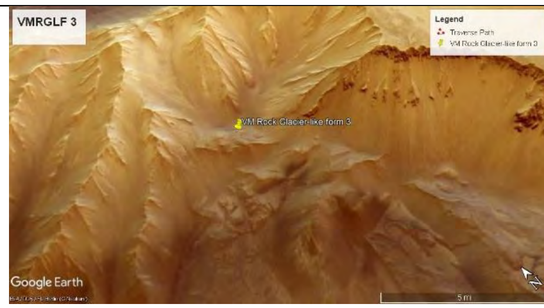	Valles Marineris, Mars 7°46'35.59"S 71°21'36.54"W	
VMRGLF 4		Valles Marineris, Mars 7°26'37.52"S 69° 7'0.54"W	
VMRGLF 5		Valles Marineris, Mars 7°45'45.98"S 68°31'33.84"W	

VMRGLF 6	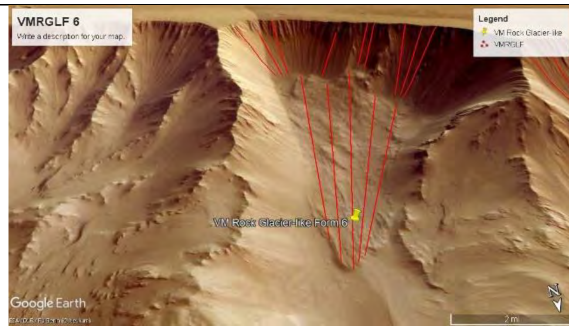	Valles Marineris, Mars 7°50'37.36"S 68°17'20.13"W	
VMRGLF 7	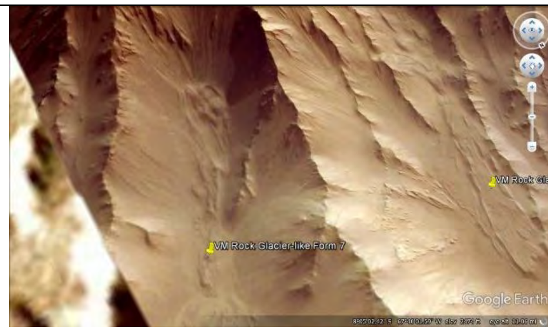	Valles Marineris, Mars 8° 3'33.23"S 67°35'19.23"W	
VMRGLF 19		Valles Marineris, Mars 15°45'45.82"S 56°55'58.48"W	
VMRGLF 32		Valles Marineris, Mars 8°39'14.93"S 63°52'9.17"W	

VMRGLF 35		Valles Marineris, Mars 4°48'57.47"S 81°43'22.24"W	
VMRGLF 37	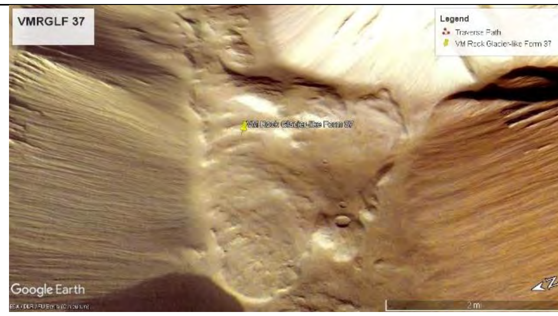	Valles Marineris, Mars 4°41'27.02"S 83°12'50.67"W	
VMGLF 38		Valles Marineris, Mars 4°47'14.68"S 84°40'43.17"W	
VMRGLF 40	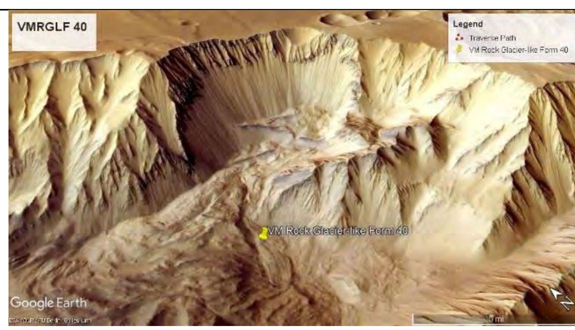	Valles Marineris, Mars 4°28'41.93"S 70°22'33.84"W	

<table>
<tr><td>PTRGLF 7</td><td>
</td><td>Promethei
Terra, Mars
37°43'15.79"S
116° 0'57.45"E</td><td></td></tr>
<tr><td>PTRGLF 8</td><td>
</td><td>Promethei
Terra, Mars
37°42'58.79"S
115°51'2.41"E</td><td></td></tr>
<tr><td>PTRGLF 9</td><td>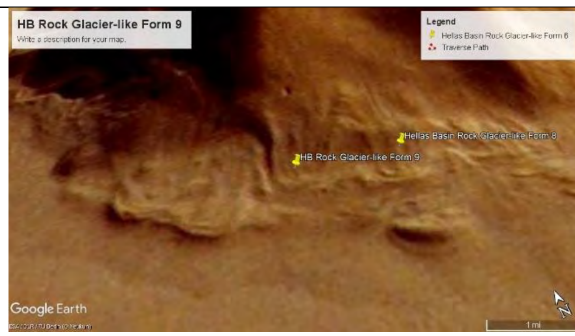
</td><td>Promethei
Terra, Mars
37°42'35.68"S
115°47'48.23"E</td><td></td></tr>
<tr><td>PTRGLF 11</td><td>
</td><td>Promethei
Terra, Mars
37°41'40.75"S
115°44'51.17"E</td><td></td></tr>
</table>

<table>
<tr><td>AMRGLF 7</td><td>
</td><td>Arsia Mons,
Mars
10°57'48.19"S
120°37'50.43"W</td><td></td></tr>
<tr><td>AMRGLF 9</td><td>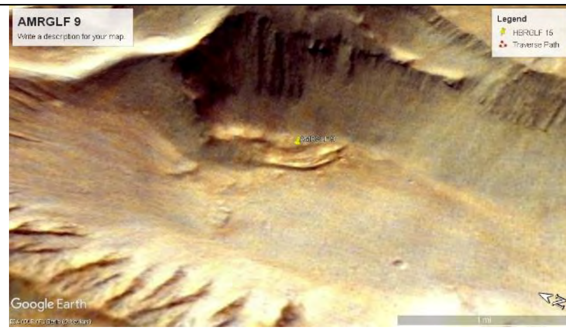
</td><td>Arsia Mons,
Mars
10°56'48.95"S
121° 3'14.12"W</td><td></td></tr>
<tr><td>AMRGLF 13</td><td>
</td><td>Arsia Mons,
Mars
10°38'21.30"S
120°33'20.78"W</td><td></td></tr>
<tr><td>VMRGLF 27</td><td>
</td><td>Valles
Marineris, Mars
4°21'56.18"S
88°47'7.07"W</td><td></td></tr>
</table>

VMRGLF 44	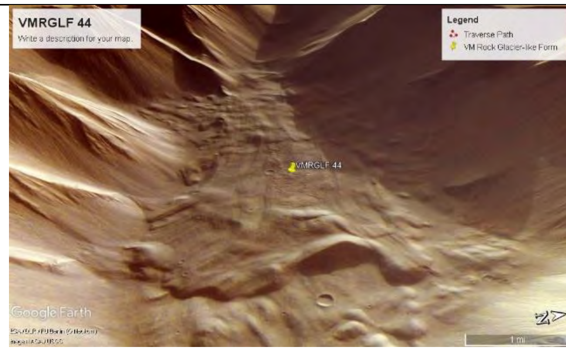	Valles Marineris Mars 4°46'51.94"S 81°57'43.24"W		
DTMRGLF 1	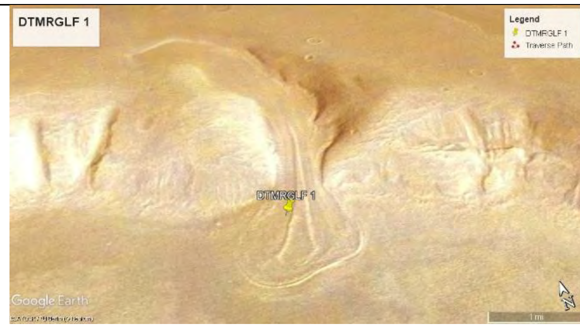	Deuteronilus Mensae, Mars 41°19'10.32"N 29°14'40.09"E		
DTMRGLF 2		Deuteronilus Mensae, Mars 41°23'34.41"N 29° 2'7.36"E		
NHRGLF 6		Deuteronilus Mensae, Mars 37°58'17.68"N 19°50'8.66"E		

NHRGLF 7	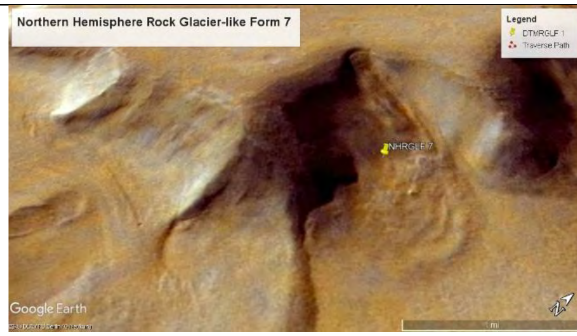	Deuteronilus Mensae, Mars 37°58'17.68"N 19°50'8.66"E	
NHRGLF 8		Deuteronilus Mensae, Mars 45°29'51.54"N 26°25'21.10"E	
PMRGLF 3		Protonilus Mensae, Mars 42°12'42.68"N 50°32'5.87"E	
PMRGLF 6	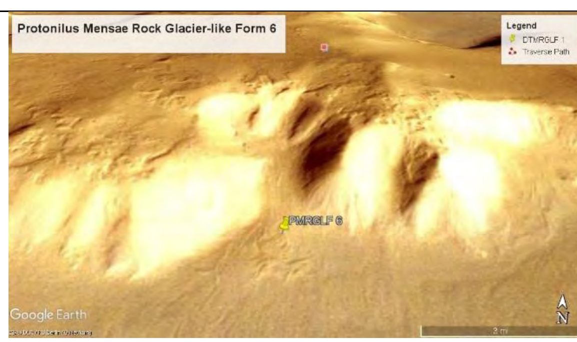	Protonilus Mensae, Mars 45° 6'10.88"N 38°11'30.67"E	

PTRGLF 28		Promethei Terra, Mars 43°12'32.39"S 96°55'19.23"E	
AMRGLF 12		Arsia Mons, Mars 10°43'3.31"S 120°40'22.65"W	
ABRGLF 1	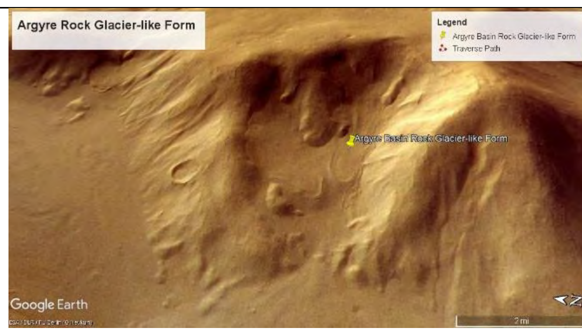	Argyre Basin, Mars 41°25'8.02"S 51°55'3.12"W	
OMRGLF 2	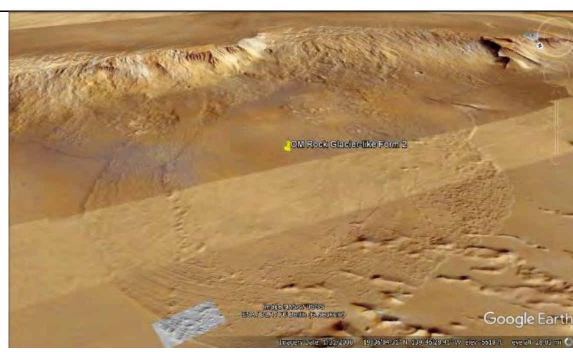	Olympis Mons, Mars 19°37'30.70"N 139°34'3.23"W	

AMRGLF 14		Arsia Mons, Mars 10°24'45.40"S 120°35'21.72"W	
NHRGLF 4	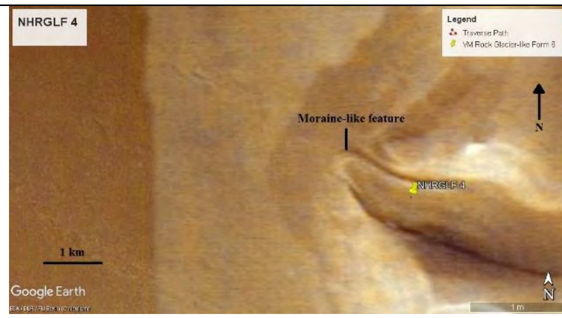	Deuteronilus Mensae, Mars 36°40'31.22"N 15°30'56.76"E	
VMRGLF 33	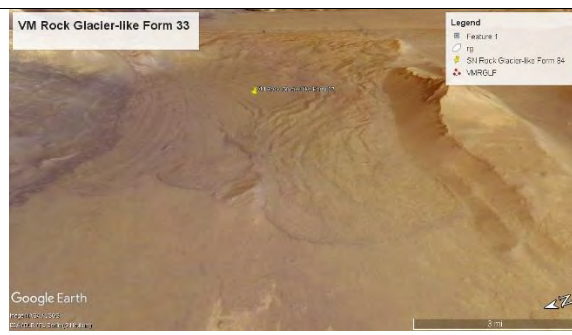	Valles Marineris, Mars 10°52'6.78"S 68°47'57.17"W	
PTRGLF 27	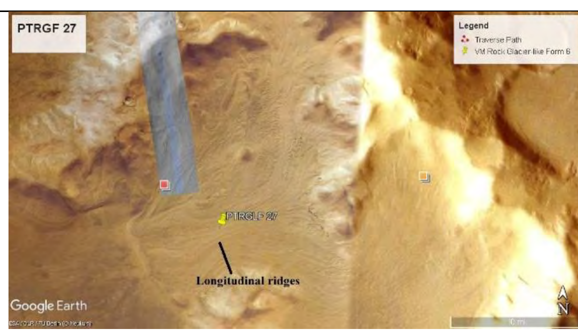	Promethei Terra, Mars 41°58'15.14"S 108°47'31.57"E	

APPENDIX 2

Earth measurement data

Rock Glacier	Height (m)	Horizontal length (m)	Headwall Slope Steepness (deg)	Rock Glacier Slope Steepness (deg)
SNRGLF 1	176.9054878	751.5853659	30.78193175	13.45509491
SNRGLF 4	173.3739837	595.8333333	30.78193175	18.26288994
SNRGLF 5	112.0934959	557.0121951	28.79246173	12.69856051
SNRGLF 12	174.9237805	658.2317073	35.0133777	14.84222706
SNRGLF 17	131.199187	351.1178862	32.65987145	21.52097056
SNRGLF 19	194.4105691	382.0121951	37.64120583	26.21256052
SNRGLF 24	171.1382114	764.796748	19.7	11.9
SNRGLF 25	145.0203252	494.2073171	35.49	16.8
SNRGLF 27	123.6788618	503.0487805	35	15.7
SNRGLF 28	178.7347561	658.0792683	30.15123298	15.70863783
SNRGLF 29	159.3495935	940.8333333	29.20519037	10.72109627
SNRGLF 31	127.5406504	906.504065	29.10140592	10.77639912
SNRGLF 32	168.2926829	471.1382114	30.14052165	20.4
SNRGLF 33	55.33536585	259.9085366	30.43119322	13.9
SNRGLF 34	107.4186992	691.1585366	33.82735747	11.12617499
SNRGLF 35	86.2296748	346.4430894	33.55859033	18
SNRGLF 37	211.8902439	828.2723577	33.96	14.86
SNRGLF 38	153.3536585	604.4512195	34.876 deg.	15.98

SNRGLF 39	183.9939024	1263.658537	33.7495258 deg.	8.922602065
SNRGLF 40	137.195122	860	34.167	9.499483015
SNRGLF 41	133.4603659	471.875	38.08123513	18.417758
SNRGLF 42	172.3323171	584.375	34	16.699
SNRGLF 43	213.9481707	647.179878	39	18
SNRGLF 44	191	435.8536585	31.4666	13.4957
SNRGLF 46	134	657.3780488	33.78	11.98
SNRGLF 48	139.2530488	387.5762195	29.17122558	20.3548538
SNRGLF 49	204.8780488	755.8943089	35.90453841	15.07396734
SNRGLF 50	197.56	405.79	32.8978183	23.0820866
SNRGLF 51	177	633.536585	36.56617603	17.47400197
SNRGLF 52	275.6	864	29.17122558	17.60596806
SNRGLF 53	95.79268293	381.9512195	34.97553679	15.71660189
SNRGLF 54	108.0792683	308.8414634	39.19724382	18.91915112
SNRGLF 55	93.52134146	343.2164634	33.65227348	17.47139544
SNRGLF 56	108.597561	481.5853659	30.45978554	18.75748723
SNRGLF 57	204.1666667	1051.707317	32.24607103	13.47767349
SNRGLF 58	142.1747967	663.8211382	33.88136058	12.84388285
SNRGLF 59	107.1138211	302.0325203	36.87513576	20.08578153
SNRGLF 60	107.1138211	302.0325203	36.87513576	20.08578153
SNRGLF 61	83.61280488	680.0304878	33.42081993	10.61965528
SNRGLF 62	88.4527439	277.3246951	34.31353651	18.398415
SNRGLF 63	103.125	421.4176829	29.93333737	15.89430317

SNRGLF 64	99.84756098	568.6737805	30.89476799	10.67499512
SNRGLF 65	94.28353659	511.3567073	29.8606122	12.01060369
SNRGLF 66	213.9481707	543.597561	32.42915578	23.67745095
SNRGLF 67	131.1768293	502.7439024	28.9557554	18.72665887
SNRGLF 68	99.35213415	375.1143293	31.18651956	16.1523379
SNRGLF 69	160.7469512	850.7012195	33.3303743	11.77194971
SNRGLF 71	140.929878	891.6768293	30.33237691	10.03739409
SNRGLF 72	247.7787456	711.1498258	34.80573907	19.26087359
SNRGLF 73	211.3414634	621.7682927	35.86282426	19.38187202
SNRGLF 74	168.0487805	410.6097561	36.8772308	21.09661443
SNRGLF 75	89.02439024	619.7560976	30.99383937	12.1776844
SNRGLF 77	54.08536585	392.0731707	29.53155351	12.1776844
SNRGLF 78	168.7804878	542.7439024	33.51504141	17.02458816
SNRGLF 79	85.5945122	228.5060976	35.19659232	21.20625313
SNRGLF 80	77.74390244	207.2408537	39.53777994	25.93133788
SNRGLF 81	45.79268293	178.3536585	31.44161549	28.31578721
SNRGLF 82	116.6158537	270.5030488	33.86725486	27.58706768
SNRGLF 83	94.3597561	457.2662602	31.40406528	13.72124923
SNRGLF 84	104.1920732	994.0243902	28.81079374	6.291450802
SNRGLF 85	203.2317073	919.9878049	30.32289087	13.1702419
SNRGLF 86	193.8262195	858.4603659	27.41802706	14.0766804
SNRGLF 87	125.3658537	378.8414634	32.02597931	18.04560951
SNRGLF 88	291.4634146	1523.902439	33.21047706	12.64402167

SNRGLF 89	235.3658537	1094.634146	29.97833251	10.79114312
SNRGLF 90	274.9237805	1536.128049	33.21750832	11.06180487
SNRGLF 91	123.597561	571.1585366	32.63730469	13.61485926
SNRGLF 92	152.6829268	476.402439	30.32763412	17.4322886
SNRGLF 93	213.6178862	664.2276423	31.03216749	18.86358756
SNRGLF 94	252.195122	622.3780488	38.74229016	24.62672132
SNRGLF 95	41.58536585	203.1097561	30.43955973	20.38506609
SNRGLF 96	112.1189024	406.6310976	32.87054443	23.80946996
SNRGLF 97	182.6219512	766.8445122	28.79612865	14.35933654
SNRGLF 98	142.1341463	378.597561	31.1679459	24.76860012
SNRGLF 99	231.9359756	776.1432927	29.82420982	16.55458148
SNRGLF 100	193.902439	779.8323171	29.8515141	14.31900044
SNRGLF 101	176.3414634	481.9512195	24.76151386	20.39513422
SNRGLF 26	165.929878	428.125	28.44785045	25.90816365
ARGLF 1	166.4634146	560.2896341	24.87951262	12.279838
ARGLF 2	186.2804878	490.9552846	16.62913196	20.42197615
ARGLF 3	191.0569106	579.8780488	16.94423111	17.71001581
APRGLF 1	396.3414634	1325.365854	25.13596966	16.3305845
APRGLF 2	337.2713415	1589.64939	26.70239597	12.2980714
APRGLF 3	79.9796748	461.1788618	22.86028813	9.74083042
APRGLF 4	228.4552846	594.1056911	28.44662004	20.75670818
APRGLF 5	200.101626	706.504065	34.74130817	15.57138148
APRGLF 6	187.0934959	741.7682927	24.83739601	13.98230535

APRGLF 8	165.8536585	611.6869919	22.7044343	15.37625125
APRGLF 10	146.3414634	442.5304878	27.35026545	18.00416161
APRGLF 14	102.6676829	314.5579268	27.45509941	18.72665887
APRGLF 15	203.5060976	602.7439024	26.72851943	18.22412953
APRGLF 19	119.2073171	591.9512195	22.75456901	10.85747319

Mars measurement data

Rock Glacier	Height (m)	Length (m)	Headwall Steepness (deg)	Rock Glacier Slope Steepness (deg)	Aspect (deg.)
VMRGLF 3	3936	8757.073171	19.82524766	15.9112415	219.7506881
VMRGLF 19	1201	4362.439024	17.75247458	16.63359276	283.8052591
VMRGLF 27	1581	9666.666667	19.4405301	9.75126259	155.916
VMRGLF 32	547	11016.09756	19.15034963	9.583466055	205.5106264
VMRGLF 35	1352	6326.341463	23.48428149	10.68902644	239.1667002
VMRGLF 44	912	10266.66667	22.85911958	4.857144369	124.1849525
VMRGLF 40	1374	15920.4878	25.96534299	9.582931856	194.717613
DTMRGLF 1	635	2500	8.971624199	12.05502989	180.6822176
DTMRGLF 2	465	1133.333	13.20476936	8.435158629	188.2985537
NHRGLF 6	632	1783.333	13.21633625	10.22040275	99.89273904
NHRGLF 7	615	2033.3333	8.6629953	10.31688002	109.1097351
NHRGLF 8	542	2666.6667	6.298313379	11.39102247	131.0684547

PMRGLF 3	1194	8000	9.620013583	8.956193816	142.5739837
PMRGLF 6	1671	3333.3333	15.41833521	14.04063713	159.1451466
PTRGLF 7	584	2366.666667	15.34892091	7.820123183	151.149175
PTRGLF 8	599	1883.33333	16.67181139	7.503440936	172.7875245
PTRGLF 28	1499	4166.666667	15.86473342	10.01157126	220.8619338
VMRGLF 6	2550	13860	25.34570716	15.28200959	71.1564857
VMRGLF 1	52.7	5104	17.49745734	13.65814813	
VMRGLF 4	2167.657774	14693.04878	25.10309019	9.550565952	
VMRGLF 5	2302.515244	11992.68293	24.89130012	10.74414159	
VMRGLF 7	1960.97561	9045.20122	25.49180617	12.06540724	
VMRGLF 19	1086.280488	4362.439024	20.25406082	14.88237175	
VMRGLF 37	461.5853659	6921.914634	25.02630265	4.699148281	
VMGLF 38	1333.689024	5775	26.62104632	13.06155108	
HBRGLF 9	328.7601626	1917.560976	17.1362745	9.350791687	
HBRGLF 11	434.5121951	2578.829268	17.58861509	9.525490784	
AMRGLF 7	255.0813008	1931.666667	22.51051422	7.894670891	
AMRGLF 9	128.4146341	717.8658537	22.50178196	10.12625808	